AD_____

Award Number: DAMD17-00-1-0081

TITLE: Targeting of Prostate Cancer with Hyaluronan-Binding Proteins

PRINCIPAL INVESTIGATOR: Charles Underhill, Ph.D.
Lurong Zhang, M.D., Ph.D.

CONTRACTING ORGANIZATION: Georgetown University
Washington, DC 20057

REPORT DATE: June 2005

TYPE OF REPORT: Final

PREPARED FOR: U.S. Army Medical Research and Materiel Command
Fort Detrick, Maryland 21702-5012

REPORT DOCUMENTATION PAGE

Form Approved
OMB No. 0704-0188

1. REPORT DATE	2. REPORT TYPE	3. DATES COVERED
01-06-2005	Final	1 Jun 2000 –31 May 2005

4. TITLE AND SUBTITLE

Targeting of Prostate Cancer with Hyaluronan-Binding Proteins

5a. CONTRACT NUMBER

5b. GRANT NUMBER
DAMD17-00-1-0081

5c. PROGRAM ELEMENT NUMBER

6. AUTHOR(S)
Charles Underhill, Ph.D.
Lurong Zhang, M.D., Ph.D.

5d. PROJECT NUMBER

5e. TASK NUMBER

5f. WORK UNIT NUMBER

7. PERFORMING ORGANIZATION NAME(S) AND ADDRESS(ES)

Georgetown University
Washington, DC 20057

8. PERFORMING ORGANIZATION REPORT NUMBER

9. SPONSORING / MONITORING AGENCY NAME(S) AND ADDRESS(ES)
U.S. Army Medical Research and Materiel Command
Fort Detrick, Maryland 21702-5012

10. SPONSOR/MONITOR'S ACRONYM(S)

11. SPONSOR/MONITOR'S REPORT NUMBER(S)

12. DISTRIBUTION / AVAILABILITY STATEMENT
Approved for Public Release; Distribution Unlimited

13. SUPPLEMENTARY NOTES
Original contains color plates: ALL DTIC reproductions will be in black and white.

14. ABSTRACT

The goal of this study is to determine the anti-tumor effect of hyaluronan (HA) binding proteins/peptides (HABPs) and to explore their underlying anti-tumor mechanisms. The idea is triggered by the facts that several known anti-tumor agents are the member of HABPs family, and that little is known about the their mechanisms.

In this grant support period, we demonstrated that: **1)** HABPs could be obtained via different approaches, such as affinity purification, genetic expression and chemical synthesis; **2)** HABPs from different sources could exert anti-cancer effect without obvious side-effect, indicating that anti-tumor effect is a universal property of members in HABPs family; **3)** HABPs could inhibit the tumor angiogenesis; **4)** some HABPs could bind to Bcl-2, promote the release of cytochrome c and trigger apoptosis of tumor cells; **5)** some HABPs could activate the classic complement pathway to kill tumor cells.

The results reveal that HABPs, a set of naturally existing biological agents is likely to be a new category of anti-tumor agent via triggering intrinsic death pathways.

We believe that study of functional domain of HABPs may lead to discover new anti-tumor agent that can be synthesized in a large quantity and safe for use in cancer treatment.

15. SUBJECT TERMS

Hyaluronan-Binding Proteins, Experimental Therapy, Prostate Cancer, Angiogenesis

16. SECURITY CLASSIFICATION OF:			17. LIMITATION OF ABSTRACT	18. NUMBER OF PAGES	19a. NAME OF RESPONSIBLE PERSON
a. REPORT	b. ABSTRACT	c. THIS PAGE			USAMRMC
U	U	U	UU	74	19b. TELEPHONE NUMBER *(include area code)*

Table of Contents

INTRODUCTION

Although much progress has been made in elucidating the underlying molecular mechanisms responsible for prostate cancer in recent years, effective treatments for this disease have not progressed at the same pace. New therapeutic approaches are badly needed.

In last decade, it has been found that some hyaluronan (HA, a major component of extracellular metrix) binding proteins, such as soluble CD44 and proteins from scapular chondrocytes or cartilage have anti-tumor or anti-angiogenesis effect (1-4). In addition, some angiogenic inhibitors, such as endostatin, have HA binding domain demonstrated by its crystal structure (5-7). Furthermore, the shake cartilage powder or its extracts have been on the shelf of health food market in USA (FDA IND# 43 033, approved on Fab 7, 1994), Europe and Asia for a decade. This substance has been widely used by patients with different tumors, in believing that avasscular cartilage might contain some natural anti-angiogenesis substance. Indeed, this substance has exhibit anti-cancer effect in some patients, which might be associated with that some components of shark cartilage escape digestion, and enter tumor sites via the blood circulation. Although the therapeutic value of shake cartilage for cancer is still controversial, Alternative Medicine Center in National Institute of Health has made decision to test the efficacy of this substance (8-21). The cartilage contains an abundance of HA binding proteins (HABP, 22-25). Whether the anti-tumor/angiogenesis effect of shark cartilage achieved in a proportion of cancer patients is due to the partially digested fragments of HABP passing through impaired mucous of gastrointestinal (GI) track remains to be investigated.

The goal of this study is to determine the anti-tumor effect of hyaluronan (HA) binding proteins/peptides (HABPs) and to explore their underlying anti-tumor mechanisms.

In this grant support period, we demonstrated that: **1)** HABPs could be obtained via different approaches, such as affinity purification, genetic expression and chemical synthesis; **2)** HABPs from different sources could exert anti-cancer effect without obvious side-effect, indicating that anti-tumor effect is a universal property of members in HABPs family; **3)** HABPs could inhibit the tumor angiogenesis; **4)** some HABPs could bind to Bcl-2, promote the release of cytochrome c and trigger apoptosis of tumor cells; **5)** some HABPs could activate the classic complement pathway to kill tumor cells.

The results reveal that HABPs, a set of naturally existing biological agents is likely to be a new category of anti-tumor agent via triggering intrinsic death pathways.

We believe that study of functional domain of HABPs may lead to discover new anti-tumor agent that can be synthesized in a large quantity and safe for use in prostate cancer treatment.

BODY

Our study approaches were in the following sequential: **1)** to obtain HABPs from different sources in the forms of either intact molecules or truncated fraction to pin down the functional domain of HABPs; **2)** to determine their anti-tumor effect; and **3)** to explore their putative action mechanisms.

A. To obtain HABPs from different sources using different approaches

1. Purification of a large quantity of intact HABP from cartilage cartilage:

The cartilage is a tissue that enriches in HA and HA binding proteins (HABP, 22-25). First, we wanted to see if we could purify cartilage intact HABP using our HA affinity column, since we speculated that the HABP might be the responsible molecule for the anti-tumor/angiogenesis effect that had be achieved in some cancer patients (8-21). The fresh cartilage was purchased from cow farm and sliced into small pieces. The purification procedure was performed according to Dr. Tengblad's method (26-27) with some modification outlined as following. The result showed that the cartilage HABP that can be purified in a large quantity using our HA affinity column. During the purification process, every effort was made to avoid the bacterial contamination. At the end, the endotoxin in each preparation was tested and the results was less then 5EU/ml, indicating that the purified cartilage HABP could be used for both in vitro and in vivo studies.

It is known that in the HABPs purified with HA affinity column have at least two major proteins with high affinity to HA: link protein and aggrecan. Since it is not possible to use human cartilage to purify these proteins, we have to use genetic expression approach.

2. Construction, expression and purification of recombinant human aggrecan and link protein:

The aggrecan is one of the major HABPs in cartilage. The only way to obtain human aggrecan is to use molecular biology approach. According to the published cDNA sequence (GenBank access number M55172 and X17405), we designed the two paired primers. One pair framed the most of HA binding domains in the N-terminal of aggrecan, which consisted of first 350 amino acids without signal peptide. The other pair framed the whole sequence of link protein (1,016 bp). The RT-PCR was performed using a cDNA library of a human sarcoma cell line derived from chondrocytes as template. The cDNAs cording for the portion of aggrecan (993 bp) and the full-length of link protein was inserted into pPICZ yeast expression vector with a-factor signal peptide for secretion from yeast cells and His_6 tag for purification. After the clones with correct cDNA were identified by DNA sequencing, the fermentation was carried out to produce truncated human aggrecan protein (termed briefly as aggrecan) and link protein. The aggrecan purified from Ni-column was identified as a single diffused band with apparent molecular weight of 68 kDa on SDS-PAGE gel, which may due to the dimerization or glycosylation of the protein. The link protein had 354 amino acids with apparent molecular weight of 46 kDa The HA binding ability of aggrecan and link protein was determined by mixing 20 μg of recombinant human aggrecan and link protein with ^{3}H-HA (see attached paper for method). The result showed that both recombinant aggrecan and link protein had a HA binding activity.

3) Synthesis of different HA binding peptides

Triggered by the fact that most biological agents that are used in treatment are small molecules, peptides, etc. We decided to study on HA binding peptides obtained by using chemical synthesis approach. The study of naturally existing HABPs reveals that there is a common property in the functional domain of HABPs, which they all contain a motif of B[X_7]B (two basic amino acids flanking a sequence of seven amino acids, 29). We used this property (B[X_7]B) to search naturally existing peptide or the motifs in the known HABP and define the sequences for the chemical synthesis. Using the ^{3}H-HA as a tool to determine their HA binding activity, we obtained several leading HA binding peptide sequence and studied them in detail summarized as following.

The study of HA binding peptide has the following advantages: **1)** it can be obtained in a large quantity without endotoxin contamination; **2)** it is much more stable than the native protein, given a long shelf-life for clinical application, if the anti-tumor activity is strong enough to be a drug; **3)** it can be chemically modified to

prevent from enzymatic digestion, which will yield a long half life in body; and **4)** it can provide a molecular structure for the design of mimic small molecule. We believe that this is a right direction to carry out our research.

a. P4, a peptide derived from HA binding sites of aggrecan and hyaluronidase: P4 consisted of 46 amino acids (CNGRCGGKQKIKHVVKLKVVVKLKSQLVKRKVVVRRRKKIQGRSKR) derived from (B[X_7]B) portions of aggrecan and hyaluronidase. It contained three (B[X_7]B, two from aggrecan and one from hyaluronidase). It was coupled together using a series of VVV residues to provide the flexible linkages. To improve the targeting of the peptide to tumor and endothelial cells the N-terminus consisted of CNGRG sequence that acts as a ligand for CD13 (30). To impede enzymatic degradation, the N–terminals of the peptides were acetylated, and the C-terminals were amidated. The peptide was synthesized by Genemed (San Francisco, CA) and dissolved in a small amount of dimethylformamide and 1% acetate acid, diluted with saline to a concentration of 1 mg/ml, and sterilized by placing in a boiling water bath for 15 min. This peptide had a high affinity to ^{3}H-HA.

b. Human brain-HABP fragment (BH-P). Using biotinylated HABP in immunohistochemic staining of brain, we found that abundant of HA existed in human brain, suggesting that its binding protein, brain-HABP, may also exist in a large quantity. Therefore, we cloned human brain HABP (GenBank accession number AY007241). Triggered by the fact that most of biologically active molecules are small peptides, we believe that the fragment form brain HABP may possess functions of its intact molecule. BH-P (CNGRCGGRRAVLGSPRVKWTFLSRGRGGRGVRVKVNEAYRFR) contains three HA binding motifs from the NH2 terminus of the human brain HABP was synthesized. It has a molecular mass of 4,736 and an isoelectric point of 12.01. The control peptide (control-P) consists of the same amino acids with a scrambled sequence. To impede enzymatic degradation, the NH2 terminus of the synthetic peptides was acetylated, and the COOH terminus was amidated. Before use, the peptides were dissolved in dimethylformamide and 1% acetate acid, diluted with saline to a concentration of 1 mg/ml, and sterilized by boiling for 15 min.

c. Tachyplesin, a naturally existing HA binding peptide: In search of naturally existing HA binding peptide, we synthesized more than 10 peptides according to their possessing of structure of (B[X_7]B) and then screened with ^{3}H-HA. One of them possessed a high binding activity was tachyplesin, an antimicrobial peptide present in leukocytes of the horseshoe crab (*Tachypleus tridentatus*). Tachyplesin has a unique structure, consisting of 17 amino acids (KWCFRVCYRGICYRRCR) with a molecular weight of 2,269 Dalton and a *pI* of 9.93. In addition, it contains two disulfide linkages, which causes all six of the basic amino acids (R: arginine; K: lysine) to be exposed on its surface. To better target on tumor/vessel, the synthetic tachyplesin was conjugated to the integrin homing domain RGD. The RGD-tachyplesin was purified with HPLC with 99% purity.

B. HABPs from different sources could exert anti-cancer effect without obvious side-effect

Fig.1. Inhibition of tumor cell growth by purified HABPs

1. Effect of affinity purified HABPs on tumor cells

1) *In vitro* effect of cartilage HABPs on anchorage-dependent growth of tumor cells.

To test if purified cartilage HABP had its bio-activity, we first performed the anchorage-dependent and independent growth assay in tumor cells. The different amounts of HABP (5, 50 μg/ml) were added to the media of tumor cells cultured in 24 well plate, at different time points (day 2, 4, 6 and 8), the cells were harvested with 10 mM EDTA and the number was counted with Coulter Counter. The result (**Fig. 1**) showed that the HABP inhibited the growth of tumor cells in a dose dependent manner. This inhibitory effect could be abolished by the heat-inactivation, indicating that

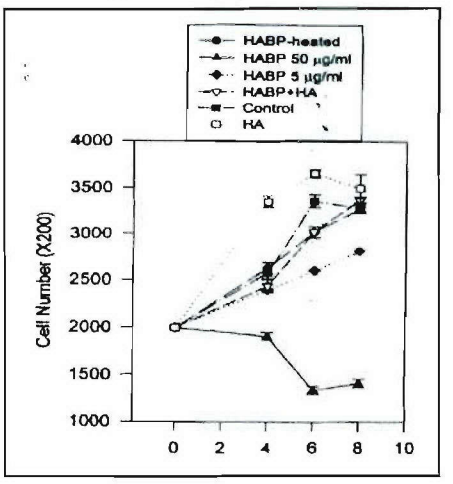

the natural structure of this protein is essential for its activity of anti-tumor cell growth.

2) *In vivo* effect of cartilage HABPs on the growth of primary TSU cancer and other tumors

To test the effect of The tumor-CAM system was used, since this was a quick, easy and cheap system (28). Furthermore, in our experience, the results from the tumor-CAM system are comparable with those obtained from the mice model system. Two million TSU or were placed on the CAMs of 10 days old chicken embryo (12 eggs/group) and allowed to grow for two day. When the established tumors could be seen by eye, 80 μg (in 200 μl saline) of HABP was iv. injected once into CAM. Four days later, the tumors were harvested, weighted and photographed. As shown in **Fig. 2**, the TSU tumors treated with HABP were smaller than those treated with vehicle alone or heat-inactivated HABP, and the difference was statistically significant ($P<0.05$). The effect was dose-dependent and required a native, active form of HABP. However, there was no difference in the chicken weight (data not shown), indicating that the HABP was not toxic and did not interrupt the normal development. Similar results were obtained with aggressive tumor formed by B16 cells, suggesting that the anti-tumor effect of HABP is not cell line specific.

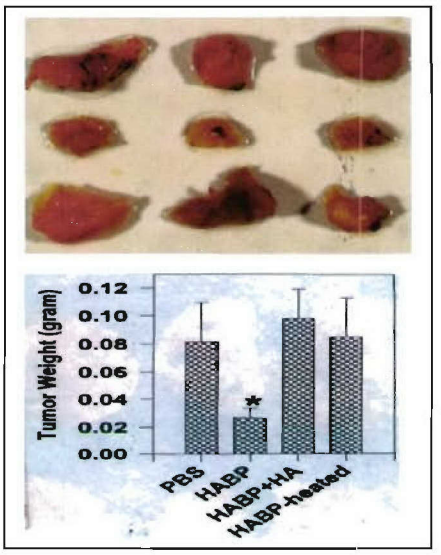

Fig 2. Effect of HABPs on TSU tumor

3) ***In vivo* effect of cartilage HABPs on the experimental metastasis**

Since the cause of death in cancer patients is mainly due to the metastasis, we were interested to see the effect of HABP on tumor metastasis (currently, there is not consistent prostate cancer metastasis model available). In this set of study, we used B16 or Lewis lung metastasis models, since they are well-recognized and reliable metastasis models. Fifty thousand tumor cells were i.v. injected via tail vein into C57BL/6 syngenic mice and allowed to establish for two days. Then, the mice were treated with i.p. injection of different doses of HABP (as test) or BSA (as non-specific protein control) or HABP pre-incubated with excess HA. As shown in **Fig. 3,** the experimental lung metastases formed by B16 or Lewis lung cancer cells were dramatically inhibited by i.v. injection of HABP every other day at doses of 15 to 50 μg. Importantly, in a side by side comparison study, HABP seems more effective than angiostatin, a well-known angiogenic inhibitor.

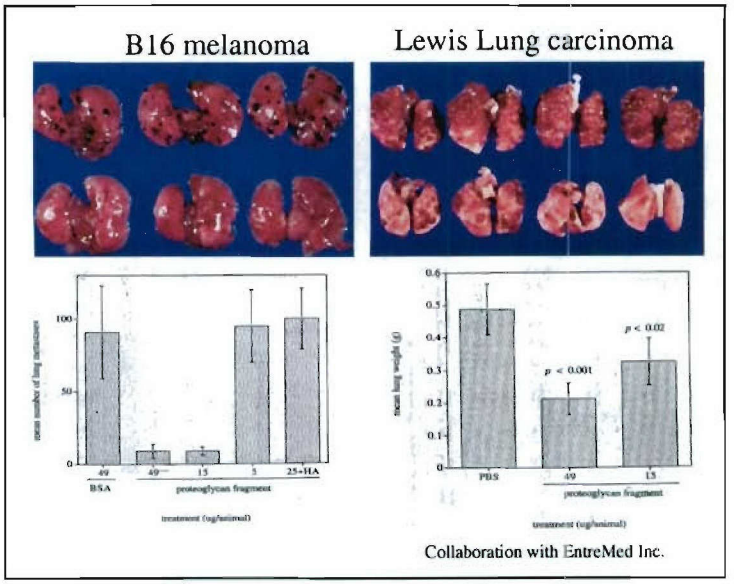

Fig 3. Inhibitory effect of HABPs on tumor metastasis

2. Anti-tumor effect of aggrecan

We were eager to see the effect of aggrecan on tumor growth. Two million of TSU tumor cells were placed on top of CAM of 10 days old chicken embryos. Two days later, 100 μg of aggrecan (expressed in yeast and purified with Ni-column) was i.v. injected into CAM and four days later, the tumors were harvested, pictured and weighted. The results showed that the tumors in the aggrecan treated group were smaller than the control (**Fig 4**) and the difference in the tumor weight between two groups was statistically significant ($p<0.05$). There was no difference in the chicken weight between two groups, indicating that

Fig 4. Inhibition of tumor growth by aggrecan

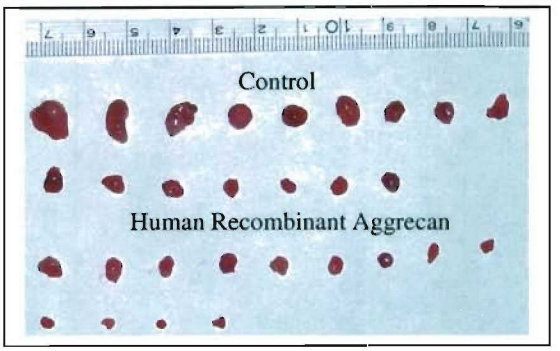

the aggrecan was not toxic to the embryo and did not impair the normal development.

3. Anti-tumor effect of link protein

To test the biological effect of a given protein, the gene transfection approach is a quick and clean approach, since the only difference between the parental and positive transfectants cells that receive either vector alone or with cDNA of link protein is the expression level of link protein at same genetical background, which allow us to obtain a clear-cut conclusion. As shown in the **Fig 5,** the cells expressing high level of link protein had a small tumor size (**A**), slow tumor growth curve (**B**) and reduced tumor weight compared to the vector alone control group (**C**). These data suggest that the level of link protein is reversely correlated with tumor growth and the anti-tumor effect of link protein can be achieved by genetic modification. Although how to deliver the effective anti-tumor gene is currently unsolved problem, the candidate therapeutic gene should still be investigated.

Fig 5. Link protein inhibits the primary tumor growth

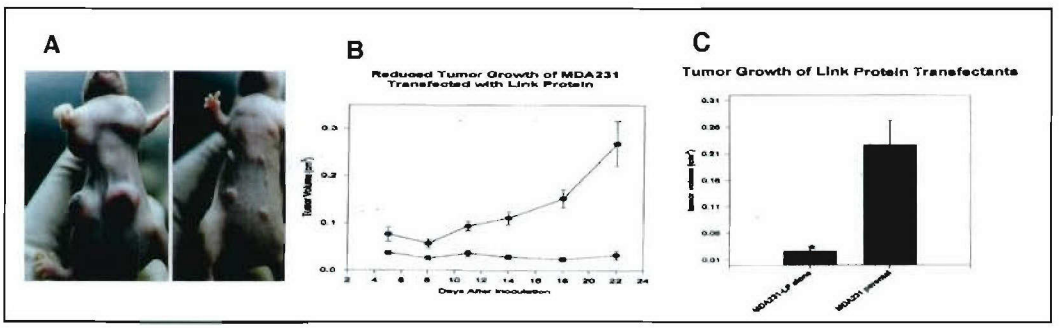

4. Anti-tumor effect of P4

a. *In vitro* effect: The anti-tumor effect of P4 was demonstrated by its ability to inhibit the growth of tumor/endothelial cells in both anchorage-dependent (3H-TdR incorporation assay, **Fig 6 A and B**) and anchorage-independent growth (soft agar assay, **Fig 6 C and D**).

Fig 6. P4 inhibits the primary tumor growth in both anchorage-dependent and anchorage-independent conditions

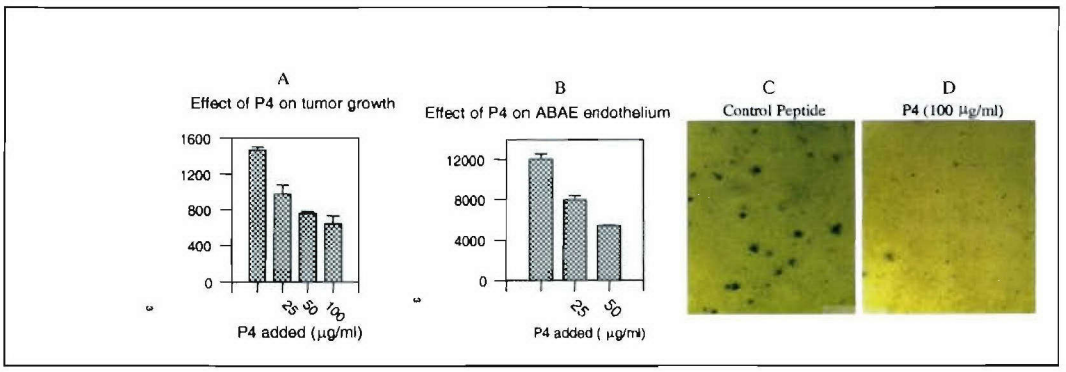

b. *In vivo* effect: To investigate the in vivo effect of P4, the amino acid sequence of P4 was back-translated into cDNA and and inserted into pSecTag2/hygro vector containing a Igκ signal peptide for secretion. The success of transfection was determined by Western blotting with antibody generated against P4 (data not shown). When two million transfectants cells were inoculated on nude mice, the tumors formed by P4 transfectants were much smaller than with the mock transfected cells (**Fig. 7 A**) and the difference was statistically significant ($P<0.05$, **Fig. 7 B**).

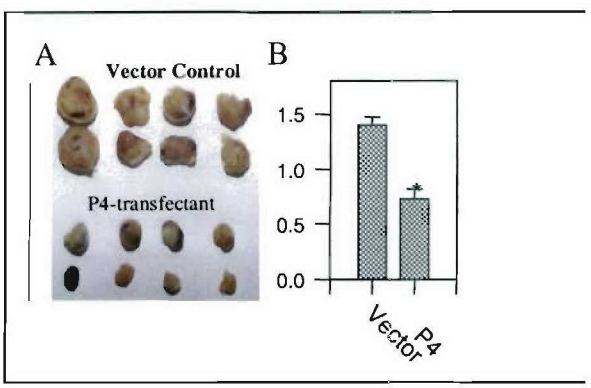

5. Anti-tumor effect of BH-P

Fig 8. Effect of BH-P on tumor growth *in vitro*

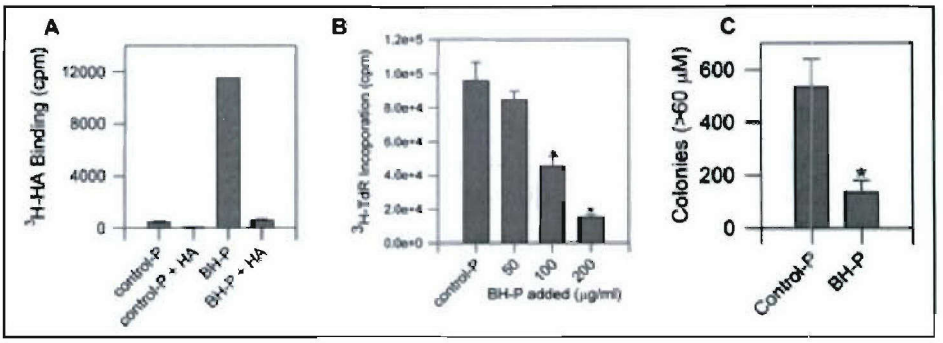

BH-P could specifically bind to HA as shown in **Fig 8 A**. When BH-P was added to the media of cultured tumor cells for 18-24 hours, it caused the cells to become rounded and detached, whereas the control peptide had no such effect (data not shown). To quantitatively measure the extent of this inhibitory effect, a [^{3}H]-thymidine incorporation assay was conducted. Figure 8 B shows that the proliferation of tumor cells was inhibited by BH-P in a dose dependent manner, with an EC_{50} of about 100 μg/ml. The In contrast, the control-P had no effect even at a concentration of 200 μg/ml (Fig. 8 B first column). In addition, BH-P also inhibited the colony formation of these tumor cells under anchorage-independent conditions on soft agar (Fig. 8 C).

In view of these *in vitro* results, we then examined the effects of BH-P *in vivo* in two different model systems.

Fig 9. Effect of BH-P on tumor growth *in vivo*

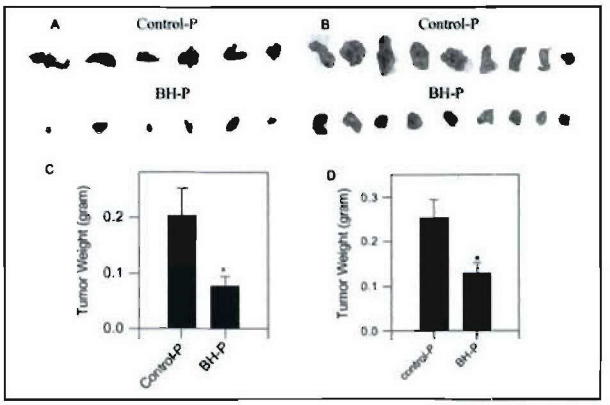

In the first model system, BH-P was directly injected into a vein of chicken embryo CAMs on which tumor xenografts were growing. As shown in Fig. 9*A*, the sizes of tumor xenografts in the BH-P treated group were much smaller than those injected with control-P. Similar results were obtained with MDA-435 cells in the same model (Fig. 9*B*). Furthermore, the difference in the tumor weights between the test and control groups was statistically significant (Fig. 9*C* and *D*). The data suggested that the antitumor effect of BH-P was not limited to one cell line and was likely to be universal.

We also transfected cDNA of BH-P into tumor cells and examined its effect. Fig. 10 *A* shows that the growth curve of the tumor cells transfected with BH-P was below that of the mock-transfected cells. Forty-two days after inoculation, the average size of tumor xenografts in the BH-P group was smaller than that in the control group (Fig. 10*B*), and the difference in tumor weight between the two groups was statistically significant (Fig. 10*C*; $P < 0.05$).

Fig 10. Inhibitory effect of BH-P on tumor growth of transfectants *in vivo*

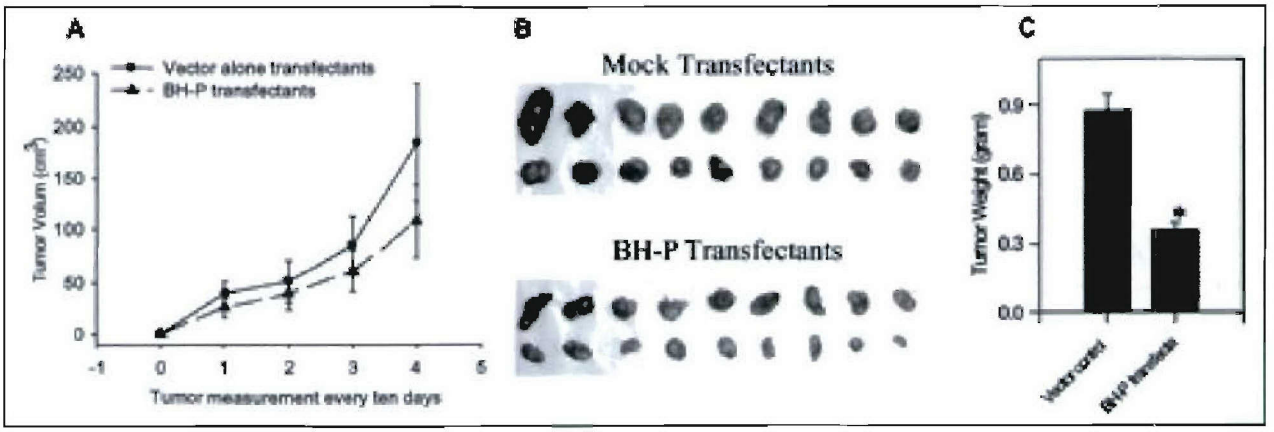

6. Anti-tumor effect of tachyplesin

Because both tumor and endothelial cells play an important role in determining tumor progression, we initially examined the effects of RGD-tachyplesin on the proliferation of both of these cells *in vitro*. As shown in Fig. 11*A*, RGD-tachyplesin inhibited the growth of the cultured cells in a dose-dependent manner, with an EC_{50} of about 75 μg/ml for TSU tumor cells and 35 μg/ml for the endothelial cells. In contrast, the scrambled peptide had no obvious effect on the proliferation of the cells at 100 μg/ml. This effect was also reflected in the morphology of the cells. After exposure to 50 μg/ml RGD-tachyplesin for 12 h, a significant fraction of treated cells had become rounded and detached, whereas few cells did so after treatment with the control peptide (data not shown).

To determine whether non-tumorigenic cells were also affected by RGD-tachyplesin, the immortalized cell lines, Cos-7 and NIH-3T3, were tested in the [^{3}H]-thymidine incorporation assay. As shown in Fig. 11*B*, when treated with 50 μg/ml RGD-tachyplesin, the extent of inhibition of Cos-7 or NIH-3T3 (0–20%) was less than that of tumor or proliferating endothelial cells (40–75%), indicating that nontumorigenic cells are less sensitive to RGD-tachyplesin.

Next, we examined the effects of the peptides on the growth of TSU cells in soft agar. The ability of cells to grow under such anchorage-independent conditions is one of the characteristic phenotypes of aggressive tumor cells. As shown in Fig. 11*C*, RGD-tachyplesin inhibited the ability of TSU cells to form colonies as compared to the groups of control peptide and vehicle alone.

Fig. 11. Anti-tumor effect of tachyplesin on tumor/endothelial cells *in vitro*

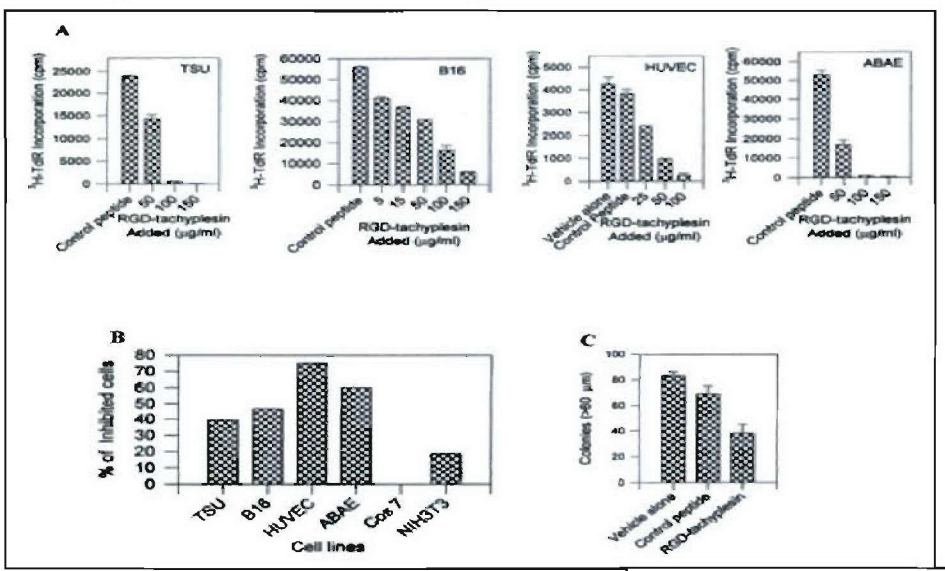

The *in vivo* effects of RGD-tachyplesin on the growth of TSU or B16 tumor cells in CAM or mouse models were examined. As shown in Fig.12, the TSU tumor xenografts growing in CAM in the group treated with RGD-tachyplesin (Fig. 12*B*) were smaller than those in the group treated with control peptide (Fig.12*A*). In addition, the average weight of the xenografts in the RGD-tachyplesin-treated group was significantly less than that of xenografts in the control group (Fig. 12*C*). Similarly, in the B16 mouse model, the B16 tumor xenografts in the RGD-tachyplesin-treated group (Fig. 12*E*) were smaller than those in the control group (Fig. 12*D*), and this difference was statistically significant ($P < 0.05$; Fig. 4*F*↓). It should be noted that RGD-tachyplesin did not appear to be

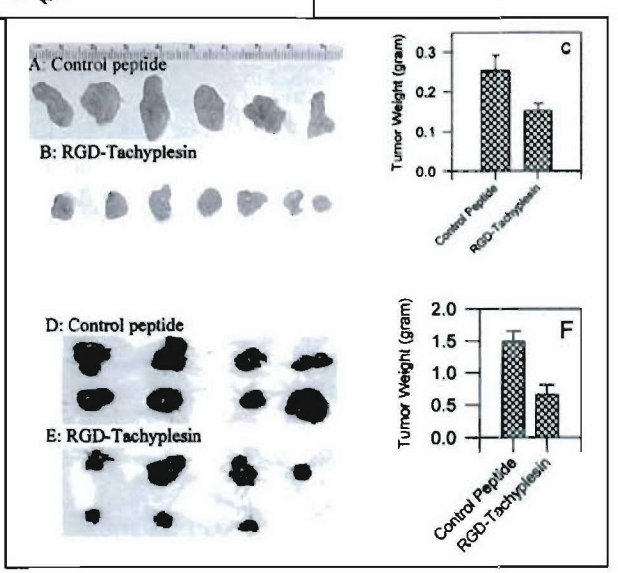

toxic to the mice, as judged by their weights and activity at the end of the experiment. Thus, the results from two models are consistent with each other, indicating that RGD-tachyplesin can inhibit tumor growth *in vivo*.

C. To explore the possible mechanisms by which HABPs exert their anti-tumor effects

1. Effect of HABPs on proliferation and migration of endothelial cells *in vitro* and angiogenesis *in vivo.*

Fig 13 Control HABP 5 ug/ml HABP 50 ug/ml

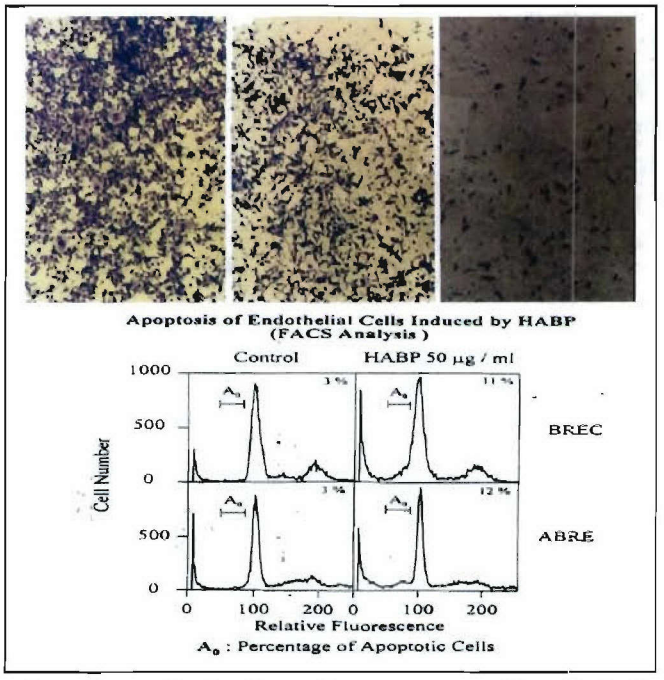

It has been reported that cartilage contains anti-angiogenesis substance that is in part responsible for the anti-tumor effect (1-4, 8-21). To test if our purified cartilage HABP had any effect on endothelial cells, we performed *in vitro* and *in vivo* studies.

First, the different amounts of HABP (5, 50 μg/ml) or heat-inactive HABP or HABP pre-incubated with excess of HA or HA alone (as control) were added to the media of endothelial cells cultured in 24 well plate. On day 2, 4, 6 and 8, the cells were harvested with 10 mM EDTA and the number was counted with Coulter Counter. The result (**Fig. 13 top panel**) showed that the HABP inhibited the growth of endothelial cells in a dose-dependent manner. This effect was abolished when HABP was heat-inactivated or pre-incubated with HA, indicating that the natural structure and the HA binding site are critical for its function of anti-endothelial cells. The cell death is likely due to apoptosis, since the flow cytometer analysis showed (**Fig. 13 bottom panel**) that the apoptotic bodies of two types of endothelium (BREC and ABAE) were increased upon the exposed to HABP.

Secondly, the HABP effect on the migration of endothelial cells was carried out with Boyden Chamber Assay. Aliquots containing 5 x 10^3 cartilage retinal endothelial cells (BREC) in 50 μl media was added to bottom wells of a 48 well Boyden chamber and then covered with a Nucleopore membrane (5 μm pore size) coated with 0.1 mg/ml gelatin. The chamber was assembled and inverted for 2 hours to allow the cells to adhere to the bottom side of membrane and then turned upright. Fifty μl of 50 μg /ml of HABP (as test) or heat-inactivated HABP was added to top wells of chamber and incubated for another 2 hours. Then, the cells on bottom side of the membrane will be carefully wiped off and the cells that have migrated to the top side of the membrane will be stained with Hema 3. The number of cells in 10 random fields will be counted. The result showed that the migration of BREC was greatly inhibited by HABP compared to the heat-inactivated HABP (**Fig. 14A and B**) and the difference was statistically significant (**Fig. 14C**).

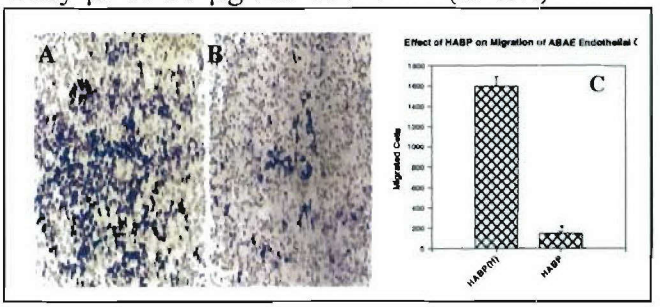

Fig. 14. Migration of endothelium was inhibited by HABP

Fig. 15. Inhibition of angiogenesis in CAM

The effect of HABP on *in vivo* angiogenesis was tested in CAM (chorioallantoic membranes). Filter disks (0.5 cm in diameter) containing 15 ng of VEGF (as stimulator) will be placed on the CAMs of 6 days-old chicken embryo (10 eggs/group). 80 μg /ml of HABP (as test) or heat-inactivated HABP or saline (as controls) was administrated i.v. into the CAM once. On day 4, the filter disks were cut out and fixed in 3.7% formaldehyde. The blood vessels on the filter disks were digitally

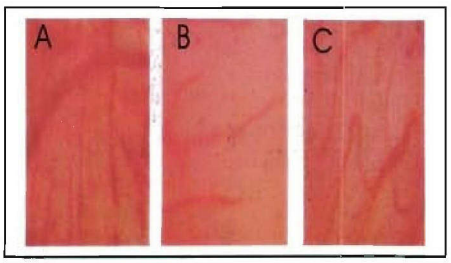

photographed and analyzed with *Optimas 5* program to determine the total vessel length. The result was expressed as vessel length index: total length of each sample/ total area measured. Indeed, the VEGF stimulated angiogenesis was inhibited by HABP (**Fig. 15B**) compared to the groups treated with heat-inactivated HABP (**Fig. 15C**) or saline (**Fig. 15A**). The difference in vessel length index among these groups was statistically significant ($P<0.05$, see attached paper).

2. HABPs alter the integrity of cell membrane

One possible mechanism to kill cancer cells is to alter their integrity of plasma or mitochondrial membrane, which, in turn, induces apoptosis. To examine this, we used JC-1 staining, which measures the membrane potential of mitochondria. As shown in Fig.16 *B* and *C*, treatment with RGD-tachyplesin caused a shift in the fluorescence profile from one that was highly red (Fig. 16*B*) to one that was less red and more green (Fig. 16*C*). This indicated that the membrane potential of mitochondria was changed by treatment with RGD-tachyplesin.

Fig.16. Impairment of integrity of cell membrane by RGD-tachyplesin

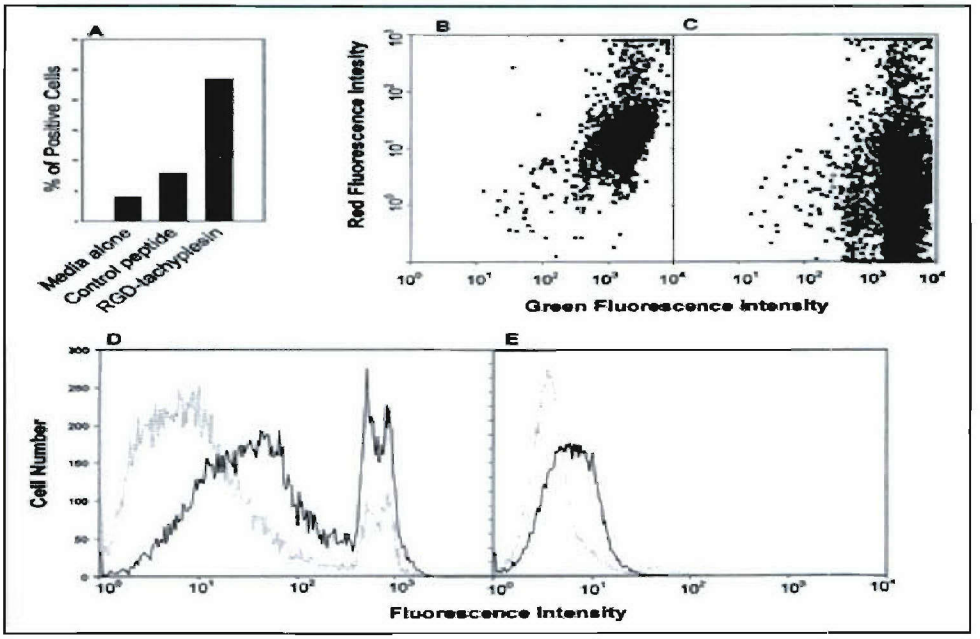

We also examined the integrity of the plasma membrane and nuclear membrane after treatment with the scrambled peptide and RGD-tachyplesin using two different fluorescent markers. YO-PRO-1 dye can only stain the nuclei of cells with damaged plasma and nuclear membranes. Fig. 16*D* shows that treatment with RGD-tachyplesin allowed the YO-PRO-1 dye to pass into the nuclei, causing an increase in the fluorescence intensity. Similar results were obtained when the cells were stained with FITC-dextran, which is not taken up by viable, healthy cells but can pass through the damaged plasma membrane of unhealthy cells. Fig. 16*E* shows that cells treated with RGD-tachyplesin took up a greater amount of FITC-dextran (M_r 40,000) than did those treated with the control peptide. These results indicated that the majority of RGD-tachyplesin-treated cells allowed these big molecules to pass their damaged membranes.

Fig 17 HABP induces apoptosis

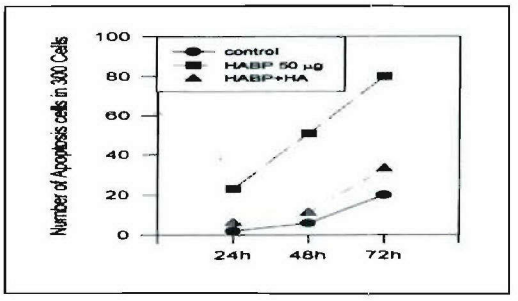

To examine the extent of apoptosis, TSU cells that had been treated for 1 day with the test or control peptides were stained with FITC-annexin and propidium iodide. FITC-annexin V binds to phosphatidylserine, which is exposed on the outer leaflet of the plasma membrane of cells in the initial stages of apoptosis, whereas propidium iodide preferentially stains the nucleus of dead cells, but not living cells. Fig. 16*A* shows that treatment with RGD-tachyplesin induced apoptosis (annexin V positive, propidium iodide negative) in a greater number of cells than did treatment with the vehicle or control peptide. Similarly, when tumor cells were treated with purified HABP, there was an increased apoptotic body as stained with Hochest 33258 (**Fig 17**), which could be abolished by pre-mixture of HABP and HA.

3. HABP triggers apoptosis pathways

Fig 18. HABP triggers apoptosis cascade

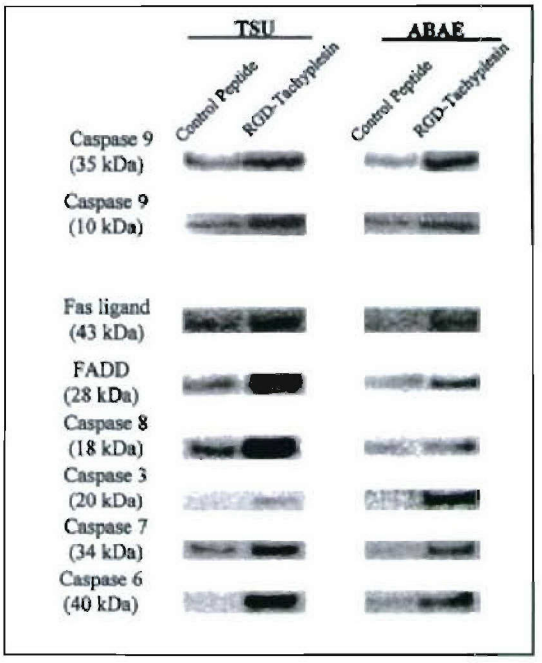

Apoptosis can be induced by two mechanisms: (*a*) the mitochondrial pathway; and (*b*) the death receptor pathway. To identify the nature of the apoptotic pathway triggered by RGD-tachyplesin, both TSU and ABAE cells were treated overnight with RGD-tachyplesin and control peptide and then analyzed by Western blotting for the alterations of molecules involved in the mitochondrial and Fas-dependent pathways. **Fig. 18** shows that treatment of both TSU tumor cells and ABAE cells with RGD-tachyplesin caused the cleavage of M_r 46,000 caspase 9 into subunits of M_r 35,000 and M_r 10,000, indicating activation of the mitochondrial-related, Fas-independent pathway. In addition, RGD-tachyplesin treatment could up-regulate the expression of upstream molecules in the Fas-dependent pathway, including Fas ligand (M_r 43,000), FADD (M_r 28,000), and activate subunits of caspase 8 (M_r 18,000). Furthermore, the downstream effectors, such as caspase 3 subunits (M_r 20,000), caspase 6 (M_r 40,000), and caspase 7 (M_r 34,000), were also up-regulated by RGD-tachyplesin. These results suggest that RGD-tachyplesin induces apoptosis through both the mitochondrial-related, Fas-independent pathway and the Fas-dependent pathway. However, because there is cross-talk between these two pathways, we do not have enough evidence to determine which one is the initiator.

Similar pattern of apoptosis related molecules was found in tumor cells treated with brain HABP (**Fig 19**). In addition, the P53, P16, P27 were up-regulated while bcl-2 and cyclin E were down-regulated. It seems that brain HABP has multiple regulatory functions to impact on several key molecules related with cell cycle and apoptosis.

Fig 19. Brain HABP alters cell cycle and apoptosis molecules

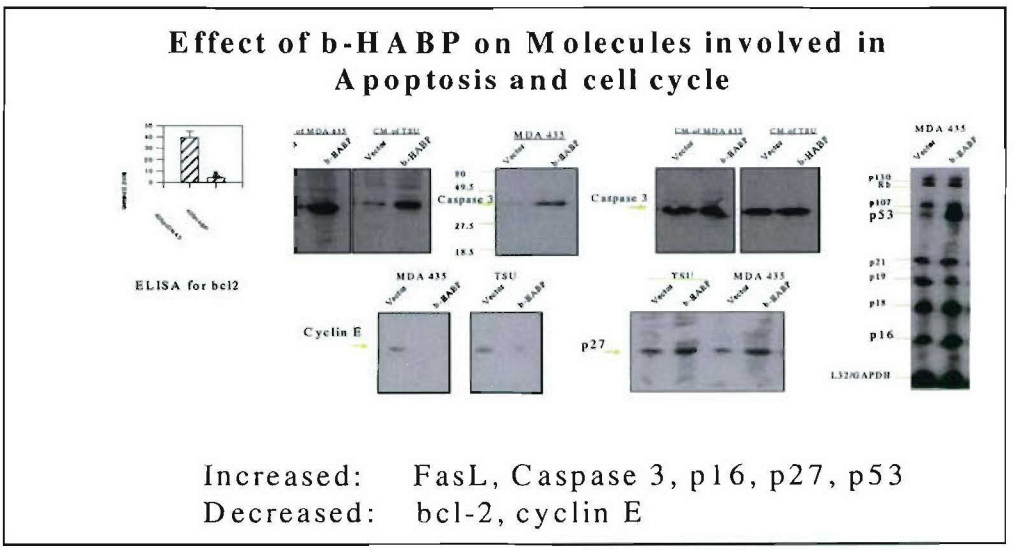

4. HABPs interacts with mitochondria and Bcl-2

Fig 20. P4 targets on mitochondria

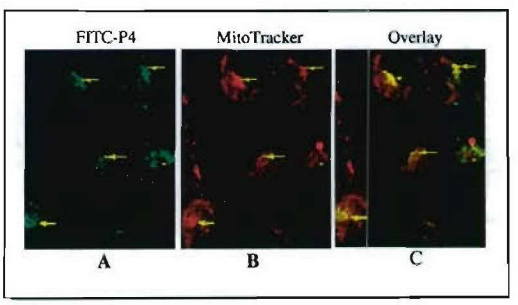

The mitochondria play a central role in regulating apoptosis. To determine if HABPs could target on mitochondria, the FITC labeled P4 was used to stain the cells and MitoTracker (red) was used as land-marker. The imaging obtained from confocal microscope was overlayed and showed that P4 could accumulate in mitochondria (**Fig 20**). Indeed, P4 and several members of the Bcl-2 family interact with the

mitochondria to control its function as well as the apoptotic cascade. Thus, it is possible that HABPs interacts with Bcl-2 or related proteins on the mitochondria. To test this possibility, we examined the binding between P4 and Bcl-2 using an ELISA. For this, immobilized P4 was probed with varying concentrations of purified Bcl-2 followed by an antibody to Bcl-2. As shown in **Figure 21**, the Bcl-2 bound to the P4 in a dose-dependent fashion but demonstrated little or no binding to the random peptide or to wells coated with vehicle alone.

We further examined the interaction between P4 and Bcl-2 by immunoprecipitation. For this, 293T cells were transiently transfected with an expression vector coding for Bcl-2 or Bcl-x_L fused to green fluorescence protein (GFP) or with GFP alone as a control (**Fig. 21*b***, lanes 1-3). The cells were then incubated with biotin-P4, extracted and mixed with streptavidin-Sepharose beads. The bound material was then analyzed by Western blotting using an antibody to GFP. **Figure 21 *b*** shows that P4 could pull down both Bcl-2-GFP and Bcl-x_L-GFP (lanes 5 and 6) but had no effect on GFP alone (lanes 4), indicating that the interaction occurs between Bcl-2/Bcl-x_L and P4. Similar results were obtained with MCF-7 cells transfected with a Bcl-2 expression vector (data not shown).

If P4 exerts its effects by blocking Bcl-2-induced apoptosis, then the overexpression of Bcl-2 should block this process. To test this possibility, MCF-7 cells were transfected with an expression vector for Bcl-2 or an empty vector and then tested for their response to P4 by thymidine incorporation. When the parental MCF-7 cells were treated with P4 overnight, they detached from the substratum, became rounded and condensed, whereas this did not occur with their counterparts treated with the random peptide. However, when the MCF-7 cells that over-expressed Bcl-2 were treated with P4, they were much less susceptible to cell damage compared to the vector transfected cells (46% of Bcl-2 high expressing cells *vs.* 70% of control cells). Thus, excess level of Bcl-2 appears to reduce the toxic effects of P4, which again suggests that Bcl-2 is the target of P4.

Fig. 21. Interaction of P4 with Bcl-2

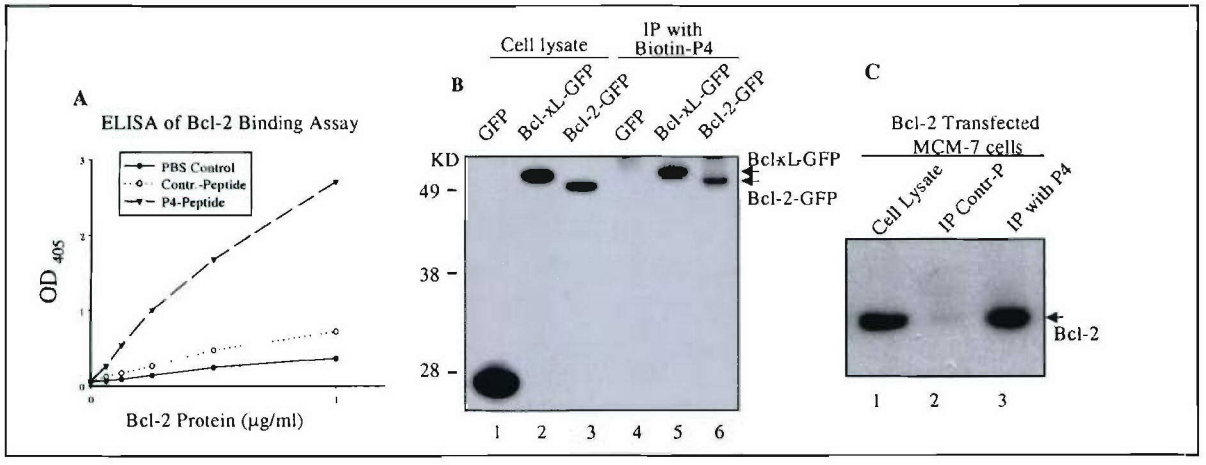

Fig. 22. P4 triggers the release of cytochrome c

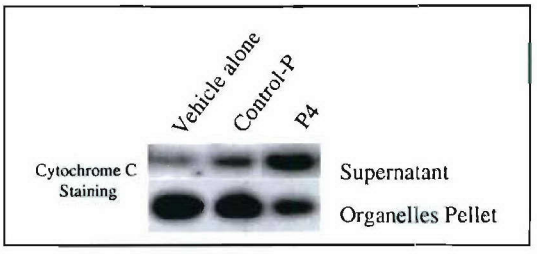

To determine if P4 initiated apoptosis by destabilizing the mitochondria, we performed an *in vitro* assay to detect the release of cytochrome c. A crude preparation of mitochondria was isolated from MDA-435 cells by differential centrifugation and divided into 3 fractions that were treated with vehicle alone, a random peptide and P4, respectively. The 3 samples were centrifuged to separate the pellets containing the particulate fraction from the supernatants containing the soluble components. All of the resulting fractions were then analyzed by Western blotting for cytochrome c. **Figure 22** shows that increased cytochrome c was detected in the supernatant of samples treated with P4 (lane 3) but not in those treated with either the random peptide or vehicle alone (lane 1 and 2).

5. HABPs activate the classic complement pathway to kill tumor cells

To identify the molecule that bind to HABPs, we also took phage display approach. We screened a phage-displayed library of some 1.6 x 10^7 unique clones expressing sequences from cancer cells ranging in size from 300 to 3,000 bp in length fused to the *T7* gene 10 capsid protein. Phage particles expressing tachyplesin-binding proteins/peptides were affinity purified on the wells of a microtiter plate coated with tachyplesin or control peptide. After four or five rounds of biopanning, the number of phages from the tachyplesin-coated plates was ~100-fold greater than that from control peptide plates. Ten plaques were then selected and amplified by PCR. Eight had the same-size PCR products and some of these were then sequenced. The deduced amino acid sequences were then subjected to a blast analysis, which repeatedly identified human C1q. The region of C1q binding to tacyplesin was located around the first 400 bp of complement C1q B chain open reading frame (Genbank accession no. NM_000491), corresponding to the NH_2-terminal collagen-like domain of C1q (31).

Fig 23. Binding of tachyplesin to C1q

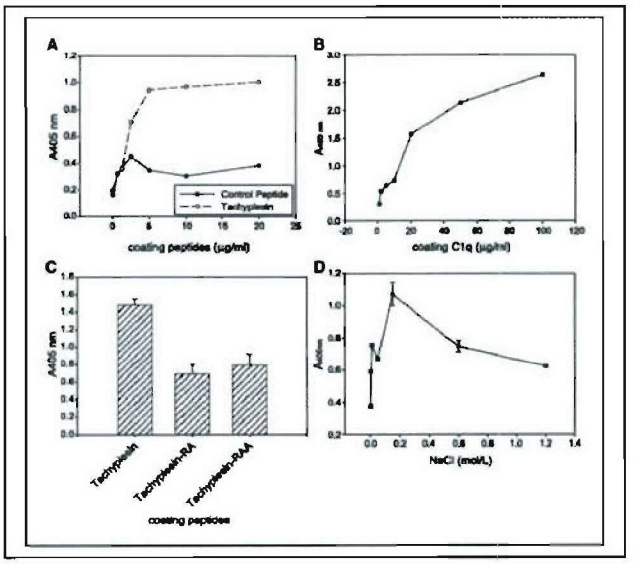

To further test the possibility that tachyplesin indeed binds to C1q, we examined the interaction between these two proteins using an ELISA-like system. In the first assay, plates were coated with tachyplesin or the control peptide, probed with C1q, and then the amount of bound C1q was detected with anti-C1q. As shown in **Fig.23*A***, C1q binds to immobilized tachyplesin in a dose-dependent manner, but not to the control peptide. Similar results were obtained when the plates were precoated with C1q and then probed with biotinylated tachyplesin (**Fig. 23*B***). However, this interaction was significantly reduced if the tachyplesin was denatured by reduction and alkylation of the disulfide bonds and further acetylation of the charged side chains (**Fig. 23*C***), which suggests that the interaction between tachyplesin and C1q depends on the secondary structure of tachyplesin.

The binding of tachyplesin to C1q was also dependent on the NaCl concentration used in the assay buffer (**Fig. 23*D***). The maximum binding occurred at 0.15 mol/L NaCl, the normal physiologic salt concentration. Both increasing and decreasing the ionic strength in the assay drastically reduced the binding.

Fig 24. binding of tachyplesin to serum C1q

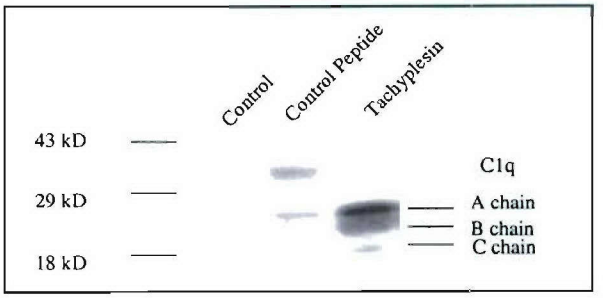

The interaction between tachyplesin and C1q was further examined by affinity precipitation and Western blotting of normal human serum. For this, a biotinylated tachyplesin was incubated with normal human serum, followed by streptavidin-Sepharose. The immobilized proteins were then eluted and analyzed by Western blotting. As shown in **Fig. 24**, probing the blot with a polyclonal antibody revealed three bands corresponding to three chains of the C1q complex (*A*: 27.5 kDa, *B*: 25.2 kDa, and *C*: 23.8 kDa, respectively) in the tachyplesin-treated sample, but not in the samples without the peptide or with the control peptide. Not surprisingly, only a small portion of C1q from the serum was pulled down because serum contains a relatively high concentration of this protein (80 μg/mL; ref. 32). Taken together, these results suggests that C1q binds to both immobilized (surface-bound) and free (liquid-phase) tachyplesin, and tachyplesin binds to both purified and serum C1q, which confirms that there is true interaction between these two molecules.

Fig 25. tachyplesin could activate the complement pathway

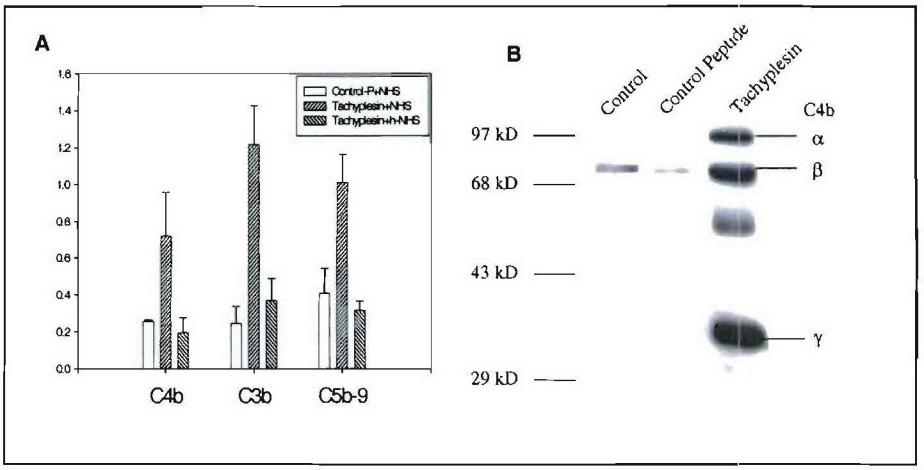

To determine if tachyplesin could activate the complement pathway, we used ELISAs with tachyplesin-coated microplates. Normal serum was diluted with VBS (containing Ca^{2+}) and applied to wells coated with tachyplesin or the control peptide, washed, and then probed with antibodies against C4, C3, and C5b-9. As shown in **Fig. 25*A***, significant amounts of activated fragments of C4b, C3b, and C5b-9 complex were bound to the immobilized tachyplesin but not to the immobilized control peptide. Furthermore, when the same fresh serum was heat-inactivated (56°C, 30 minutes) before use, then the amount of C4b, C3b, and C5b-9 complex was greatly reduced. These results show that tachyplesin is able to trigger the activation of whole classic complement cascade, which is characterized by the appearance of C4b, C3b, and C5b-9 complex.

To further test for the presence of activated C4b fragments, Western blotting was done. For this, normal fresh human serum was mixed with the biotinylated tachyplesin or control peptide, affinity-precipitated with streptavidin-Sepharose, and then subjected to SDS-PAGE and Western blotting using antibodies to C4. **Figure 25*B*** shows that the three peptide chains of C4b (α 97 kDa, ß 75 kDa, and γ33 kDa, respectively) were affinity-precipitated in the tachyplesin-treated sample, but not in those treated with the control peptide or in the absence of peptide. This is consistent with the results obtained from ELISA and further supports the conclusion that tachyplesin can activate the classic complement cascade. Whereas it is possible that tachyplesin binds directly to C4b, the phage display results suggest that this is not the case. Tachyplesin seems to initially and mainly bind to C1q and then to C4b.

Fig 26. HA-mediated attachment of tachyplesin to TSU tumor cells

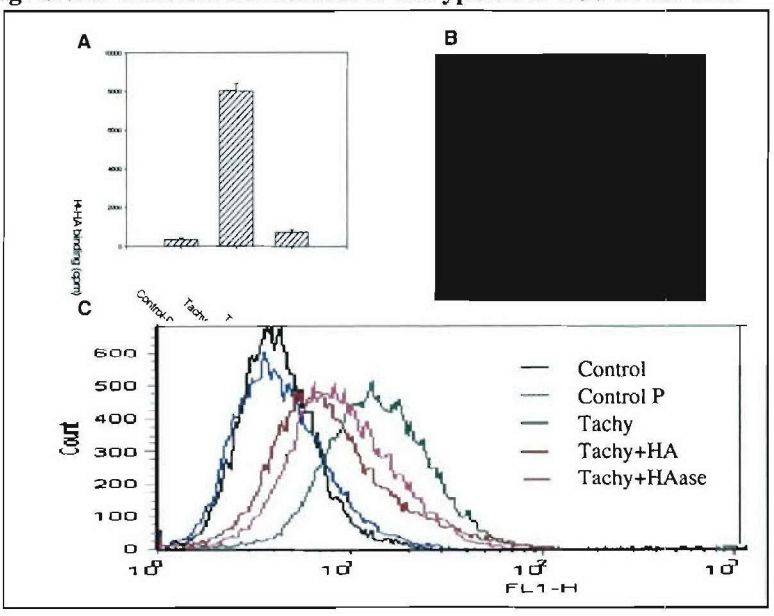

Because tachyplesin contains a hyaluronan-binding motif $[B(X)_7B]$, we investigated the possibility that tachyplesin can bind to hyaluronan (both free and cell associated). We took advantage of the fact that hyaluronan by itself does not bind to nitrocellulose but will do so in the presence proteins or peptides that bind to it (33). In the assay, tachyplesin was mixed with [^{3}H]hyaluronan and then applied to a nitrocellulose membrane. The free [^{3}H]hyaluronan was washed away and the complex of [^{3}H]hyaluronan-tachyplesin retained on the filter membrane was analyzed. **Figure 26*A*** shows that tachyplesin binds strongly to hyaluronan and this could be abolished by a 100-fold excess of unlabeled hyaluronan. In contrast, the control peptide showed little or no binding to [^{3}H]hyaluronan, indicating that the binding of tachyplesin to hyaluronan was specific.

We then examined the binding of FITC-tachyplesin to TSU cells that express large amounts of hyaluronan on their surfaces (34, 35). As shown in **Fig. 26*B***, tachyplesin was distributed on the surface of the cells. This binding was significantly reduced by the addition of an excess of free hyaluronan on pretreatment

with hyaluronidase (**Fig. 26*C***) as shown by flow cytometry analysis. These results suggest that hyaluronan or related molecules, such as chondroitin sulfate (36), act as targets for tachyplesin on the cell surface.

Fig 27. Effect of tachyplesin on induction of complement on the cell surfaces

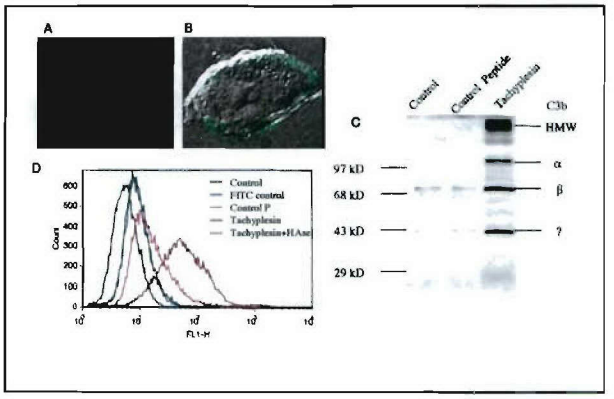

In the classic pathway of complement activation, 4- to 5-fold more C3b than C4b is deposited on the surfaces of target cells (37). In addition, C3 contains a thioester moiety that can form covalent bonds with nearby molecules in the transition from C3 to C3b. Thus, C3b deposition represents an index of complement activation. For this reason, we tested whether tachyplesin could induce the deposition of C3b on tumor cells. TSU cells were incubated in a mixture of normal serum and tachyplesin, stained with antibodies to C3, then examined by confocal microscopy. As shown in **Fig. 27*A* and *B***, C3b was indeed deposited on the surfaces of TSU cells.

The presence of activated C3b was also shown by Western blotting of TSU cells following treatment with serum and tachyplesin. **Figure 27*C*** shows that in the samples treated with tachyplesin, two subunits of C3b (α 115 kDa and ß 75 kDa) and possibly degraded iC3b (? band for α1). Significantly, a high molecular weight band (*HMW* in **Fig. 27*C***) was found with Western blotting under reducing conditions, indicating a covalent linkage to large membrane constituents. Scans of these Western blots revealed that the majority of deposited C3b (70-80%) was present in this high molecular weight form. This is consistent with the fact that in the transition from C3 to C3b, a thioester moiety, can form covalent bonds with nearby molecules. FACS analysis of cells treated with tachyplesin and serum (**Fig. 27*D***) showed that there was a significant increase in FITC-tagged antibody to C3, indicating that C3b was deposited on the tumor cells, which did not occur with cells treated with the control peptide. These results are consistent with those from confocal microscopy and Western blotting.

Fig 28. Effect of HAase on tachyplesin function.

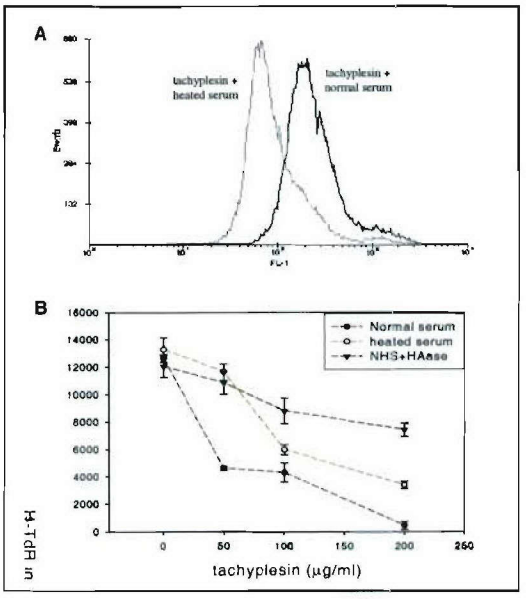

Because tachyplesin can bind to hyaluronan, we investigated the possibility that membrane-bound hyaluronan plays a role the binding of tachyplesin-mediated activation of complement on the surface of tumor cells. Suspensions of TSU cells were pretreated with hyaluronidase before the addition of tachyplesin and human serum; the presence of C3b was detected by immunostaining followed by FACS analysis. As shown in **Fig. 27*D***, hyaluronidase pretreatment markedly reduced the intensity of fluorescence, indicating a reduction in C3b deposition. Thus, hyaluronan or related glycosaminoglycans seems to play a key role in the activation of complement on the cell surface by tachyplesin.

The complement membrane attack complex (MAC, C5b-9) can damage the cell membrane, which results in the killing of the target cells. The possibility that tachyplesin can trigger the deposition of complement and the formation of C5b-9 on the surfaces of tumor cells via the classic pathway suggests that it might kill cells by disrupting the integrity of the plasma membrane. To test this possibility, we examined the permeability of cell membrane with macromolecule FITC-dextran, which is excluded by the membranes of viable, healthy cells but can pass through the damaged plasma membrane of unhealthy cells. **Figure 28*A*** showed that when cells were treated with tachyplesin and human serum, the fluorescence spectrum shifted, indicating that more FITC-dextran had passed through the plasma membrane and entered the cytoplasm. Thus, it seems that treatment with

tachyplesin disrupted the cell membrane and increased its permeability.

Fig 29. Tachyplesin induced death via activated complement

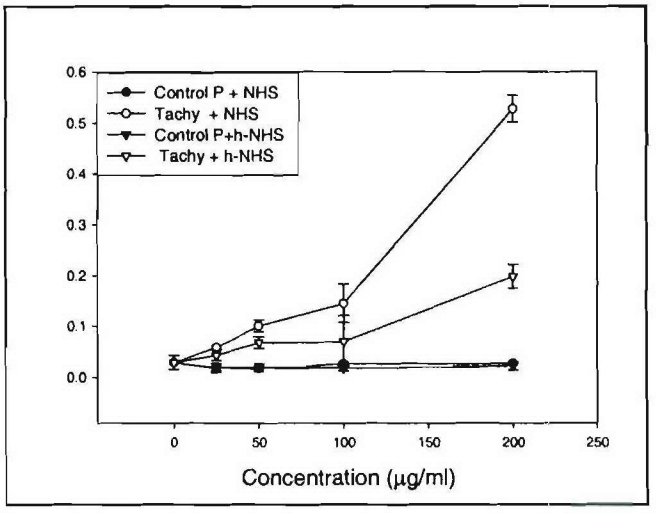

Finally, we examined the effect of tachyplesin and normal human serum on tumor cell proliferation as measured by thymidine incorporation and cell death as measured by trypan blue uptake. As indicated in **Figs. 28*B* and 29**, TSU cells treated with tachyplesin in the presence of complete human serum showed a marked inhibition of proliferation and an increased extent of cell death. **Figure 28*B*** also showed that treatment with hyaluronidase significantly reversed the effects, again suggesting that cell-surface hyaluronan plays a critical role in tachyplesin-induced inhibition of tumor cell growth. Significantly, heat-inactivated serum also attenuated the effects of tachyplesin, but to a lesser extent than hyaluronidase treatment. These results imply that tachyplesin may have multiple effects on the cells leading to both growth arrest and death.

Taken together, the members in HABPs family seem to utilize multiple mechanisms to exert their anti-tumor effect. Among these action points, there may be a initial target that HABPs have a high affinity to it, which needs to be further investigated.

This study reveals that several HABPs from different sources have the anti-tumor effect. Although their action mechanism is still not well elucidated, they still have potential to be developed as new anti-tumor agent due to non-toxicity and easy to make a large quantity.

Key Research Accomplishments

In this grant support period, we demonstrated that: **1)** HABPs could be obtained via different approaches, such as affinity purification, genetic expression and chemical synthesis; **2)** HABPs from different sources exerted anti-cancer effect without obvious side-effect, indicating that anti-tumor effect is a universal property of members in HABPs family; **3)** HABPs could inhibit the tumor angiogenesis; **4)** some HABPs could bind to Bcl-2, promote the release of cytochrome c and trigger apoptosis of tumor cells; **5)** some HABPs could activate the classic complement pathway to kill tumor cells.

The results reveal that HABPs, a set of naturally existing biological agents is likely to be a new category of anti-tumor agent via triggering intrinsic death pathways.

We believe that study of functional domain of HABPs may lead to discover new anti-tumor agent that can be synthesized in a large quantity and safe for use in cancer treatment.

Reportable Outcomes

Publications during the grant support period

(Due to or partially due to this grant support;
papers or abstracts marked ** are scientifically related with this grant)

Original papers

1. Zeqiu Han, Jian Ni, Patrick Smits, Charles B. Underhill, Bin Xie, Ningfei Liu, Przemko Tylzanowski, David Parmelee, Ping Feng, Ivan Ding, Feng Gao, Reiner Gentz, Danny Huylebroeck, Jozef Merregaert and Lurong Zhang : **Extracellular matrix protein 1(ECM1): a novel angiogenic factor expressed in breast cancer cells.** FASEB J: 2001; 988-994

2. Ningfei Liu, Charles B. Underhill, Randall Lapevich , Zeqiu Han, Feng Gao, Lurong Zhang and Shawn Green: **Metastatin: A hyaluronan binding complex from cartilage that inhibits tumor growth.** Cancer Res 2001; 61:1022-1028

3. **Yixin Chen, XueMing Xu, Shuigen Hong, Jinguo Chen, Ningfei Liu, Charles B. Underhill, Karen Creswell and Lurong Zhang: **RGD-Tachyplesin inhibits tumor growth.** Cancer Res. 2001; 61: 2434-2438

4. Ningfei Liu, Feng Gao, Zeqiu Han, Charles B. Underhill and Lurong Zhang: **Over-expression of Human Hyaluronan Synthase 3 in TSU Prostate Cancer Cells Promotes Tumor Growth**. Cancer Res.2001, 61: 5207-5214

5. Hamada T, McLean WH, Ramsay M, Ashton GH, Nanda A, Jenkins T, Edelstein I, South AP, Bleck O, Wessagowit V, Mallipeddi R, Orchard GE, Wan H, Dopping-Hepenstal PJ, Mellerio JE, Whittock NV, Munro CS, van Steensel MA, Steijlen PM, Ni J, Zhang L, Hashimoto T, Eady RA, McGrath JA.: **Lipoid proteinosis maps to 1q21 and is caused by mutations in the extracellular matrix protein 1 gene (ECM1).** Hum Mol Genet 2002; 11(7): 833-840

6. Liu N, Shao L, Xu X, Chen J, Song H, He Q, Lin Z, Zhang L, Underhill CB.: **Hyaluronan metabolism in rat tail skin following blockage of the lymphatic circulation**. Lymphology 2002; 35 (1):15-22

7. Gao F, Zhang L, Underhill CB.: **Promotion of growth of human breast cancer cells MDA231 by human sperm membrane-bound hyaluronidase: an experimental study**. Zhonghua Yi Xue Za Zhi. 2002; 82(3):207-10

8. Shanmin Yang, Jinguo Chen, Zhen Guo, Xue-Ming Xu, Luping Wang, Xu-Fang Pei, Jing Yang Charles B. Underhill and Lurong Zhang **Triptolide Inhibits the Growth and Metastasis of Solid Tumors**. Mol Cancer Ther. 2003; 2(1):65-72.

9. Okunieff P, Fenton BM, Zhang L, Kern FG, Wu T, Greg JR, Ding I. **Fibroblast growth factors (FGFS) increase breast tumor growth rate, metastases, blood flow, and oxygenation without significant change in vascular density**. Adv Exp Med Biol. 2003; 530:593-601.

10. Okunieff P, Ding I, Liu W, Fenton B, Zhang L, Cheng S. **FGF1 not VEGF transfection induces in-vitro radiation resistance, in-vivo radiation modifying effects of angiogenic peptides probably relate more to vascularity than apoptosis.** Int J Radiat Oncol Biol Phys. 2003;57(2):S318

11. Luping Wang, Jiyao Yu, Jian Ni, Xue-Ming Xu, Jianjin Wang, Haoyong Ning, Xu-Fang Pei, Jinguo Chen, Shanmin Yang, Charles B. Underhill, Lei Liu, Joeri Liekens, Joseph Merregaert and Lurong Zhang: **Extracellular Matrix Protein1 (ECM1) is Over-expressed in Malignant Epithelial Tumors.** Cancer Lett. 2003; 200(1):57-67.

12. **Xue-Ming Xu, Yixin Chen, Feng Gao, Jinguo Chen, Shanmin Yang, Charles B. Underhill and Lurong Zhang: **A Peptide with Three Hyaluronan Binding Motifs Inhibits Tumor Growth by Inducing Apoptosis**. Cancer Res. 2003; 63(18):5685-90.

13. **Ninfei Liu, Xue-Ming Xu, Jinguo Chen, Luping Wang, Shanmin Yang, Charles B. Underhill, and Lurong Zhang: **A Hyaluronan-Binding Peptide Can Inhibit Tumor Growth by Interacting with Bcl-2**. International Journal of Cancer 2004; 109 : 49-57

14. Chen J, Zhang L and Kim S: **Quantification and detection of DcR3, a decoy receptor in TNFR family**. Journal of Immunological Methods 2004; 285(1):63-70.

15. Wang L, Xu X, Ning H, Yang S, Chen J, Yu J, Ding H, Underhill CB, Zhang L.: **Expression of PH20 in primary and metastatic breast cancer and its pathological significance**. Zhonghua Bing Li Xue Za Zhi. 2004;33(4):320-3.

16. Kim S, McAuliffe W, Zaritskaya L, Zhang L, and Nardelli, B: **Selective induction of TR6/DcR3 release by bacterial antigens in human monocytes and a dendritic cell subset**. Infection and Immunity 2004; 72(1):89-93.

17. Wang H, MaoY, Ju L, Zhang J, Liu Z, Zhou X, Li Q, Wang Y, Kim S, Zhang L: **Detection and Monitoring of SARS-Coronavirus in the Plasma and Peripheral Blood Lymphocytes of Patients with Severe Acute Respiratory Syndrome.** Clinical Chemistry 2004; 50 (7): 1237-40.

18. ** Jinguo Chen, Xue-Ming Xu, Charles B. Underhill, Shanming Yang, Luping Wang, Yixin Chen, Shuigen Hong, Karen Creswell, Lurong Zhang: **Tachyplesin Activates the Classical Complement Pathway to Kill Tumor Cells.** Cancer Res. 2005; 65(11):4614-22.

19. Huixiang Li, Lurong Zhang, Hong Lou, Ivan Ding, Jiaoti Huang, P. Anthony di Sant'Agnese, Jun-Yi Lei: **Over-expression of decoy receptor 3 in precancerous lesion and adenocarcinoma of the esophagus.** Am. J Clinical Pathology 2005, 124 (2):282-7

20. Kim S, Zhang L: **Identification of naturally secreted soluble form of TL1A, a TNF-like cytokine**. J Immunol Methods. 2005;298(1-2):1-8.

Meeting abstracts

(marked ** are scientifically related with this grant)

1. ** Xue-Ming Xu, Yixin Chen[1], Ningfei Liu, Jinguo Chen, Feng Gao, Zequi Han, Charles B. Underhill and Lurong Zhang. **Targeted peptide of human brain hyaluronan binding protein inhibits tumor growth.** Proc. Annu. Meet. Am. Assoc. Cancer Res 2001; 42: 71:383

2. ** Feng Gao, Xue-Ming Xu, Charles B. Underhill, Shimin Zhang, Ningfei Liu, Zeqiu Han, Jiaying Zhang and Lurong Zhang. **Human brain hyaluronan binding protein inhibits tumor growth via induction of apoptosis.** Proc. Annu. Meet. Am. Assoc. Cancer Res 2001; 42: 815:4375

3. ** Ningfei Liu, Xue-Ming Xu, Charles B. Underhill, Susette Mueller, Karen Creswell, Yixin Chen, Jinguo Chen and Lurong Zhang. **Inhibition of tumor growth by hyaluronan binding motifs (P4) is mediated by apoptosis pathway related with lysosome and mitochondria.** Proc. Annu. Meet. Am. Assoc. Cancer Res 2001; 42: 644: 3465

4. ** Ningfei Liu, Xue-Ming Xu, Charles B. Underhill, Yixin Chen, Jinguo Chen, Feng Gao, Zeqiu Han and Lurong Zhang. **Hyaluronan binding motifs inhibit tumor growth**. Proc. Annu. Meet. Am. Assoc. Cancer Res 2001; 42: 71:382

5. ** Yixin Chen, Xue-Ming Xu, Jinguo Chen, Ningfei Liu, Charles B. Underhill, Karen Creswell, and Lurong Zhang. **Anti-tumor effect of RGD-tachyplesin**. Proc. Annu. Meet. Am. Assoc. Cancer Res 2001; 42: 69: 369

6. ** Jinguo Chen, Yixin Chen, Shuigen Hong, Fabio Leonessa, Robert Clake, Xue-Ming Xu, Ningfei Liu, Charles B. Underhill, Karen Creswell and Lurong Zhang. **Effect of tachyplesin on MDR overexpressing tumor cells.** Proc. Annu. Meet. Am. Assoc. Cancer Res 2001; 42: 812:4358

7. ** Xue-Ming Xu, Jinguo Chen, Luping Wang, Xu-Fang Pei, Shanmin Yang, Charles B. Underhill and Lurong Zhang: **Peptides derived endostatin and angiostatin inhibits tumor growth**. Proc. Annu. Meet. Am. Assoc. Cancer Res 2002; 43:1084:5364

8. Luping Wang, Jianjin Wang, Jiyao Yu, Haoyong Ning, Xu-Fang Pei, Jinguo Chen, Xue-Ming Xu, Shanmin Yang, Charles B. Underhill, Lei Liu and Lurong Zhang: **Expression pattern of ECM1 in human tumors**. Proc. Annu. Meet. Am. Assoc. Cancer Res 2002; 43: 729: 3618

9. ** Luping Wang, Xu-Fang Pei, Jinguo Chen, Xue-Ming Xu, Shanmin Yang, Ningfei Liu, Charles B. Underhill and Lurong Zhang: **A peptide derived from hemopexin-like domain of MMP9 exerts anti-tumor effect**. Proc. Annu. Meet. Am. Assoc. Cancer Res 2002; 43: 159:794

10. Shanmin Yang, Jinguo Chen, Xue-Ming Xu, Luping Wang, Shimin Zhang, Xu-Fang Pei, Jing Yang, Charles B. Underhill and Lurong Zhang: **Triptolide, a potent anti-tumor/metastasis agent.** Proc. Annu. Meet. Am. Assoc. Cancer Res 2002; 43: 854: 4233

11. ** Yixin Chen, Shuigen Hong, Ningfei Liu, Xu-Fang Pei, Luping Wang, Shanmin Yang[1], Xue-Ming Xu, Jinguo Chen, Charles B. Underhill and Lurong Zhang: **Targeted hyaluronan binding peptide inhibits the growth of ST88-14 Schwann cells.** Proc. Annu. Meet. Am. Assoc. Cancer Res 2002; 43: 888:4404

12. Ku-chuan Hsiao, Shanmin Yang, Jinguo Chen, Xue-Ming Xu, Luping Wang, Jing Yang, Charles B. Underhill and Lurong Zhang. **A peptide antagonist of Fas acts as strong stimulus for cell proliferation**. Proc. Annu. Meet. Am. Assoc. Cancer Res 2002; 43: 706:3502

13. ** Jinguo Chen, Xueming Xu, Shanmin Yang, Luping Wang, Charles B. Underhill, Lurong Zhang: **Over-expression of tumor necrosis factor-stimulated gene-6 protein (TSG-6) suppresses tumor growth *in vivo*.** Proc. Annu. Meet. Am. Assoc. Cancer Res 2002; 43: 799:3962

14. Jinguo Chen, Glenn D. Prestwich, Yi Luo, Xueming Xu, Shanmin Yang, Luping Wang, Charles B. Underhill and Lurong Zhang.: **Inhibition of tumor growth and metastasis by hyaluronan conjugated Taxol**. Proc. Annu. Meet. Am. Assoc. Cancer Res 2003; 44:1654

15. Luping Wang, Sunghee Kim, Jinguo Chen, Xue-Ming Xu, Shanmin Yang, Charles B. Underhill, and Lurong Zhang: **Decoy TR6 (DcR3) protects tumor cells from apoptosis**. Proc. Annu. Meet. Am. Assoc. Cancer Res 2003; 44: 149

16. ** Xue-Ming Xu, Ningfei Liu, Jinguo Chen, Luping Wang, Shanmin Yang, Charles B. Underhill, and Lurong Zhang. **A Hyaluronan Binding Peptide Triggers Apoptosis by Antagonizing Members of the Bcl-2 Family**. Proc. Annu. Meet. Am. Assoc. Cancer Res 2003; 44: 5589

17. Shanmin Yang, Jinguo Chen, Xue-Ming Xu, Luping Wang, Charles B. Underhill and Lurong Zhang. **Liposomal Triptolide inhibits tumor growth at a low dose.** Proc. Annu. Meet. Am. Assoc. Cancer Res 2003; 44: 6461

18. Weimin Liu, Ivan Ding, Keqiang Chen, John Olschowka, Lurong Zhang and Paul Okunieff: **Elevation of IL-1β and matrix metalloproteinases (MMPs) in radiation induced mouse dermatitis and fibrosis**. Proc. Annu. Meet. Am. Assoc. Cancer Res. 2004; 3119

19. Lurong Zhang, Weimin Liu, Xiaoqi Gong, Jian Wang, Dading Fu, Yuanying Jiang, Ivan Ding and Okunieff Paul, **Elevation of Hyaluronan After Radiation *in Vitro* and *in Vivo***. Proc. Annu. Meet. Am. Assoc. Cancer Res. 2004; 335

20. Paul Okunieff, Weimin Liu, Jainhua Xu, Keqiang Chen, Lurong Zhang and Ivan Ding: **Effect of Cytokines on radiation induced cutaneous toxicity in mice**. Proc. Annu. Meet. Am. Assoc. Cancer Res. 2004; 3117

21. Lurong Zhang, Shanmin Yang, Luping Wang, Weimin Liu and Sunghee Kim: **Regulation of DcR3 in cancer cells by modulators of protein kinase C**. Proc. Annu. Meet. Am. Assoc. Cancer Res. 2004; 3395

22. Luping Wang, Feng Gao, Zeqiu Han, Shanmin Yang, Jinguo Chen, Charles B. Underhill and Lurong Zhang. **Alterations of hyaluronan and hyaluronidase induced by Hypoxia**. Proc. Annu. Meet. Am. Assoc. Cancer Res. 2004; 3587

23. ** Jinguo Chen, Xue-Ming Xu, Charles B. Underhill, Shanming Yang, Karen Creswell and Lurong Zhang: **Tachyplesin can kill tumor cells by activation of the classical complement pathway**. Proc. Annu. Meet. Am. Assoc. Cancer Res. 2004; 4375

24. Shanmin Yang, Jinguo Chen, Charles B. Underhill, Sunghee Kim, Luping Wang, Xu-Ming Xu and Lurong Zhang: **Effect of Triptolide on the Telomerase Activity in Human Cancer Cells**. Proc. Annu. Meet. Am. Assoc. Cancer Res. 2004, 993

25. Sunghee Kim, Shanmin Yang, Weimin Liu, Xue-Ming Xu and Lurong Zhang: **Transcriptional regulation of DcR3 in colon cancer cells.** Proc. Annu. Meet. Am. Assoc. Cancer Res. 2004, 3342

26. Shanmin Yang, Luping Wang, Jinguo Chen, Xue-Ming Xu, Sunghee Kim, Charles B. Underhill and Lurong Zhang: **Radiation-sensitizing effect of DcR3 siRNA on human colon cancer SW480 cells.** Proc. Annu. Meet. Am. Assoc. Cancer Res. 2004; 4151

27. Ross JS, Sheehan CE, Kallakury BVS, Azumi N, Kim S,Yang S, Zhang L: **Immunohistochemical expression of decoy receptor DcR3 in human colorectal and ovarian carcinomas.** Proc. Annu. Meet. Am. Assoc. Cancer Res. 2004; 3362

28. Zhenyu Xiao, Ying Su, Shanmin Yang, Ivan Ding, Shimin Zhang, Lurong Zhang and Paul Okunieff. **Esculentoside A Ameliorates Soft Tissue Toxicity Following Ionizing Radiation**. Proc. Annu. Meet. Am. Assoc. Cancer Res. 2005:

29. Ying Su, Sunghee kim, Shanmin Yang, Zhenyu Xiao, Peter Keng, Ivan Ding, Paul Okunieff and Lurong Zhang. **DcR3 regulation and its effect on radiation treatment.** Proc. Annu. Meet. Am. Assoc. Cancer Res. 2005:

30. Shanmin Yang, Zhenyu Xiao, Ying Su, Bruce Fenton, Ivan Ding, Paul Okunieff and Lurong Zhang. **Tritolide is a Breast Cancer Radiosensitizer**. Proc. Annu. Meet. Am. Assoc. Cancer Res. 2005:

Conclusions

- HA-Sepharose 4B affinity column is a good method to purify bioactive form of HABP with little endotoxin contamination.
- HABPs can be genetically expressed and modified.
- HABPs can be chemically synthesized in a large quantity with modification of functional HA binding domain ($B[X_7]B$) and targeting domain (RGD).
- HABPs can inhibit the anchorage-dependent and independent growth of tumor cells *in vitro*.
- HABPs can reduce the growth of TSU prostate cancer and other tumor *in vivo*.
- HABPs can inhibit the experimental metastasis.
- HABPs can inhibit the proliferation and migration of endothelial cells *in vitro* and angiogenesis *in vivo*.
- HABPs interact with Bcl-2, promote the release of cytochrome c and trigger apoptosis of tumor cells.
- HABPs activate the classic complement pathway to kill tumor cells.

References

1. Moses, M A, Sudhalter, J., and Langer, R.: Identification of an inhibitor of neovascularization from cartilage. Science 1990; 248: 1408-1410
2. Moses, M A, Sudhalter, J., and Langer, R.: Isolation and characterization of an inhibitor of neovascularization from scapular chondrocytes. J. Cell Biol. 1992: 119 (2):473-482
3. Sy, M-S., Guo, Y. J., and Stamenkovic, I.: Inhibition of tumor growth in vivo with a soluble CD44-immunoglobulin fusion protein. J. Exp. Med. 1992; 176: 623-627
4. Langer R. Brem H. Falterman K. Klein M. Folkman J. Isolations of a cartilage factor that inhibits tumor neovascularization. Science; 1976. 193(4247):70-2
5. O'Reilly MS. Boehm T. Shing Y. Fukai N. Vasios G. Lane WS. Flynn E. Birkhead JR. Olsen BR. Folkman J.: Endostatin: an endogenous inhibitor of angiogenesis and tumor growth. Cell 1997; 88(2):277-85
6. Sasaki T. Fukai N. Mann K. Gohring W. Olsen BR. Timpl R. Structure, function and tissue forms of the C-terminal globular domain of collagen XVIII containing the angiogenesis inhibitor endostatin. EMBO Journal 1998; 17(15):4249-56
7. Zetter BR. Angiogenesis and tumor metastasis. Annual Review of Medicine 1998; 49:407-24
8. Hohenester E. Sasaki T. Olsen BR. Timpl R.: Crystal structure of the angiogenesis inhibitor endostatin at 1.5 A resolution. EMBO Journal 1998; 17(6):1656-64
9. Horsman MR, et al: The effect of shark cartilage extracts on the growth and metastatic spread of the SCCVII carcinoma. Acta Oncol. 1998; 37(5): 441-5.

10. Miller DR, et al: Phase I/II trial of the safety and efficacy of shark cartilage in the treatment of advanced cancer. J Clin Oncol. 1998; 16(11):3649-55
11. Simone CB, et al: Shark cartilage for cancer. Lancet. 1998; 9; 351(9113): 1440.
12. Newman V, et al: Dietary supplement use by women at risk for breast cancer recurrence. The Women's Healthy Eating and Living Study Group. J Am Diet Assoc. 1998; 98(3): 285-92.
13. Ernst E: Shark cartilage for cancer? Lancet. 1998; 24; 351(9098): 298.
14. Markman M: Shark cartilage: the Laetrile of the 1990s. Cleve Clin J Med. 1996; 63(3): 179-80.
15. Hunt TJ, et al: Shark cartilage for cancer treatment. Am J Health Syst Pharm. 1995; 52(16): 1756, 1760.
16. Blackadar CB: Skeptics of oral administration of shark cartilage. J Natl Cancer Inst. 1993; 85(23): 1961-2.
17. Mathews J: Media feeds frenzy over shark cartilage as cancer treatment. J Natl Cancer Inst. 1993; 4; 85(15): 1190-1.
18. Oikawa T, et al: A novel angiogenic inhibitor derived from Japanese shark cartilage (I). Extraction and estimation of inhibitory activities toward tumor and embryonic angiogenesis.Cancer Lett. 1990;51(3):181-6.
19. Lee A, et al: Shark cartilage contains inhibitors of tumor angiogenesis. Science. 1983; 221 (4616):1185-7.
20. Langer R. Brem H. Falterman K. Klein M. Folkman J. Isolations of a cartilage factor that inhibits tumor neovascularization. Science; 1976. 193(4247):70-2
21. Couzin J.: Beefed-up NIH center probes unconventional therapies. Science. 1998 Dec 18; 282(5397):2175-6
22. Laurent ,T. C. (1987): Biochemistry of hyaluronan. Acta Otolaryngol; 442: 7-24
23. Schwatz, N. B. : Proteoglycans. In Devlin, T. M. ed (1992) Textbook of biochemistry with clinical correlations. A John wiley & Sons , Inc., New York 378-379
24. Laurent, T. C. (1970) Structure of hgyaluronic acid. In Balazs EA.ed. Chemistry and molecular biology of the intercellular matrix. London: Academic Press. 703-732
25. Roden, L. (1980) Structure and metabolism of connective tissue proteoglycans. In: Lennarz, W. J. ed. The biochemistry of glycoprotein and proteoglycans. New York: Plenum Publ. 267-371
26. Tengblad A.: Affinity chromatography on immobilized hyaluronate and its application to the isolation of hyaluronate binding properties from cartilage. Biochimica et Biophysica Acta. 578(2):281-9, 1979
27. Tengblad A: A comparative study of the binding of cartilage link protein and the hyaluronate-binding region of the cartilage proteoglycan to hyaluronate-substituted Sepharose gel. Biochimica et Biophysica Acta. 578(2):281-9, 1979
28. Brooks PC, Silletti S, von Schalscha TL, Friedlander M, Cheresh DA: Disruption of angiogenesis by PEX, a noncatalytic metalloproteinase fragment with integrin binding activity. Cell 1998; 92(3):391-400
29. Yang B, Yang BL, Savani RC, Turley EA. Identification of a common hyaluronan binding motif in the hyaluronan binding proteins RHAMM, CD44 and link protein. EMBO J 1994;13: 286-96.
30. Arap W, Pasqualini R, Ruoslahti E. Cancer treatment by targeted drug delivery to tumor vasculature in a mouse model. Science 1998; 279:377-80.
31. Kishore U, Reid KB. C1q: structure, function, and receptors. Immunopharmacology 2000;49:159–70
32. Kohro-Kawata J, Wener MH, Mannik M. The effect of high salt concentration on detection of serum immune complexes and autoantibodies to C1q in patients with systemic lupus erythematosus. J Rheumatol 2002;29:84–9
33. Agren UM, Tammi R, Tammi M. A dot-blot assay of metabolically radiolabeled hyaluronan. Anal Biochem 1994;217:311–5
34. Xu XM, Chen Y, Chen J, et al. A peptide with three hyaluronan binding motifs inhibits tumor growth and induces apoptosis. Cancer Res 2003;63:5685–90
35. Liu N, Gao F, Han Z, Xu X, Underhill CB, Zhang L. Hyaluronan synthase 3 overexpression promotes the growth of TSU prostate cancer cells. Cancer Res 2001;61:5207–14
36. Hautmann SH, Lokeshwar VB, Schroeder GL, et al. Elevated tissue expression of hyaluronic acid and hyaluronidase validates the HA-HAase urine test for bladder cancer. *J Urol* . 2001; 165:2068-2074
37. Barilla-LaBarca ML, Liszewski MK, Lambris JD, Hourcade D, Atkinson JP. Role of membrane cofactor protein (CD46) in regulation of C4b and C3b deposited on cells. *J Immunol*. 2002; 168:6298-6304.

Personals involved in this study

Major contributors

Lurong Zhang, MD, Ph.D.
Charles B. Underhill, Ph.D.
Ningfei Liu, MD, Ph.D.
Feng Gao, MD, Ph.D.
Zeqiu Han, MD
Yixin Chen, Ph.D.
Xue-Ming Xu, MD, Ph.D.
Shanmin Yang, MD
Jinguo Chen, MD
Luping Wang, MD

Collaborators

Susette Mueller, Ph.D.
Karen Creswell, Ph.D.

BIOGRAPHICAL SKETCH

NAME	POSITION TITLE
Zhang, Lurong, M.D., Ph.D.	**Res. Professor**

EDUCATION *(Begin with baccalaureate or other initial professional education, such as nursing, and include postdoctoral training.)*

INSTITUTION AND LOCATION	DEGREE *(If applicable)*	YEAR(s)	FIELD OF STUDY
Fujian Medical College, Fuzhou, P. R. C.	M.D.	1978-82	Medicine
Second Medical College, Shanghai, P. R. C.	Ph.D.	1983-89	Biochem./Immunol.
VA Medical Center, Boise, Idaho	Post-Doc	1990-91	Immunol./Pharmacol.
Bristol-Myers Squibb Research Inst., Seattle, WA	Post-Doc	1991-92	Mol. Bio./Canc Therap.
Lombardi Cancer Center, Georgetown Univ,Wash.DC	Post-Doc	1992-94	Mol. Bio./Canc Therap.

POSITION AND EMPLOYMENT

2004-present Res. Professor, Dept. of Radiation Oncology, School of Medicine, University of Rochester
1999-04: Res. Associate. Professor, Dept. of Oncology, School of Medicine, Georgetown University
1996-99: Res. Assist. Professor, Dept. of Cell Biology, School of Medicine, Georgetown University
1994-96: Res. Assist. Professor, Dept. of Biochemistry & Molecular Biology, Lombardi cancer center, School of Medicine, Georgetown University, Washington DC
1992-94: Postdoctoral fellow, Lombardi Cancer Center, Georgetown University, Washington DC
1991-92 Postdoctor, Immunotherapy, Dept. of Drug Discovery, Bristol-Myers Squibb Research Institute
1990-91 Postdoctoral Research Associate, Immunopharmacology Research Lab, VA Medical Center, Dept.of Pharmaceutical Sciences, College of Pharmacy, Idaho State Univ., Boise, Idaho
1987-90 Senior Researcher, Center of Clinical Immunology, Second Medical College, Shanghai, China
1985-87 Instructor, Clinical Immunology, Changzheng Hospital, Second Medical College, Shanghai, China
1975-78 Midwife, Dept. of OBG, Fujian People's Hospital, Fujian Medical School, P.R. China

PROFESSIONAL EXPERIENCE

1999-present Reviewer for basic, clinical and translational research grant, Susan G. Komen breast cancer foundation
2001-2003 Committee member of FCM Shared Resource, Lombardi Cancer Center
1992-2003 Active member, Lombardi Cancer Center
1996-present Active member, American Association for Cancer Research

PUBLICATIONS (selected from more than 60 publications)

1. Gregoire CD, **Zhang L** & Daniels CK: Expression of Polymeric Immunoglobulin Receptor by Cultured aged Rat Hepatocytes. *Gastroenterology* 1992; 103 (1): 296-301
2. **Zhang L,** Hellstrom KE & Chen L: Luciferase Activity as a Marker of Tumor Burden and an Indicator of Tumor Response to Antineoplastic Therapy *in vivo. Clinical & Experimental Metastasis* 1994;12:(2):87-2
3. Daniels, C. K. **Zhang L**, Musser B, and Vestal RE: A Solid-phase Radioimmunoassay for Cyclic AMP. *J. Pharmacol. Toxicol. Meth.* 1994; 31 (1): 41-46
4. **Zhang L**, Underhill CB & Chen L: Hyaluronic Acid on the Surface of Tumor Cells is Correlated with Metastatic Behavior. *Cancer Res.* 1995; 55:428-433
5. Kern F.G., McLeskey S.W., **Zhang L**, Kurebayashi J., Liu Y., Ding IYF., Chen D., Miller D.L., Kullen K., Paik S., Dickson R. B., Transfected MCF-7 Cells as a Model for Breast Cancer Progression. *Breast Cancer Res. Treatment.* 1996; 31:153-65
6. McLeskey SW; **Zhang L;** Trock BJ; Kharbanda S; Liu Y; Gottardis MM; Lippman ME; Kern FG: Effects of AGM-1470 and pentosan polysulphate on tumorigenicity and metastasis of FGF-transfected MCF-7 cells. *Br J Cancer* 1996; 73 (9): 1053-62
7. McLeskey SW; **Zhang L;** Kharbanda S; Kurebayashi J; Lippman ME; Dickson RB; Kern FG: Fibroblast growth factor overexpressing breast carcinoma cells as models of angiogenesis and metastasis. *Breast Cancer Res Treat* 1996; 39 (1):103-1
8. Ding I; Huang K; Snyder ML; Cook J; **Zhang L**; Wersto N; Okunieff P: Tumor growth and tumor radiosensitivity in mice given myeloprotective doses of fibroblast growth factors. *J Natl Cancer Inst* 1996; 88 (19): 1399-404
9. **Zhang L;** Kharbanda S; Chen D; Bullocks J; Miller DL; Ding IY; Hanfelt J; McLeskey SW; Kern FG: MCF-7 breast carcinoma cells overexpressing FGF-1 form vascularized, metastatic tumors in ovariectomized or tamoxifen-treated nude mice. *Oncogene* 1997;15, 2093
10. **Zhang L;** Kharbanda S; Hanfelt J; Kern FG: Both autocrine and paracrine effects of transfected acidic fibroblast growwth factor are involved in the estrogen-independent and antiestrogen-resistant growth of MCF-7 breast cancer cells. *Cancer Res* 1998; 8(2):352-61.

11. McLeskey S.W., **Lurong Zhang**, Samir K, Kern FG: Tamoxifen resistance of FGFs transfected MCF-7 cells are cross-resistance in vivo to anti-estrogen ICI 182,278 and aromatase inhibitors. *Clinical Can Res*1998; 4: 697-711
12. Ningfei Liu & **Lurong Zhang:** Changes of tissue fluid hyluronan (hyluronic acid) in peripheral lymphedema. *Lymphology* 1998,31: 173
13. Underhill CB, Andrews P and **Zhang L**:Hypertrophic chondracytes are surrounded by a condensed layer of hyaluronan.Matrix 1999;
14. **Zhang L**, Kharbanda S, Mcleskey SW and.Kern FG: Overexpression of fibroblast growth factor 1 in MCF-7 breast cancer cells facilitates tumor cell dissemination but does not support the development of macrometastases in the lung or lymph nodes. *Cancer Res.* 1999; 59: 5023
15. Underhill,C.B. and **Zhang L**: Analysis of hyaluronan using biotinylated hyaluronan-Binding proteins. *Method in Mol. Biol.* 2000;137: 441
16. Han Z, Ni J, Smits P, Underhill CB, Xie B, Chen Y, Liu N, Tylzanowski P, Parmelee D, Feng P, Ding I, Gao F, Gentz R, Huylebroeck D, Merregaert J, and **Zhang L:**Extracellular matrix protein 1(ECM1): a novel angiogenic factor expressed in breast cancer cells. *FASEB J:* 2001; 988-994
17. Ningfei Liu, Charles B. Underhill, Randall Lapevich , Zeqiu Han, Feng Gao, **Lurong Zhang** and Shawn Green: Metastatin: A hyaluronan binding complex from cartilage that inhibits tumor growth. *Cancer Res* 2001; 61:1022-28
18. Yixin Chen, XueMing Xu, Shuigen Hong, Jinguo Chen, Ningfei Liu, Charles B. Underhill, Karen Creswell and **Lurong Zhang:** RGD-Tachyplesin inhibits tumor growth. *Cancer Res.* 2001; 61: 2434-2438
19. Ningfei Liu, Feng Gao, Zeqiu Han, Charles B. Underhill and **Lurong Zhang:** Over-expression of Human Hyaluronan Synthase 3 in TSU Prostate Cancer Cells Promotes Tumor Growth . *Cancer Res.*2001, 61: 5207-5214
20. Okunieff P, Li M, Liu W, Sun J, Fenton B, Zhang L, Ding I.: Keratinocyte growth factors radioprotect bowel and bone marrow but not KHT sarcoma. *Am J Clin Oncol.* 2001; 24 (5):491-5
21. Hamada T, McLean WH, Ramsay M, Ashton GH, Nanda A, Jenkins T, Edelstein I, South AP, Bleck O, Wessagowit V, Mallipeddi R, Orchard GE, Wan H, Dopping-Hepenstal PJ, Mellerio JE, Whittock NV, Munro CS, van Steensel MA, Steijlen PM, Ni J, **Zhang L**, Hashimoto T, Eady RA, McGrath JA.: Lipoid proteinosis maps to 1q21 and is caused by mutations in the extracellular matrix protein 1 gene (ECM1). *Hum Mol Genet* 2002; 11(7): 833-840
22. Liu N, Shao L, Xu X, Chen J, Song H, He Q, Lin Z, **Zhang L**, Underhill CB.: Hyaluronan metabolism in rat tail skin following blockage of the lymphatic circulation. *Lymphology* 2002; 35 (1):15-22
23. Gao F, **Zhang L**, Underhill CB.: Promotion of growth of human breast cancer cells MDA231 by human sperm membrane-bound hyaluronidase: an experimental study. *Zhonghua Yi Xue Za Zhi.* 2002; 82(3):207-10
24. Yang S, Chen J, Guo Z , Xu XM, Luping Wang, Xu-Fang Pei, Jing Yang Charles B. Underhill and **Lurong Zhang** Triptolide Inhibits the Growth and Metastasis of Solid Tumors. *Mol Cancer Ther.* 2003; 2 (1):65-72.
25. Okunieff P, Fenton BM, **Zhang L**, Kern FG, Wu T, Greg JR, Ding I. Fibroblast growth factors (FGFS) increase breast tumor growth rate, metastases, blood flow, and oxygenation without significant change in vascular density. *Adv Exp Med Biol.* 2003; 530:593-601.
26. Okunieff P, Ding I, Liu W, Fenton B, **Zhang L**, Cheng S. FGF1 not VEGF transfection induces in-vitro radiation resistance, in-vivo radiation modifying effects of angiogenic peptides probably relate more to vascularity than apoptosis. *Int J Radiat Oncol Biol Phys.* 2003;57(2):S318
27. Wang L, Yu J, Ni J, Xu X, Wang J, Ning H, PeiX, Chen J, Yang S, Underhill CB, Liu L, Liekens J, Merregaert J and **Zhang L:** Extracellular Matrix Protein1 (ECM1) is Over-expressed In Malignant Epithelial Tumors. *Cancer Letter.* 2003; 200 (1):57-67.
28. Xu, XM, Chen Y, Gao F, Chen J, Shanmin Yang, Charles B. Underhill and **Lurong Zhang:** A Peptide with Three Hyaluronan Binding Motifs Inhibits Tumor Growth by Inducing Apoptosis. *Cancer Res.* 2003; 63 (18):5685-90
29. Liu N, Xu X, Chen J, Wang L, Yang S, Underhill CB, and **Zhang L**: A Hyaluronan-Binding Peptide Can Inhibit Tumor Growth by Interacting with Bcl-2. *Int. J of Cancer* 2004, 109 : 49-57
30. Chen J, **Zhang L** and Kim S: Quantification and detection of DcR3, a decoy receptor in TNFR family. J Im. Meth. 2004; 285(1):63-70
31. Kim S, McAuliffe W, Zaritskaya L, **Zhang L,** and Nardelli, B: Selective induction of TR6/DcR3 release by bacterial antigens in human monocytes and a dendritic cell subset. *Infection and Immunity* 2004; 72(1):89-93.
32. Wang H, MaoY, Ju L, Zhang J, Liu Z, Zhou X, Li Q, Wang Y, Kim S, **Zhang L**: Detection and Monitoring of SARS-Coronavirus in the Plasma and Peripheral Blood Lymphocytes of Patients with Severe Acute Respiratory Syndrome. *Clinical Chemistry* 2004; 50 (7):
33. Chen J, Xu XM, Underhill CB, Yang S, Wang L, Chen Y, Hong S, Creswell K, **Zhang: L.** Tachyplesin activates the classic complement pathway to kill tumor cells. Cancer Res. 2005 ;65 (11):4614-22
34. Kim S and **Zhang L**: Identification of naturally secreted soluble form of TL1A, a TNF-like cytokine. J Immunol. Meth. 2005;298(1):1-8.
35. Li, H, **Zhang L**, Lou H, Ding I, Kim S,Wang L, Huang J, P. di Sant'Agnese A, Lei J: Over-expression of decoy receptor 3 in precancerous lesion and adenocarcinoma of the esophagus. Am. J Clinical Pathology 2005, (in press)

Active/Pending Other Support

Active:

1. U19 AI067733-01 (PI: Okunieff)**:** Center for Biophysical Assessment and Risk Management Following Irradiation

Project 1 (Co-PI) Inflammatory Molecules in Radiation Toxicity:Risk Assessment and Intervention
09/01/05-8/31/10 50%
Aims: **1):** Determine beneficial and deleterious IM patterns following IR: measure soft tissue inflammatory response to local or whole abdomen irradiation (IR) in FV sensitive and resistant mice; **2)** Identify single agent mitigating inflammatory and FV toxicity following IR**; 3)** Test early and late therapeutic programs for mitigation of soft tissue inflammation and FV.

Overlap: None

2. DAMD-BC033799 **Co-PI** 09/01/04-8/31/06 5%
Targeting of Beast Cancer with Triptolide Nanoparticle
Aims: 1) To examine the effects of RGD/NGR-PA-TPL-lipo on primary and metastatic breast cancer; and 2) To examine the targeting of RGD/NGR-PA-TPL-lipo on angiogenesis.

Overlap: None

3. 1R41AI066756-01 **PI** 09/31/05-9/30/06 5%
ESA, a novel anti-inflammation agent

Aims: 1) Test for beneficial anti-inflammatory effects of EsA in a standard arthritis model; 2) Demonstrate that oral and other administrative routes have utility, and determine the optimal dose and ED_{50}; 3) Measure the therapeutic window and side effect profile of EsA in mice.

Overlap: None

Completed projects in past 3 years:

1 R29 CA71545 **PI** 9/1/97---8/31/03 50%
NCI/NIH
Role of Hyaluronan in Tumor Progression

Aims: To test the hypothesis that: 1) high level of HA synthesis will promote the angiogenesis, tumor growth and metastasis; 2) inhibition of HA expression will attenuate the malignancy of tumor cells; 3) *in vivo* spontaneous metastatic process preferentially selects high HA-expressing cells for growth in distant sites; and 4) the expression of HA is regulated by hypoxia.

DAMD17-98-1-8099 **PI** 09/01/98--08/31/03 5%
U. S. Army Med. Res. & Mat. Command
Role of Membrane-bound Hyaluronidase in Tumor Progression

Aims: To test the hypothesis that: 1) over-expression of HAase is capable of increasing the malignant potential of tumor cells; 2) inhibition of HAase activity will attenuate tumor progression; and 3) to determine if the process of spontaneous metastases preferentially selects HAase-high expressing cells.

Susan G. Koman Breast Cancer Foundation: PI 3/31/99--3/30/03 5%
Role of ECM1 in Breast Cancer

Aims: 1) To transfect MCF-7 cells with cDNA for ECM1 and examine phenotype alteration; 2) To study the expression of ECM1 in human breast cancer.

DAMD17-00-1-0081 **PI** 06/01/00-5/31/05 30%
Targeting of Prostate Cancer with Hyaluronan Binding Proteins
Aims: 1) To see the effect of bovine HABP on prostate cancer cells; 2) To examine the effect of link protein on prostate cancer cells; 2) To examine the possible anti-angiogenesis effect of bovine HABP.

Susan G. Koman Breast Cancer Foundation **PI** 10/1/01--11/30/04 5%
A potent anti-tumor agent for breast cancer
Aims: 1) To examine the anti-tumor effect of triptolide (TPL) on breast cancer; 2) To study the mechanism of TPL
Overlap: None

DAMD17-01-1-0708 **PI** 09/01/01-8/31/05 20%

Therapeutic Effect of Targeted Hyaluronan Binding Peptide on Neurofibromatosis
Aims: 1) To examine the anti-tumor effect of synthetic targeted HA binding peptide on malignant neurofibromatosis cells; 2) To examine the anti-tumor effect of genetically expressed targeted HA binding peptide; 2) To examine the effect of targeted HA binding peptide on molecules involved in apoptosis.

[CANCER RESEARCH 61, 1022–1028, February 1, 2001]

Metastatin: A Hyaluronan-binding Complex from Cartilage That Inhibits Tumor Growth[1]

Ningfei Liu,[2] Randall K. Lapcevich,[2] Charles B. Underhill, Zeqiu Han, Feng Gao, Glenn Swartz, Stacy M. Plum, Lurong Zhang,[2] and Shawn J. Green[2, 3]

Department of Oncology, Georgetown University Medical Center, Washington, D.C. 20007 [N. L., C. B. U., Z. H., F. G., L. Z.], and EntreMed, Inc., Rockville, Maryland 20902 [R. K. L., G. S., S. M. P., S. J. G.]

ABSTRACT

In this study, a hyaluronan-binding complex, which we termed Metastatin, was isolated from bovine cartilage by affinity chromatography and found to have both antitumorigenic and antiangiogenic properties. Metastatin was able to block the formation of tumor nodules in the lungs of mice inoculated with B16BL6 melanoma or Lewis lung carcinoma cells. Single i.v. administration of Metastatin into chicken embryos inhibited the growth of both B16BL6 mouse melanoma and TSU human prostate cancer cells growing on the chorioallantoic membrane. The *in vivo* biological effect may be attributed to the antiangiogenic activity because Metastatin is able to inhibit the migration and proliferation of cultured endothelial cells as well as vascular endothelial growth factor-induced angiogenesis on the chorioallantoic membrane. In each case, the effect could be blocked by either heat denaturing the Metastatin or premixing it with hyaluronan, suggesting that its activity critically depends on its ability to bind hyaluronan on the target cells. Collectively, these results suggest that Metastatin is an effective antitumor agent that exhibits antiangiogenic activity.

INTRODUCTION

A potential therapeutic target on angiogenic endothelial cells is hyaluronan, a large negatively charged glycosaminoglycan that plays a role in the formation of new blood vessels (1). Particularly high concentrations of hyaluronan are associated with endothelial cells at the growing tips or sprouts of newly forming capillaries (2, 3). Similarly, when cultured endothelial cells are stimulated to proliferate by cytokines, their synthesis of hyaluronan is significantly increased (4). Interestingly, this stimulation is restricted to endothelial cells derived from the small blood vessels and is not seen in endothelial cells derived from larger ones (4). In the case of mature blood vessels, hyaluronan is present in perivascular regions and in the junctions between the endothelial cells (5, 6). Earlier studies have shown that exogenously applied hyaluronan has different effects on angiogenesis depending on its size, with macromolecular hyaluronan inhibiting vascularization in chicken embryos, and oligosaccharide fragments of hyaluronan stimulating vascularization in the chorioallantoic membrane (7–9). Thus, hyaluronan appears to be specifically associated with the endothelial cells of newly forming blood vessels and can influence their behavior.

In addition to hyaluronan, endothelial cells involved in neovascularization also express CD44 and other cell surface receptors for hyaluronan (10–12). In particular, endothelial cells associated with tumors express large amounts of CD44 (11). In previous studies, we have shown that CD44 allows cells to bind hyaluronan so that it can be internalized into endosomal compartments, where the hyaluronan is degraded by the action of acid hydrolases (13, 14). Thus, the expression of CD44 by endothelial cells allows them to bind and internalize hyaluronan as well as any associated proteins. The fact that both hyaluronan and CD44 are up-regulated in endothelial cells involved in neovascularization suggests that the turnover of hyaluronan by these cells is much greater than that by cells lining mature blood vessels.

The increased turnover of hyaluronan in tumor-associated endothelial cells suggested a possible mechanism to specifically target these cells. Our initial idea was to use a hyaluronan-binding complex isolated from cartilage to deliver chemotherapeutic agents specifically to these endothelial cells. Purified by affinity chromatography, this hyaluronan-binding complex consists of tryptic fragments of the link protein and aggrecan core protein (5, 15, 16). We intended to couple the hyaluronan-binding complex to a chemotherapeutic agent such as methotrexate and use this derivative to attack endothelial cells. We hoped that this derivative would bind to the hyaluronan on the endothelial cells and then be internalized into lysosomes, where the methotrexate would be released by the action of acid hydrolyses. Surprisingly, however, in the course of these experiments, we found that the hyaluronan-binding complex by itself (*i.e.*, in the absence of a chemotherapeutic agent) inhibited angiogenic activity. Functionally, we termed the hyaluronan-binding complex, which inhibits tumor growth, Metastatin.

In the present study, we demonstrate that Metastatin has a number of intriguing biological activities, including inhibition of endothelial cell proliferation and migration, inhibition of angiogenesis, and suppression of tumor cell growth in chicken embryos and pulmonary metastasis in mice. These effects are blocked by preincubating Metastatin with hyaluronan, suggesting that the activity of Metastatin depends on its ability to bind hyaluronan on the target cells.

MATERIALS AND METHODS

Preparation of Metastatin. The hyaluronan-binding complex was prepared by a modified version of the method originally described by Tengblad (15, 16). Briefly, bovine nasal cartilage (Pel-Freez, Rogers, AR) was shredded with a Sure-Form blade (Stanley), extracted overnight with 4 M guanidine-HCl and 0.5 M sodium acetate (pH 5.8), and dialyzed against distilled water to which 10× PBS was added to a final concentration of 1× PBS (pH 7.4). The protein concentration was measured, and for each 375 mg of protein, 1 mg of trypsin (type III; Sigma, St. Louis, MO) was added. After digestion for 2 h at 37°C, the reaction was terminated by the addition of 2 mg of soybean trypsin inhibitor (Sigma) for each milligram of trypsin. The digest was dialyzed against 4 M guanidine-HCl and 0.5 M acetate (pH 5.8), mixed with hyaluronan coupled to Sepharose, and then dialyzed against a 10-fold volume of distilled water. The hyaluronan-Sepharose beads were placed into a chromatography column and washed with 1.0 M NaCl, followed by a gradient of 1.0–3.0 M NaCl. Metastatin was eluted from the hyaluronan affinity column with 4 M guanidine-HCl and 0.5 M sodium acetate (pH 5.8), dialyzed against saline, and sterilized by passage through a 0.2-μm-pore filter. For SDS-PAGE analysis, the purified preparation was loaded onto a 10% BisTris nonreducing gel (Novex, Inc.) and subsequently stained with Coomassie Blue. To identify the

Received 7/12/00; accepted 11/28/00.

The costs of publication of this article were defrayed in part by the payment of page charges. This article must therefore be hereby marked *advertisement* in accordance with 18 U.S.C. Section 1734 solely to indicate this fact.

[1] Supported in part by the United States Army Medical Research and Materiel Command under DAMD1717-94-J-4284, DAMD17-98-1-8099, and DAMD17-99-1-9031. Additional support was obtained from the Susan G. Komen Foundation and NIH Grant R29CA71545.

[2] These authors contributed equally to this work.

[3] To whom requests for reprints should be addressed, at EntreMed, Inc., Medical Center Drive, Suite 200, Rockville, MD 20902. Phone: (301) 738-2494; Fax (301) 217-9594; E-mail shawng@entremed.com.

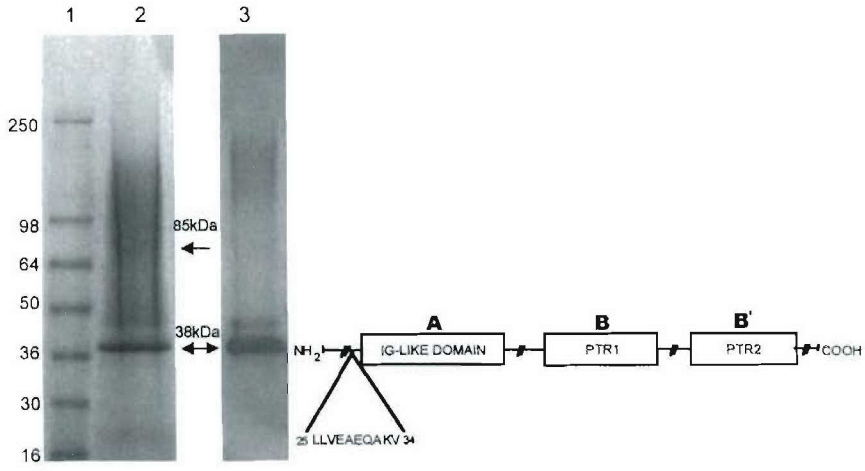

Fig. 1. SDS-PAGE and NH_2-terminal analysis of Metastatin. *Lane 1*, molecular mass markers; *Lane 2*, Metastatin stained with Coomassie blue; *Lane 3*, Western blot of Metastatin immunostained with an antibody against the link protein. The fragment of aggrecan migrated as a diffuse band at ~85 kDa, whereas the truncated link protein was at 38 kDa. NH_2-terminal sequence analysis of the 38-kDa band indicated that the first 24 amino acids of the link protein have been cleaved and is indicated on the schematic diagram.

link protein by Western blotting, the proteins on the gel were transferred to a sheet of nitrocellulose and immunostained with the 9/30/8-A-4 monoclonal antibody. (The monoclonal antibody, developed by Dr. B. Caterson, was obtained from the Developmental Studies Hybridoma Bank under the auspices of the NICHD and maintained by the University of Iowa, Department of Biological Sciences, Iowa City, IA 52242.) This identity was further confirmed by NH_2-terminal sequencing (Fig. 1). In tests of the biological activity of Metastatin, controls consisted of Metastatin mixed with an excess mass of hyaluronan (Lifecore, Chaska, MN) or a heat-inactivated preparation made by placing it in a boiling water bath for 30 min.

Endothelial and Tumor Cell Lines. HUVECs[4] were obtained from the Tumor Bank of the Lombardi Cancer Center (Georgetown University, Washington, DC). ABAEs were kindly provided by Dr. Luyuan Li (Lombardi Cancer Center), and BRECs were provided by Dr. Rosemary Higgins (Pediatrics, Georgetown University). These endothelial cells were cultured in 90% DMEM, 10% fetal bovine serum, and 10 ng/ml bFGF. The B16BL6 melanoma tumor line was obtained from the National Cancer Institute Central Repository (Frederick, MD). TSU cells were obtained from the American Type Culture Collection (Rockville, MD), and Lewis lung carcinoma cells were kindly supplied by Dr. Michael O'Reilly (Children's Hospital, Boston, MA). The tumor cells were grown in 90% DMEM, 10% fetal bovine serum, and 2 mM L-glutamine. For the mouse metastasis assays, cells were generally used between passages 6 and 18.

Mice. Specific pathogen-free, male, 6–8-week-old C57Bl/6 mice were obtained from The Jackson Laboratory (Bar Harbor, ME). Animals were cared for and treated in accordance with the procedures outlined in the Guide for the Care and Use of Laboratory Animals (NIH Publication No. 86-23). Animals were housed in a pathogen-free environment and provided with sterilized animal chow (Harlan Sprague Dawley, Indianapolis, IN) and water *ad libitum*.

Mouse Metastasis Model System. For the experimental melanoma model, mice were inoculated i.v. in the lateral tail vein with B16Bl6 cells (5×10^4 cells/animal) on day 0. Treatment was initiated on day 3 with 5 (0.2 mg/kg), 15 (0.6 mg/kg), and 49 μg (2 mg/kg) of Metastatin and continued daily until animals were sacrificed on day 14. After euthanasia, the lungs were removed, and surface metastatic lesions were enumerated under a dissecting microscope.

Mice were also inoculated with Lewis lung carcinoma cells, which aggressively form pulmonary metastases. Mice were injected i.v. in the lateral tail vein with 2.5×10^5 cells/animal (day 0), and beginning on day 3, the Metastatin was administered by daily i.p. injections of 15 (0.6 mg/kg) and 49 μg (2 mg/kg) or by three i.v. injections of 100 μg (4 mg/kg) on days 1, 3, and 5. Animals were euthanized, and their lungs were removed and weighed. To obtain the lung weight gain, the average lung weight of nontreated mice (0.2 g) was subtracted from that of the treated animals.

The number of pulmonary metastases and lung weight gains were reported as mean ± SD, and the differences were compared using Student's *t* test. The groups were considered to be different when the probability (P) value was <0.05.

Chicken Chorioallantoic Membrane Assays. To measure angiogenesis, a chick chorioallantoic membrane assay was performed using a modification of the methods of Brooks *et al.* (17). For this, holes were drilled in the tops of 10-day-old chicken eggs to expose the chorioallantoic membranes, and filter discs (0.5 cm in diameter) containing 20 ng of human recombinant VEGF [20 μl (1 μg/ml); Pepro, Rocky Hill, NJ] were placed on the surface of each chorioallantoic membrane (day 0). The holes were covered with parafilm, and the eggs were incubated at 37°C in a humidified atmosphere. One day later, the eggs were given injections (via a blood vessel in the chorioallantoic membrane using a 30-gauge needle) of the various substances [Metastatin (80 μg/egg) or controls consisting of PBS or heat-inactivated Metastatin]. Three days later (day 4), the chorioallantoic membranes and associated discs were cut out and immediately immersed in 3.7% formaldehyde. For computer-assisted image analysis, the discs were divided into quarters with fine wires, and the blood vessels in each quarter were digitally photographed and analyzed by an Optimas 5 program to calculate the vessel area and length normalized to the total area measured. The means and the SEs were calculated from all quadrants within each group, and the statistical significance was determined by Student's *t* test. Twelve or more eggs were used for each sample point.

For the growth of xenografts on the chorioallantoic membrane, holes were cut into the sides of 10-day-old eggs exposing the membrane (day 0), and then 1×10^6 B16BL6 or TSU cells were applied to the membranes. Two days later, the eggs were given i.v. injections of the various substances. On day 7, the tumor masses were fixed in formalin, dissected free from the normal membrane tissue, and weighed.

Cell Growth Assays. To determine the effects of Metastatin on cell growth, the cell lines were subcultured into 24-well dishes at a density of approximately 5×10^4 cells/well for the endothelial cell lines (HUVEC, ABAE, and BREC) and 5×10^4 cells/well for tumor cell lines (B16BL6, TSU, and Lewis lung carcinoma). For the dose-response experiments, the medium was changed every other day, and at the end of 6 days, the cells were released with 0.5 mM EDTA in PBS, and the cell number was determined with a Coulter counter (Hialeah, FL).

ELISA Assay for Hyaluronan. Cells were grown to confluence in 24-well dishes, and the conditioned medium was collected, incubated with a biotinylated version of the Metastatin (16), and then transferred to plates precoated with hyaluronan (umbilical cord; Sigma). The hyaluronan present in the conditioned medium interacts with the biotinylated Metastatin so that less of it will be left to bind to hyaluronan attached to the plate. At the end of the incubation, the plates were washed, and the amount of biotinylated Metastatin remaining attached was determined by incubating the plates with streptavidin coupled to peroxidase (Kirkegard & Perry, Gaithersburg, MD) followed by a soluble substrate for peroxidase. The amount of hyaluronan in the conditioned medium was calculated by comparison with a standard curve with known amounts of hyaluronan (16).

[4] The abbreviations used are: HUVEC, human umbilical vein endothelial cell; ABAE, adult bovine aorta endothelial cell; BREC, bovine retinal endothelial cell; VEGF, vascular endothelial growth factor; bFGF, basic fibroblast growth factor.

Wound Migration Assay. A suspension of HUVECs (5×10^5 cells in 5 ml of 98% M199 and 2% fetal bovine serum) was added to 60-mm tissue culture plates that had been precoated with gelatin (2 ml of 1.5% gelatin in PBS, 37°C, overnight) and allowed to grow for 3 days to confluence. An artificial "L"-shaped wound was generated in the confluent monolayer with a sterile razor blade by moving the blade down and across the plate. Plates were then washed with PBS, and 2 ml of PBS were added to each plate along with 2 ml of sample in M199 and 2% fetal bovine serum in the presence and absence of 5 ng/ml bFGF. After an overnight incubation, the plates were treated with Diff-Quik for 2 min to fix and stain the cells. The number of cells that migrated were counted under ×200 magnification using a 10-mm micrometer over a 1 cm distance along the wound edge. Ten fields for each plate were counted, and an average for the duplicate was calculated.

RESULTS

Characterization of Metastatin. Metastatin was isolated from bovine nasal cartilage by affinity chromatography on hyaluronan-Sepharose. As shown in Fig. 1, Metastatin consisted of two molecular factions as determined by SDS-PAGE, a sharp band at 38 kDa that corresponds to the link protein, and a diffuse band at approximately 85 kDa that represents a tryptic fragment of the aggrecan core protein (5, 15, 16). The diffuse nature of this latter fraction is probably due to variations in the degree of glycosylation and glycosaminoglycan content. The identity of the link protein was verified by immunoblotting with a specific monoclonal antibody against this protein (Fig. 1). In addition, NH_2-terminal sequence analysis of the 38-kDa band revealed that the purified protein was missing the first 24 amino acids. Previous studies have shown that this complex binds to hyaluronan with high affinity and specificity (5, 16). Indeed, a biotinylated version of the preparation has been widely used as a histochemical stain to localize hyaluronan in tissue sections (5, 16).

Because cartilage is known to contain various protease inhibitors, which may contribute to its antitumor properties (18), we wanted to determine whether Metastatin possessed such attributes. For this reason, we used a chromogenic assay (Diapharma Group, Inc., West Chester, OH) to assess the effect of Metastatin on the following enzymes: (*a*) trypsin; (*b*) chymotrypsin; (*c*) plasmin; and (*d*) elastase. At concentrations as high as 100 μg/ml, Metastatin did not inhibit the activity of any of the enzymes tested (data not shown).

Effect of Metastatin on Metastatic Tumors. In initial experiments, we found that Metastatin was effective at inhibiting pulmonary metastases of B16BL6 cells. When mice were given daily i.p. injections of Metastatin 3 days after tumor inoculation, lung metastases were strikingly reduced (Fig. 2*A*). Fig. 2*B* shows that the number of surface lung metastases (>0.5 mm) in the mice treated with 15 and 49 μg Metastatin/day were reduced by more than 80%. The dose-response curve shown in Fig. 2*C* was constructed from two independent experiments and shows that Metastatin decreased the number of metastatic colonies in a dose-dependent manner with an ED_{50} of approximately 10 μg (0.4 mg/kg). Significantly, when Metastatin preparations were premixed with macromolecular hyaluronan, the antimetastatic activity was blocked, and the mean number of surface pulmonary metastases was comparable to that seen in control mice (Fig. 2*B*). This suggests that the ability of Metastatin to bind hyaluronan is required for its anti-tumor activity.

Similar results were obtained with the Lewis Lung carcinoma cell line, which is a more aggressive mouse tumor model. As shown in Fig. 3, *A* and *B*, Metastatin inhibited pulmonary metastasis of Lewis lung carcinoma cells in a dose-related fashion, as reflected in the weight gain of the lungs. Furthermore, Metastatin was effective when given by two different routes, i.p. and i.v. (Fig. 3, *B* and *C*).

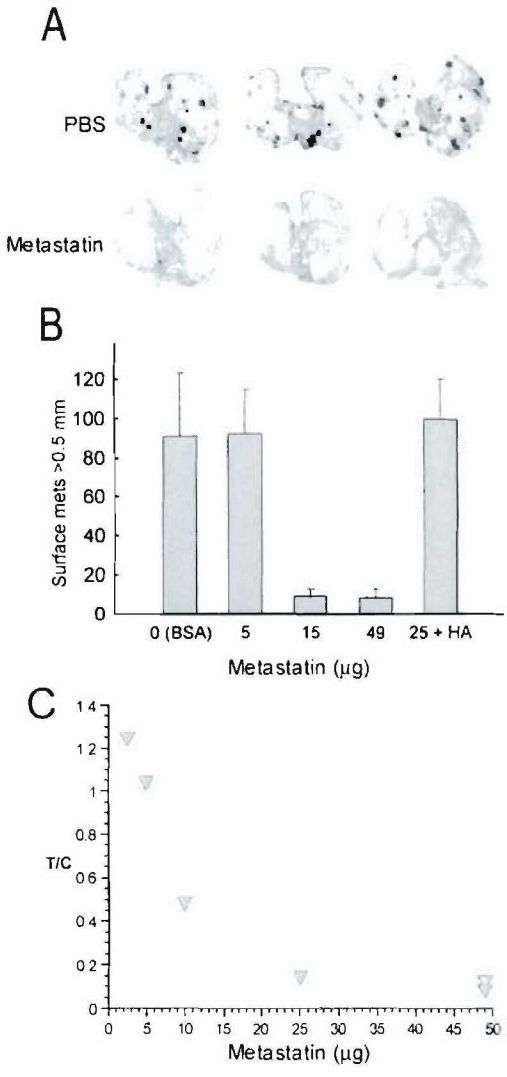

Fig. 2. Effect of Metastatin on B16BL6 melanoma metastasis. B16BL6 melanoma cells were injected into the tail veins of C57Bl/6 mice, and 3 days later, the mice were injected i.p. with increasing doses of Metastatin. After 14 days, the lungs were removed, and surface pulmonary metastases were counted. *A*, the lungs from control animals had a greater number of metastases than those from the Metastatin (49 μg)-treated animals. *B*, the number of pulmonary metastases larger than 0.5 mm is plotted against the concentration of Metastatin injected. Metastatin inhibits the number of metastases, and the addition of hyaluronan to Metastatin blocked its inhibitory activity. The values shown are the mean of at least five mice/group; *bars*, SD. *C*, this dose-response curve was derived from two independent experiments ($n = 5$ for each point) and shows the ratio of pulmonary metastasis in the test and control animals (*T/C*) as a function of the Metastatin dose.

Effect of Metastatin on *in Vitro* Cell Proliferation and Migration. In the next series of experiments, we wanted to determine whether Metastatin has any effect on the growth of either endothelial or tumor cells in tissue culture. For these experiments, the cells were grown in the presence of varying concentrations of Metastatin for 6 days, and then the final cell numbers were determined. Metastatin inhibited the proliferation of the endothelial cell lines HUVEC, ABAE, and BREC (Fig. 4*A*) and two of the tumor cell lines (B16BL6 and Lewis lung carcinoma cells) but had no effect on the TSU cells (Fig. 4*B*). Similar results were obtained when proliferation was monitored by incorporation of bromodeoxyuridine (data not shown). It is important to note that the growth inhibition of B16BL6 cells was partially blocked when the preparation of Metastatin was premixed with an excess of hyaluronan (Fig. 4*B*).

One possible explanation for the lack of TSU cell sensitivity to

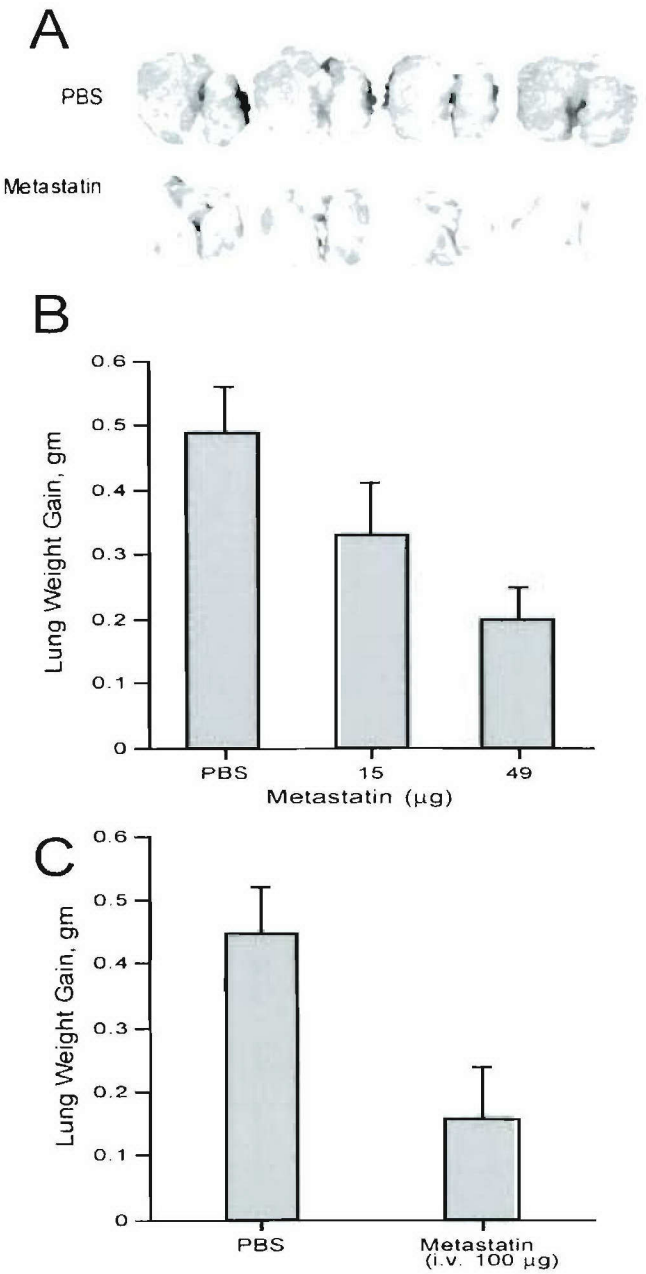

Fig. 3. Inhibition of pulmonary metastasis of Lewis lung carcinoma cells. Lewis lung carcinoma cells were injected into the tail veins of C57Bl/6 mice, and 3 days later, mice were treated with PBS or Metastatin. Once the treatment was stopped, animals were euthanized, and lungs were removed and weighed. *A*, shows representative lungs from control and treated animals and illustrates that Metastatin lowers the tumor burden. *B*, Metastatin injected i.p. daily beginning on day 4 decreased the relative lung weights in a dose-dependent fashion. *C*, the weight of the lungs in animals was also decreased when Metastatin was administered by three separate i.v. injections (100 μg/injection on days 1, 3, and 5). The values shown are the mean of at least five mice/group; *bars*, SD.

Metastatin could be the amount of hyaluronan that they secrete because it has an inhibitory effect. To test this possibility, conditioned media from confluent cultures of the different cell lines were collected and analyzed for hyaluronan by a modified ELISA. TSU cells were found to secrete significantly larger amounts of hyaluronan into the medium than the other cell lines (7 μg/ml *versus* <0.5 μg/ml, respectively). Indeed, this level of hyaluronan would be sufficient to block the effects of added Metastatin.

We also examined the effects of Metastatin on the migration of endothelial cells, another important factor in the process of angiogenesis (19). In this assay, we examined the effect of Metastatin on the migration of HUVECs using the wound migration assay. Fig. 5 shows that at a concentration of 10 μg/ml, Metastatin inhibited the migration of HUVECs by 50% as compared with controls treated with bFGF alone. Again, similar results were obtained when migration was monitored using Nucleopore filters (data not shown).

Effect of Metastatin on VEGF-induced Angiogenesis. The fact that Metastatin could inhibit both the growth and migration of endothelial cells *in vitro* suggested that it might also be able to block angiogenesis *in vivo*. To test this possibility, we examined the effect

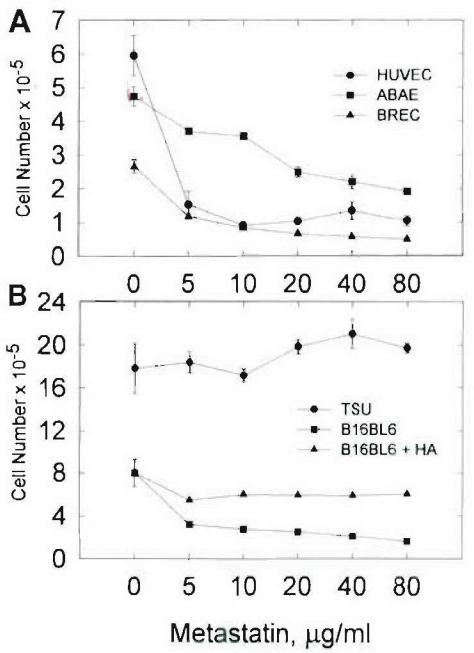

Fig. 4. The effects of varying concentrations of Metastatin on the growth of cultured cells. The cell lines were cultured in 24-well dishes in complete medium containing the indicated amounts of Metastatin, with medium changes ever other day. After 6 days, the cells were harvested with a solution of EDTA in PBS, and the cell numbers were determined with a Coulter counter. *A*, a dose-response curve is shown for the effects of Metastatin on the growth of the endothelial cell lines HUVEC, ABAE, and BREC. In each case, the growth of the cells was inhibited by Metastatin. *B*, a dose-response plot is shown for the tumor cell lines B16BL6 and TSU. Whereas Metastatin inhibited the growth of the B16BL6 cells, it had little or no effect on the TSU cells. The addition of an equal mass of hyaluronan to the Metastatin significantly reduced its effect on the proliferation of B16BL6 cells

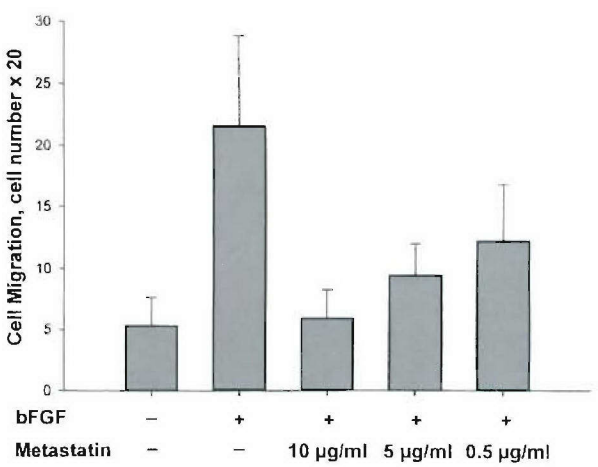

Fig. 5. Dose-dependent inhibitory effect of Metastatin on the migration of endothelial cells. HUVECs were grown to confluence on gelatin-coated culture plates, wounded with a sterile razor blade, and induced to migrate with bFGF in the presence of varying amounts of Metastatin. The number of cells that migrated were enumerated using a micrometer and microscope at ×200 magnification.

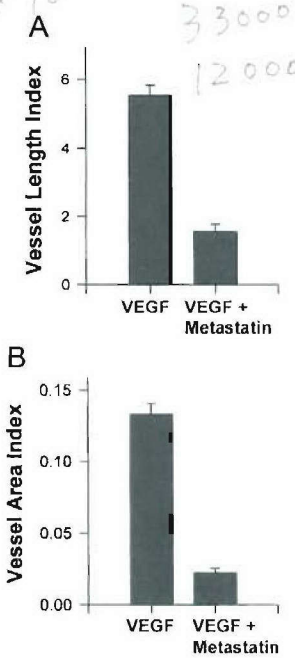

Fig. 6. Effect of Metastatin on VEGF-induced angiogenesis. The top of air sacs of 10-day-old chicken eggs were opened, exposing the chorioallantoic membranes, and filter discs containing 20 ng of VEGF were applied. The treated group was then injected i.v. with Metastatin (80 μg/egg), and the control group did not receive injections. The chorioallantoic membranes and associated discs were cut out on day 3 and analyzed by computer-assisted image analysis as described in "Materials and Methods". Metastatin had a significant inhibitory effect on both the (*A*) vessel length index and (*B*) vessel area index.

of Metastatin on angiogenesis induced in the chick chorioallantoic membrane. In this assay, filter papers containing recombinant human VEGF were placed on the chorioallantoic membrane of 10-day-old eggs, which were then given a single i.v. injection of the Metastatin or control preparations. Three days later, the extent of vascularization in the region of the filters was determined by computer-assisted image analysis. As shown in Fig. 6, treatment with Metastatin reduced both the length and area of vessels as compared with the control group, suggesting that Metastatin does indeed have the ability to block VEGF-induced angiogenesis.

Inhibition of Tumor Growth on the Chorioallantoic Membrane. To further explore the antitumor activity of Metastatin, we examined its effect on the growth of B16BL6 and TSU cells on the chicken chorioallantoic membrane. Tumor cells were applied to the chorioallantoic membranes of 10-day-old chicken embryos and allowed to grow for 1 week. Pilot experiments revealed that after inoculation with 10^6 cells, the take rate was almost 100% and resulted in xenografts with weights from 50–150 mg in 7 days. However, when the inoculated eggs were given a single i.v. injection of the Metastatin, the growth of the B16BL6 and TSU xenografts was greatly inhibited (Fig. 7). Again, this inhibitory effect was abolished if the preparation of Metastatin was heat inactivated or preincubated with its ligand, hyaluronan (Fig. 7*B*). It is important to note that Metastatin did not appear to adversely affect the development of the chicken embryos.

DISCUSSION

In this study we report that Metastatin, a cartilage-derived hyaluronan-binding complex consisting of proteolytic fragments of bovine link protein and aggrecan, is able to block the growth and metastasis of tumor cells under the following conditions: (*a*) a single i.v. injection of Metastatin into the chorioallantoic membrane of chicken embryos inhibited the growth of B16BL6 mouse melanoma cells and TSU human prostate cancer cells; (*b*) multiple i.p. injections of Metastatin prevented the experimental metastasis of B16BL6 and Lewis lung carcinoma cells to the lungs of mice; and (*c*) three i.v. injections of Metastatin were sufficient to inhibit the formation of Lewis lung carcinoma metastasis. In each case, Metastatin did not have an obvious detrimental effect on the host and was neutralized by complexing with soluble hyaluronan.

Metastatin is a member of a family of hyaluronan-binding proteins that also includes CD44, tumor necrosis factor-stimulated gene 6 (TSG-6), versican, neurocan, and brevican (20). Interestingly, Metastatin is similar to other factors that influence angiogenesis in that it is a fragment of a larger complex. For example, Angiostatin is a fragment of plasminogen, Endostatin represents a fragment of collagen XVIII, and serpin consists of a fragment of antithrombin (21–24). It is possible that the production of the peptide fragments is part of a feedback loop important in the down-regulation of angiogenesis.

In addition to Metastatin, a number of other antiangiogenic factors have been isolated from cartilage. Indeed, cartilage has been extensively studied as a source of molecules that could account for its avascular nature. Langer *et al.* (25) first reported a bovine cartilage fraction isolated by guanidine extraction and purified by trypsin affinity chromatography that inhibited tumor-induced vascular proliferation. In addition, Moses *et al.* (26) have recently isolated Troponin I from veal scapulae, which was shown to have antitumor and antiangiogenic properties. Lee and Langer (27) have described a guanidine-extracted factor from shark cartilage that inhibited angiogenesis and suppressed tumor vascularization. Similarly, Moses *et al.* (18) isolated a factor from cultures of scapular chondrocytes that inhibited angiogenesis in the chicken chorioallantoic membrane and appeared to be a protease inhibitor. However, it is likely that our preparation of Metastatin acts through a distinct mechanism because it has no detectable antiprotease activity and is inhibited by the addition of hyaluronan. It is tempting to speculate that Metastatin may contribute to the avascular nature of cartilage. Along these lines, we have previously found that hypertrophic chondrocytes produce large amounts of free hyaluronan, which may neutralize the effects of Metastatin in this region and thereby allow blood vessels to invade (28).

The results of this study suggest that Metastatin has antiangiogenic properties as demonstrated by its ability to block VEGF-induced formation of blood vessels in the chicken chorioallantoic membrane. The antiangiogenic effect of Metastatin was also consistent with our finding that it blocked both the proliferation and migration of cultured endothelial cells. Whereas Metastatin can directly attach tumor cells, we believe that most of its antitumor activity is due to its inhibition of angiogenesis because after its injection, the first cells that it would encounter are the endothelial cells, which would be exposed to the highest concentration. In addition, this antiangiogenic mechanism is suggested by the fact that Metastatin blocked the growth of TSU cells *in vivo* (*i.e.*, on the chicken chorioallantoic membrane) but had little or no effect on their proliferation *in vitro*. In this particular case, it seems likely that Metastatin was acting indirectly on the TSU tumor cells by blocking angiogenesis.

In other cases, the antitumor activity of Metastatin may be due to the combined action of direct killing of the tumor cells and the inhibition of angiogenesis. Indeed, Metastatin does appear to partially inhibit the growth of B16BL6 in tissue culture, and it could presumably have a similar effect *in vivo*. Because many blood vessels that are associated with tumors are leaky (29), Metastatin may be able to escape the circulation to interact directly with the tumor cells and block their proliferation. Along these lines, a recent study by Maniotis *et al.* (30) has indicated that some tumors have the ability to form

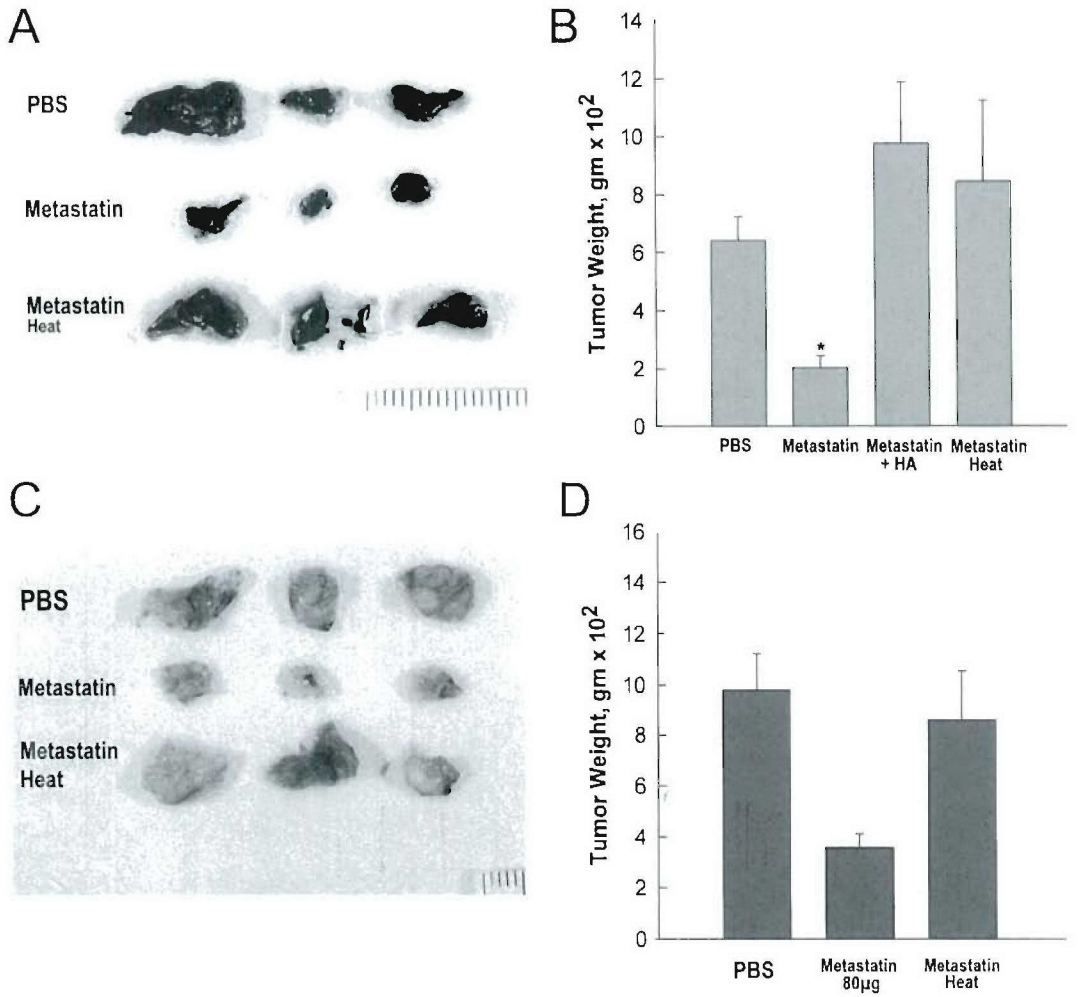

Fig. 7. Effect of Metastatin on the growth of tumor cells on the chicken chorioallantoic membrane. The top of the air sacs of 10-day-old chicken eggs were opened, exposing the chorioallantoic membrane, and pellets containing B16BL6 melanoma or TSU prostate tumor cells were placed on the membrane. On day 3, the embryos were given a single i.v. injection of PBS or Metastatin (80 μg). The tumors and associated chorioallantoic membranes were removed on day 6 and weighed. *A* and *C*, examples of the B16BL6 and TSU xenografts from eggs treated with PBS, Metastatin, or heat-denatured Metastatin. *B* and *D*, the weights of B16BL6 and TSU xenografts from eggs treated with Metastatin and control preparations are shown.

vasculature independent of endothelial cells. The tumor cells themselves appear to take on the characteristics of endothelial cells and are responsible for the formation of blood vessels. It is possible that such dual-acting tumor cells could also respond to Metastatin.

The biological effects of Metastatin appear to be closely linked to its ability to bind hyaluronan. If the preparation of Metastatin was premixed with hyaluronan, then this reversed its inhibitory effects on tumor growth *in vivo* and *in vitro* and its effects on the growth and migration of cultured endothelial cells. This indirectly suggests that Metastatin is binding to hyaluronan associated with the target cell. In the case of endothelial cells, particularly high levels of hyaluronan are localized to the tips of newly forming capillaries in the chicken chorioallantoic membrane and rabbit cornea (2, 3). A variety of other cell types show a similar relationship between proliferation and the production of hyaluronan (31–34). Whereas the hyaluronan present on proliferating tumor and endothelial cells could interact directly with Metastatin in the blood, the hyaluronan in other locations would not be exposed to high concentrations of the complex. Most normal cells would be protected by the fact that high concentrations of hyaluronan are present in connective tissues such as the dermis, lamina propria, and capsules (5, 35, 36), which would help to neutralize the Metastatin that diffused into these regions. It is important to note that under normal physiological conditions, hyaluronan in the blood is maintained at low levels by the liver and lymphatic system (37, 38). Thus, the circulating Metastatin should retain its hyaluronan binding activity.

Cell surface hyaluronan may serve as a target for other inhibitors of angiogenesis and tumor growth. For example, Endostatin, a ~20-kDa fragment of the COOH-terminal of collagen XVIII that inhibits angiogenesis (21, 22), may also be able to bind hyaluronan, as suggested by the presence of specific structural motifs (39). Secondly, a soluble, recombinant version of immunoglobulin fused with CD44 that binds to hyaluronan can inhibit the growth of human lymphoma cells that express CD44 in nude mice (40, 41). TSG-6, which is secreted by a variety of cells after stimulation with inflammatory cytokines, is able to both bind hyaluronan and block tumor cell growth (42). In each of these cases, these factors may be interacting with hyaluronan on the surfaces of target cells to exert their effects on angiogenesis and tumor growth.

In preliminary studies, we have found that Metastatin induces apoptosis in the target cells. However, at present, the mechanism by which Metastatin is able to do this is unclear. One possibility is that after Metastatin has bound to hyaluronan on the cell surface, it is taken up by the cells into lysosomes, where it is broken down into smaller fragments that enter the cytoplasm and induce apoptosis, perhaps by interacting with the mitochondrial membrane. Alternatively, Metasta-

tin could be interacting directly with the plasma membrane of the target cells, causing damage that in turn induces the apoptotic cascade. Clearly, future experiments will be directed toward elucidating the mechanism by which Metastatin induces apoptosis in the target cells.

In conclusion, we have found that Metastatin is able to block tumor growth in two model systems, and this effect depends on its ability to bind hyaluronan. Metastatin appears to target both tumor cells and endothelial cells that are involved in neovascularization. We postulate that during angiogenesis, the endothelial cells up-regulate their synthesis of hyaluronan, which then serves as a target for the injected Metastatin. Thus, Metastatin may represent a new type of antitumor agent, which targets cell surface hyaluronan.

ACKNOWLEDGMENTS

We are grateful to Dr. Theresa LaVallee and Wendy Hembrough for their assistance with the migration assay.

REFERENCES

1. Rooney, P., Kumar, S., Ponting, J., and Wang, M. The role of hyaluronan in tumor neovascularization. Int. J. Cancer, *60:* 632–636, 1995.
2. Ausprunk, D. H., Boudreau, C. L., and Nelson, D. A. Proteoglycans in the microvasculature. II. Histochemical localization in proliferating capillaries of the rabbit cornea. Am. J. Pathol., *103:* 367–375, 1981.
3. Ausprunk, D. H. Distribution of hyaluronic acid and sulfated glycosaminoglycans during blood vessel development in the chick chorioallantoic membrane. Am. J. Pathol., *177:* 313–331, 1986.
4. Mohamadzadeh, M., DeGrendele, H., Arizpe, H., Estess, P., and Siegelman, M. Proinflammatory stimuli regulate endothelial hyaluronan expression and CD44/HA-dependent primary adhesion. J. Clin. Investig., *101:* 97–108, 1998.
5. Green, S. J., Tarone, G., and Underhill, C. B. The distribution of hyaluronate and hyaluronate receptors in the adult lungs. J. Cell Sci., *89:* 145–156, 1988.
6. Eggli, P. S., and Graber, W. Association of hyaluronan with rat vascular endothelial and smooth muscle cells. J. Histochem. Cytochem., *43:* 689–697, 1995.
7. Feinberg, R. N., and Beebe, D. C. Hyaluronate in vasculogenesis. Science (Washington DC), *220:* 1177–1179, 1983.
8. West, D. C., Hampson, I. N., and Kumar, S. S. Angiogenesis induced by degradation products of hyaluronic acid. Science (Washington DC), *228:* 1324–1326, 1985.
9. Deed, R. P., Rooney, P. L., Kumar, J. D., Norton, J., Smith, A., Freemont, J., and Kumar, S. Early-response gene signaling is induced by angiogenic oligosaccharides of hyaluronan in endothelial cells. Inhibition by non-angiogenic, high-molecular-weight hyaluronan. Int. J. Cancer, *71:* 251–256, 1997.
10. Banerjee, S. D., and Toole, B. P. Hyaluronan-binding protein in endothelial cell morphogenesis. J. Cell Biol., *119:* 643–652, 1992.
11. Griffioen, A. W., Goenen, M. J. H., Damen, C. A., Hellwig, S. M. M., van Weering, D. H. J., Vooys, W., Blijham, G. H., and Groenewegen, G. CD44 is involved in tumor angiogenesis; an activation antigen on human endothelial cells. Blood, *90:* 1150–1159, 1997.
12. Banerji, S., Ni, J. Wang, S-X., Clasper, S., Su, J., Tammi, R., Jones, M., and Jackson, D. G. LYVE-1, a new homologue of the CD44 glycoprotein, is a lymph-specific receptor for hyaluronan. J. Cell Biol., *144:* 789–801, 1999.
13. Culty, M., Nguyen, H. A., and Underhill, C. B. The hyaluronan receptor (CD44) participates in the uptake and degradation of hyaluronan. J. Cell Biol., *116:* 1055–1062, 1992.
14. Culty, M., Shizari, M., Thompson, E. W., and Underhill, C. B. Binding and degradation of hyaluronan by human breast cancer cell lines expressing different forms of CD44: correlation with invasive potential. J. Cell. Physiol., *160:* 275–286, 1994.
15. Tengblad, A. Affinity chromatography on immobilized hyaluronate and its applications to the isolation of hyaluronate binding proteins from cartilage. Biochim. Biophys. Acta., *578:* 281–289, 1979.
16. Underhill, C. B., and Zhang, L. Analysis of hyaluronan using biotinylated hyaluronan-binding proteins. Methods Mol. Biol., *137:* 441–447, 1999.
17. Brooks, P. C., Silletti, S., von Schalscha, T. L., Friedlander, M., and Cheresh, D. A. Disruption of angiogenesis by PEX, a noncatalytic metalloproteinase fragment with integrin binding activity. Cell, *92:* 391–400, 1998.
18. Moses, M. A., Sudhalter, J., and Langer, R. Isolation and characterization of an inhibitor of neovascularization from scapular chondrocytes. J. Cell Biol., *119:* 473–482, 1992.
19. Ausprunk, D. H., and Folkman, J. Migration and proliferation of endothelial cells in preformed and newly formed blood vessels during tumor angiogenesis. Microvasc. Res., *14:* 53–65, 1977.
20. Neame, P. J., and Barry, F. P. The link protein. Experientia (Basel), *49:* 393–402, 1993.
21. Folkman, J., and Shing, Y. Angiogenesis. J. Biol. Chem., *267:* 10931–10934, 1992.
22. O'Reilly, M. S., Boehm, T., Shing, Y., Fukai, N., Vasios, G., Lane, W. S., Flynn, E., Birkhead, J. R., Olsen, B. R., and Folkman, J. Endostatin. An endogenous inhibitor of angiogenesis and tumor growth. Cell, *88:* 277–285, 1997.
23. O'Reilly, M. S., Holmgren, L., Shing, Y., Chen, C., Rosenthal, R. A., Moses, M., Lane, W. S., Cao, Y., Sage, E. H., and Folkman, J. Angiostatin. A novel angiogenesis inhibitor that mediates the suppression of metastases by a Lewis lung carcinoma. Cell, *79:* 315–328, 1994.
24. O'Reilly, M. S., Pirie-Sheperd, S., Lane, W. S., and Folkman, J. Antiangiogenic activity of the cleaved conformation of the serpin antithrombin. Science (Washington DC), *285:* 1926–1928, 1999.
25. Langer, R., Brem, H., Falterman, K., Klein, M., and Folkman, J. Isolations of a cartilage factor that inhibits tumor neovascularization. Science (Washington DC), *193:* 70–72, 1976.
26. Moses, M. A., Wiederschain, D., Wu, I., Fernandez, C. A., Ghazizadeh, V., Lane, W. S., Flynn, E., Sytkowski, A., Tao, T., and Langer, R. Troponin I is present in human cartilage and inhibits angiogenesis. Proc. Natl. Acad. Sci. USA, *96:* 2645–2650, 1999.
27. Lee, A., and Langer, R. L. Shark cartilage contains inhibitors of tumor angiogenesis. Science (Washington DC), *221:* 1185–1187, 1983.
28. Pavasant, P., Shizari, M., and Underhill, C. B. Distribution of hyaluronan in the epiphysial growth plate: Turnover by CD44 expressing osteoprogenitor cells. J. Cell Sci., *107:* 2669–2677, 1994.
29. Dvorak, H. F., Nagy, J. A., Dvorak, J. T., and Dvorak, A. M. Identification and characterization of the blood vessels of solid tumors that are leaky to circulating macromolecules. Am. J. Pathol., *133:* 95–109, 1988.
30. Maniotis, A. J., Folberg, R., Hess, A., Seftor, E. A., Gardner, L. M. G., Pe'er, J., Trent, J. M., Meltzer, P. S., and Hendirx, M. J. Vascular channel formation by human melanoma cells *in vivo* and *in vitro:* vasculogenic mimicry. Am. J. Pathol., *155:* 739–752, 1999.
31. Main, N. Analysis of cell-growth-phase-related variation in hyaluronate synthase activity of isolated plasma-membrane fractions of cultured human skin fibroblasts. Biochem. J., *237:* 333–342, 1986.
32. Tomida, M., Koyama, H., and Ono, T. Induction of hyaluronic acid synthetase activity in rat fibroblasts by medium change of confluent cultures. J. Cell. Physiol., *86:* 121–130, 1975.
33. Hronowski, L., and Anastassiades, T. P. The effect of cell density on net rates of glycosaminoglycan synthesis and secretion by cultured rat fibroblasts. J. Biol. Chem., *255:* 10091–10099, 1980.
34. Matuoka, K., Namba, M., and Mitsui, Y. Hyaluronate synthetase inhibition by normal and transformed human fibroblasts during growth reduction. J. Cell Biol., *104:* 1105–1115, 1987.
35. Alho, A. M., and Underhill, C. B. The hyaluronate receptor is preferentially expressed on proliferating epithelial cells. J. Cell Biol., *108:* 1557–1565, 1989.
36. Underhill, C. B. The interaction of hyaluronate with the cell surface: the hyaluronate receptor and the core protein. CIBA Found. Symp., *143:* 87–106, 1989.
37. Fraser, J. R. E., Appelgren, L. E., and Laurent, T. C. Tissue uptake of circulating hyaluronic acid. Cell Tissue Res., *233:* 285–293, 1983.
38. Laurent, T. C., and Fraser, J. R. E. The properties and turnover of hyaluronan. Laurent, removal of HA from the blood. CIBA Found. Symp., *124:* 9–29, 1986.
39. Hohenester, E., Sasaki, T., Olsen, B. R., and Timpl, R. Crystal structure of the angiogenesis inhibitor endostatin at 1.5 A resolution. EMBO J., *17:* 1656–1664, 1998.
40. Sy, M-S., Guo, Y. J., and Stamenkovic, I. Inhibition of tumor growth *in vivo* with a soluble CD44-immunoglobulin fusion protein. J. Exp. Med., *176:* 623–627, 1992.
41. Yu, Q., Toole, B. P., and Stamenkov, I. Induction of apoptosis of metastatic mammary carcinoma cells *in vivo* by disruption of tumor cell surface CD44 function. J. Exp. Med., *186:* 1985–1996, 1997.
42. Wisniewski, H. G., Hua, J-C., Poppers, D. M., Naime, D., Vilcek, J., and Cronstein, B. N. TSG-6, a glycoprotein associated with arthritis, and its ligand hyaluronan exert opposite effects in a murine model of inflammation. J. Immunol., *156:* 1609–1615, 1996.

[CANCER RESEARCH 61, 2434–2438, March 15, 2001]

Advances in Brief

RGD-Tachyplesin Inhibits Tumor Growth[1]

Yixin Chen, Xueming Xu, Shuigen Hong, Jinguo Chen, Ningfei Liu, Charles B. Underhill, Karen Creswell, and Lurong Zhang[2]

Department of Oncology, Lombardi Cancer Center, Georgetown University Medical School, Washington, D.C. 20007 [X-M. X., J. C., N. F., C. B. U., K. C., L. Z.], and The Key Laboratory of China Education Ministry on Cell Biology and Tumor Cell Engineering, Xiamen University, Fujian 361005, People's Republic of China [Y. C., S. H.]

Abstract

Tachyplesin is an antimicrobial peptide present in leukocytes of the horseshoe crab (*Tachypleus tridentatus*). In this study, a synthetic tachyplesin conjugated to the integrin homing domain RGD was tested for antitumor activity. The *in vitro* results showed that RGD-tachyplesin inhibited the proliferation of both cultured tumor and endothelial cells and reduced the colony formation of TSU prostate cancer cells. Staining with fluorescent probes of FITC-annexin V, JC-1, YO-PRO-1, and FITC-dextran indicated that RGD-tachyplesin could induce apoptosis in both tumor and endothelial cells. Western blotting showed that treatment of cells with RGD-tachyplesin could activate caspase 9, caspase 8, and caspase 3 and increase the expression of the Fas ligand, Fas-associated death domain, caspase 7, and caspase 6, suggesting that apoptotic molecules related to both mitochondrial and Fas-dependent pathways are involved in the induction of apoptosis. The *in vivo* studies indicated that the RGD-tachyplesin could inhibit the growth of tumors on the chorioallantoic membranes of chicken embryos and in syngenic mice.

Introduction

Tachyplesin, a peptide from hemocytes of the horseshoe crab (*Tachypleus tridentatus*), can rapidly inhibit the growth of both Gram-negative and -positive bacteria at extremely low concentrations (1, 2). Tachyplesin has a unique structure, consisting of 17 amino acids (KWCFRVCYRGICYRRCR) with a molecular weight of 2,269 and a pI of 9.93. In addition, it contains two disulfide linkages, which causes all six of the basic amino acids (R, arginine; K, lysine) to be exposed on its surface (3). The cationic nature of tachyplesin allows it to interact with anionic phospholipids present in the bacterial membrane and thereby disrupt membrane function (4, 5).

The structural nature of tachyplesin suggested that it might also possess antitumor properties. Tachyplesin can interact with the neutral lipids in the plasma membrane of eukaryotic cells (4, 5). More importantly, because it can interact with the membranes of prokaryotic cells, it is likely that tachyplesin can also interact with the mitochondrial membrane of eukaryotic cells. Indeed, these membranes are structurally similar because mitochondria are widely believed to have evolved from prokaryotic cells that have established a symbiotic relationship with the primitive eukaryotic cell (6). Recent studies have indicated that mitochondria play a critical role in regulating apoptosis in eukaryotic cells (7). The disruption of mitochondrial function results in the release of proteins that normally are sequestered by this organelle. The release of factors, such as cytochrome *c* and Samc, can activate caspases that, in turn, trigger the apoptotic cascade (8, 9). Along these lines, Ellerby *et al.* (10) have found that a cationic antimicrobial peptide (KLAKLAKKLAKLAK) conjugated with a CNGRC homing domain exhibits antitumor activity through its ability to target mitochondria and trigger apoptosis. Because the proapoptotic peptide and tachyplesin belong to the same category of cationic antimicrobial peptide, it seems possible that tachyplesin could have similar antitumor activity.

To explore this possibility, we have examined a chemically synthesized preparation of tachyplesin that was linked to a RGD sequence, which corresponds to a homing domain that allows it to bind to integrins on both tumor and endothelial cells and thereby facilitates internalization of the peptide (11, 12). We found that this synthetic RGD-tachyplesin could inhibit the proliferation of TSU prostate cancer cells and B16 melanoma cells as well as endothelial cells in a dose-dependent manner *in vitro* and reduce tumor growth *in vivo*.

Materials and Methods

Synthesis of RGD-Tachyplesin. Two peptides were chemically synthesized. The test peptide was RGD-tachyplesin (CRGDCGGKWCFRVCYRGICYRRCR), and the control peptide was a scrambled sequence with a similar molecular weight and pI. To impede enzymatic degradation, the NH_2-terminal of the peptide was acetylated, and the COOH-terminal was amidated. Before use, the peptides were dissolved in dimethylformamide and 1% acetate acid, diluted with saline to a concentration of 1 mg/ml, and sterilized by boiling for 15 min in a water bath.

Cell Lines. The TSU human prostate cancer cells, B16 melanoma, Cos-7, and NIH-3T3 were maintained in 10% calf serum and 90% DMEM. The human umbilical vein endothelial cells and ABAE[3] cells were cultured in 20% fetal bovine serum and 80% DMEM containing 10 ng/ml fibroblast growth factor 2 and vascular endothelial growth factor, respectively.

Cell Proliferation Assay. Aliquots of complete medium containing 5000 cells were distributed into a 96-well tissue culture plate. The next day, the media were replaced with 160 μl of fresh media and 40 μl of a solution containing different concentrations of the peptides. One day later, 30 μl of 0.3 μCi of [^{3}H]thymidine in serum-free media were added to each well, and after 8 h, the cells were harvested, and the amount of incorporated [^{3}H]thymidine was determined with a beta counter.

Colony Formation Assay. TSU cells (2×10^4) were suspended in 1 ml of 0.36% agarose in 90% DMEM and 10% calf serum containing 100 μg/ml control peptide or RGD-tachyplesin and then immediately placed on the top of a layer of 0.6% solid agarose in 10% calf serum and 90% DMEM in 6-well plates. Two weeks later, the number of colonies larger than 60 μm in diameter was determined using an Omnicon Image Analysis system (Imaging Products International Inc., Chantilly, VA).

Analysis of Tachyplesin-damaged Cells by Flow Cytometry. Cultures of TSU cells at 80% confluence were treated overnight with 50 μg/ml control peptide or RGD-tachyplesin. The next day, the cells were harvested with 5 mM EDTA in PBS, washed, resuspended in 10% calf serum and 90% DMEM, and then stained with the fluorescent dyes annexin V and propidium iodide, JC-1.

Received 11/22/00; accepted 1/30/01.

The costs of publication of this article were defrayed in part by the payment of page charges. This article must therefore be hereby marked *advertisement* in accordance with 18 U.S.C. Section 1734 solely to indicate this fact.

[1] Supported in part by National Cancer Institute/NIH Grant R29 CA71545; United States Army Medical Research and Materiel Command Grants DAMD17-99-1-9031, DAMD17-98-1-8099, DAMD17-00-1-0081, and PC970502; and Susan G. Komen Breast Cancer Foundation (C. B. U. and L. Z.). Y. C. was a recipient of China Scholarship Council, and L. Z. was a recipient of funding from the visiting scholar foundation for key laboratory at Xiamen University, China.

[2] To whom requests for reprints should be addressed, at Department of Oncology, Lombardi Cancer Center Georgetown University Medical School, 3970 Reservoir Road, NW, Washington, D.C. 20007. Phone: (202) 687-6397; Fax: (202) 687-7505; E-mail: Zhangl@georgetown.edu.

[3] The abbreviations used are: ABAE, adult bovine aorta endothelial; FADD, Fas-associated death domain; CAM, chorioallantoic membrane.

YO-PRO-1, and FITC-dextran, according to manufacturer's instructions (Molecular Probes, Eugene, OR).

Western Blotting. Cultures of TSU and ABAE cells at approximately 80% confluence were treated overnight with 100 μg/ml peptides and then harvested with 1 ml of lysis buffer (1% Triton X-100, 0.5% sodium deoxycholate, 0.5 μg/ml leupetin, 1 mM EDTA, 1 μg/ml pepstatin, and 0.2 mM phenylmethylsulfonyl fluoride). The protein concentration was determined by the BCA method (Pierce, Rockford IL), and 20 μg of protein lysate were loaded onto 4–12% BT NuPAGE gel (Invitrogen, Carlsbad CA), electrophoresed, and transferred to a nitrocellulose membrane. The loading and transfer of equal amounts of protein were confirmed by staining with Ponceau S solution (Sigma, St. Louis, MO). The membranes were blocked with 5% nonfat milk and 1% polyvinylpyrrolidone in PBS for 30 min and then incubated for 1 h with 1 μg/ml antibodies to Fas ligand, FADD, caspase 9, caspase 8, caspase 3, caspase 7, and caspase 6 (Oncogene, Boston, MA). After washing, the membrane was incubated for 1 h with 0.2 μg/ml of peroxidase-labeled antirabbit IgG followed by a chemiluminescent substrate for peroxidase and exposed to enhanced chemiluminescence Hyperfilm MP (Amersham, Piscataway, NJ).

Effect of RGD-Tachyplesin on TSU Tumor Growth on the Chicken CAM. TSU cells (2×10^6) were mixed with equal amounts of control peptide or RGD-tachyplesin (100 μg in 200 μl of saline) and immediately placed on top of the CAMs of 10-day-old chicken embryos (15 eggs/group) and incubated at 37.8°C. Every other day thereafter, 200 μl of PBS containing 100 μg of the peptides were added tropically to the xenografts on the CAMs. Five days later, the xenografts were dissected from the membrane, photographed, and weighed.

Effect of RGD-Tachyplesin on B16 Tumor Growth in Mice. B16 melanoma cells were injected s.c. into the flank of 5-week-old male C57BL/6 mice (5×10^5 cells/site; 5 mice/group) and allowed to establish themselves for 2 days. Every other day thereafter, 250 μg of the control peptide or RGD-tachyplesin was injected i.p. into the mice. At the end of 2 weeks, the mice were sacrificed, and the tumor xenografts were removed, photographed, and weighed.

Statistical Analysis. The mean and SE were calculated from the raw data and then subjected to Student's t test. $P < 0.05$ was regarded as statistical significance.

Results

RGD-Tachyplesin Inhibits the Growth of Tumor and Endothelial Cells *in Vitro*. Because both tumor and endothelial cells play an important role in determining tumor progression, we initially examined the effects of RGD-tachyplesin on the proliferation of both of these cells *in vitro*. As shown in Fig. 1*A*, RGD-tachyplesin inhibited the growth of the cultured cells in a dose-dependent manner, with an EC_{50} of about 75 μg/ml for TSU tumor cells and 35 μg/ml for the endothelial cells. In contrast, the scrambled peptide had no obvious effect on the proliferation of the cells at 100 μg/ml. This effect was also reflected in the morphology of the cells. After exposure to 50 μg/ml RGD-tachyplesin for 12 h, a significant fraction of treated cells had become rounded and detached, whereas few cells did so after treatment with the control peptide (data not shown).

To determine whether nontumorigenic cells were also affected by RGD-tachyplesin, the immortalized cell lines, Cos-7 and NIH-3T3, were tested in the [^{3}H]thymidine incorporation assay. As shown in Fig. 1*B*, when treated with 50 μg/ml RGD-tachyplesin, the extent of inhibition of Cos-7 or NIH-3T3 (0–20%) was less than that of tumor or proliferating endothelial cells (40–75%), indicating that nontumorigenic cells are less sensitive to RGD-tachyplesin.

Next, we examined the effects of the peptides on the growth of TSU cells in soft agar. The ability of cells to grow under such anchorage-independent conditions is one of the characteristic phenotypes of aggressive tumor cells. As shown in Fig. 1*C*, RGD-tachyplesin inhibited the ability of TSU cells to form colonies as compared to the groups of control peptide and vehicle alone.

Treatment with RGD-Tachyplesin Alters Membrane Function. We then examined the mechanism by which RGD-tachyplesin inhibited the proliferation of the tumor and endothelial cells. One possibility was that RGD-tachyplesin damages cell membranes, and this damage, in turn, induces apoptosis.

To examine the extent of apoptosis, TSU cells that had been treated for 1 day with the test or control peptides were stained with FITC-annexin and propidium iodide. FITC-annexin V binds to phosphatidylserine, which is exposed on the outer leaflet of the plasma membrane of cells in the initial stages of apoptosis, whereas propidium iodide preferentially stains the nucleus of dead cells, but not living cells. Fig. 2*A* shows that treatment with RGD-tachyplesin induced apoptosis (annexin V positive, propidium iodide negative) in a greater number of cells than did treatment with the vehicle or control peptide.

This induction of apoptosis could have been due to the disruption of mitochondrial function. To examine this, we used JC-1 staining, which measures the membrane potential of mitochondria. As shown in Fig. 2, *B* and *C*, treatment with RGD-tachyplesin caused a shift in the fluorescence profile from one that was highly red (Fig. 2*B*) to one that was less red and more green (Fig. 2*C*). This indicated that the membrane potential of mitochondria was changed by treatment with RGD-tachyplesin.

We also examined the integrity of the plasma membrane and nuclear membrane after treatment with the scrambled peptide and RGD-tachyplesin using two different fluorescent markers. YO-PRO-1 dye can only stain the nuclei of cells with damaged plasma and nuclear membranes. Fig. 2*D* shows that treatment with RGD-tachyplesin allowed the YO-PRO-1 dye to pass into the nuclei, causing an increase in the fluorescence intensity. Similar results were obtained when the cells were stained with FITC-dextran, which is not taken up by viable, healthy cells but can pass through the damaged plasma membrane of unhealthy cells. Fig. 2*E* shows that cells treated with RGD-tachyplesin took up a greater amount of FITC-dextran (M_r 40,000) than did those treated with the control peptide. These results indicated that the majority of RGD-tachyplesin-treated cells allowed these big molecules to pass their damaged membranes.

The above-mentioned experiments were also carried out with ABAE cells, and similar results were obtained (data not shown). Presumably, RGD-tachyplesin induces apoptosis in both TSU and ABAE cells by damaging their membranes.

RGD-Tachyplesin Triggers Apoptotic Pathways. Apoptosis can be induced by two mechanisms: (*a*) the mitochondrial pathway; and (*b*) the death receptor pathway (13). To identify the nature of the apoptotic pathway triggered by RGD-tachyplesin, both TSU and ABAE cells were treated overnight with RGD-tachyplesin and control peptide and then analyzed by Western blotting for the alterations of molecules involved in the mitochondrial and Fas-dependent pathways. Fig. 3 shows that treatment of both TSU tumor cells and ABAE cells with RGD-tachyplesin caused the cleavage of M_r 46,000 caspase 9 into subunits of M_r 35,000 and M_r 10,000, indicating activation of the mitochondrial-related, Fas-independent pathway. In addition, RGD-tachyplesin treatment could up-regulate the expression of upstream molecules in the Fas-dependent pathway, including Fas ligand (M_r 43,000), FADD (M_r 28,000), and activate subunits of caspase 8 (M_r 18,000). Furthermore, the downstream effectors, such as caspase 3 subunits (M_r 20,000), caspase 6 (M_r 40,000), and caspase 7 (M_r 34,000), were also up-regulated by RGD-tachyplesin. These results suggest that RGD-tachyplesin induces apoptosis through both the mitochondrial-related, Fas-independent pathway and the Fas-dependent pathway. However, because there is cross-talk between these two pathways (13), we do not have enough evidence to determine which one is the initiator.

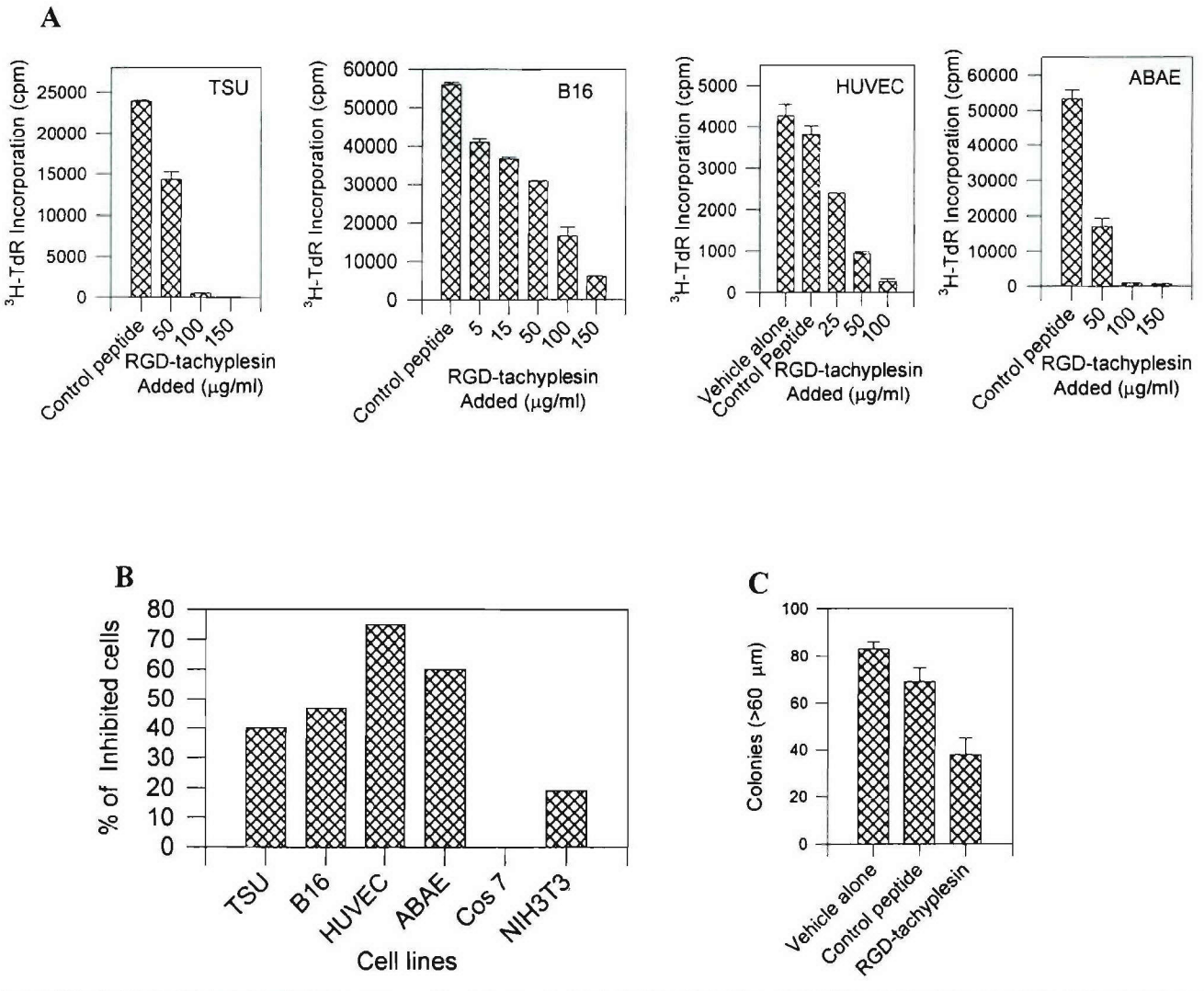

Fig. 1. Effects of RGD-tachyplesin and scrambled peptide on cell proliferation. *A*, effect of RGD-tachyplesin on cell proliferation. TSU cells were treated with vehicle alone, 100 μg/ml control peptide, or different doses of RGD-tachyplesin for 24 h, followed by a [^{3}H]thymidine incorporation assay. The proliferation of both the tumor and endothelial cells was greatly inhibited by RGD-tachyplesin in a dose-dependent manner ($P < 0.01$). *B*, effect of RGD-tachyplesin on different cell lines. The cells were treated overnight with 50 μg/ml control peptide or RGD-tachyplesin and then treated with [^{3}H]thymidine. The rate of inhibition was calculated as follows: (1 − cpm of cells treated with RGD-tachyplesin/cpm of cells treated with control peptide) × 100%. The nontumorigenic cell lines Cos-7 and NIH-3T3 were inhibited to a lesser degree than the tumor or endothelial cells ($P < 0.05$). *C*, effect of RGD-tachyplesin on colony formation of TSU cells. TSU cells were suspended in 0.36% agarose containing 100 μg/ml control peptide or RGD-tachyplesin and then placed on top of 0.6% agarose. Two weeks later, colonies larger than 60 μm were counted with the Omnicon Image Analysis system. The colony formation of TSU cells was inhibited by RGD-tachyplesin ($P < 0.01$). All of the experiments were repeated three times, and similar results were obtained.

RGD-Tachyplesin Inhibits the Growth of TSU and B16 Tumor *in Vivo*. In the final series of experiments, we examined the *in vivo* effects of RGD-tachyplesin on the growth of TSU or B16 tumor cells in CAM (14) or mouse models. As shown in Fig. 4, the TSU tumor xenografts growing in CAM in the group treated with RGD-tachyplesin (Fig. 4*B*) were smaller than those in the group treated with control peptide (Fig. 4*A*). In addition, the average weight of the xenografts in the RGD-tachyplesin-treated group was significantly less than that of xenografts in the control group (Fig. 4*C*). Similarly, in the B16 mouse model, the B16 tumor xenografts in the RGD-tachyplesin-treated group (Fig. 4*E*) were smaller than those in the control group (Fig. 4*D*), and this difference was statistically significant ($P < 0.05$; Fig. 4*F*). It should be noted that RGD-tachyplesin did not appear to be toxic to the mice, as judged by their weights and activity at the end of the experiment. Thus, the results from two models are consistent with each other, indicating that RGD-tachyplesin can inhibit tumor growth *in vivo*.

Discussion

The major conclusion of this study is that RGD-tachyplesin can inhibit tumor growth by inducing apoptosis in the tumor cells and the associated endothelial cells. This conclusion was supported by the following observations. First, RGD-tachyplesin was able to inhibit the growth of TSU tumor cells on the CAM of chicken embryos as well as the growth of B16 tumor cells in syngenic mice. Second, RGD-tachyplesin also blocked the proliferation of both tumor and endothelial cells in culture in a dose-dependent fashion, whereas proliferation was relatively unaffected in nontumorigenic cell lines Cos-7 and NIH-3T3. Third, RGD-tachyplesin induced apoptosis in cultured TSU cells, as indicated by staining with fluorescent markers for apoptosis including FITC-annexin V, which detects exposed phosphatidylserine, and JC-1, which tracks mitochondrial membrane potential. Finally, RGD-tachyplesin stimulated the activation and production of several molecules in the apoptotic cascade in both TSU and endothelial cells, as judged by Western blotting.

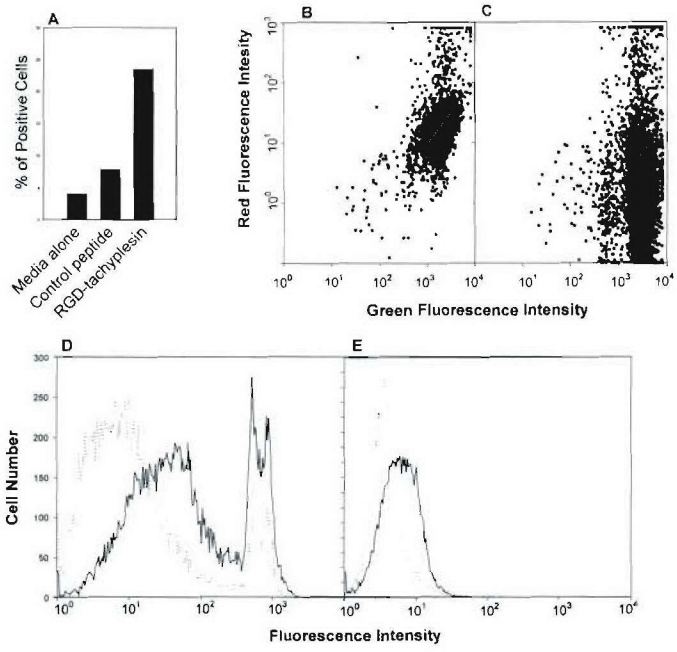

Fig. 2. The effect of RGD-tachyplesin on the function of TSU cells. TSU cells were treated overnight with 50 μg/ml control peptide or RGD-tachyplesin and then stained with different membrane probes. *A*, staining with annexin V and propidium iodide for apoptotic cells. The percentage of cells that were positive for FITC-annexin V and negative for propidium iodide was analyzed by flow cytometry. The RGD-tachyplesin-treated cells had a high percentage of apoptotic cells ($P < 0.01$). *B* and *C*, staining with JC-1 for mitochondrial membrane potential. The cells treated with the control peptide (*B*) and RGD-tachyplesin (*C*) were stained with 10 μg/ml JC-1 for 10 min and then analyzed by flow cytometry. The RGD-tachyplesin shifted the spectrum of the cells from high red (*B*, healthy) to high green and low red (*C*, loss mitochondrial potential). *D*, staining with YO-PRO-1 for integrity of nuclei membrane. The peptide-treated cells were stained with 0.1 μg/ml YO-PRO-1 dye, an indicator for damaged nuclei membranes (the *first peak* represents the dye-stained G_0-G_1-phase cells; the *second peak* represents the dye-stained S-M-phase cells). The RGD-tachyplesin treated cells shift from right to left, indicating the loss of integrity of the nuclei membrane. *E*, staining with FITC-dextran for integrity of plasma membrane. The peptide-treated cells were incubated with 50 μg/ml FITC-dextran (M_r 40,000) for 30 min and analyzed with flow cytometry. A higher proportion of RGD-tachyplesin-treated cells allowed FITC-dextran to pass through their plasma membrane as compared to the control.

Our results also suggest that RGD-tachyplesin up-regulates apoptosis related to both the mitochondrial and the death receptor pathways. The involvement of the mitochondrial pathway was suggested by the facts that staining with JC-1 indicated the membrane potential of mitochondria was decreased (Fig. 2, *B* and *C*) and that the caspase 9 was activated (Fig. 3) in cells treated with RGD-tachyplesin. Presumably, this resulted from the release of cytochrome *c*, which, in turn, bound to Apaf-1 and activated caspase 9 and then caspase 3, caspase 7, and caspase 6 (13, 15–17). This is the mechanism by which the peptide described by Ellerby *et al.* (10) induced apoptosis. In addition, we found that members of the death receptor pathway (Fas ligand, FADD, and caspase 8) were also up-regulated. Thus, RGD-tachyplesin may have multiple effects on the target cells. It is difficult at this point to determine what initial event is responsible for the RGD-tachyplesin-induced activation of apoptosis.

There appears to be considerable cross-talk between the mitochondrial apoptotic pathway and Fas-dependent pathway. The caspase 6 activated by the mitochondrial pathway (cytochrome *c*→Apaf-1→caspase 9→caspase 3) could act on FADD and then on caspase-8, which triggered the Fas-dependent pathway. On the other hand, the caspase 8-activated Fas-FADD pathway could act on BID that stimulates the mitochondrial pathway (15–17). This cross-talk creates positive feedback and enhances the apoptosis cascade.

RDG-tachyplesin also appeared to be relatively nontoxic to cells not associated with tumors. When RGD-tachyplesin was administered at a concentration that inhibited tumor growth, there was no notable side effects on either the chicken embryos or mice with regard to animal body weight and activity at the end of each experiment. In addition, studies on cultured cells indicated that the sensitivity to RGD-tachyplesin varied depending on cell type. In comparison to tumor cells and proliferating endothelial cells, immortalized cells such as Cos-7 (green monkey kidney cells) and NIH-3T3 (fibroblast cells) were less sensitive to RGD-tachyplesin. Taken together, these results suggest that RGD-tachyplesin is a well-tolerated peptide.

RGD-tachyplesin also appears to be more potent than similar cationic peptides. The unique cyclic structure of tachyplesin maintained by two disulfide bonds may make it more effective in targeting membranes than the linear antimicrobial peptides, such as KLAK-LAKKLAKLAK (a proapoptotic peptide; Ref. 10), which is suggested by its lower minimal inhibition concentration on both *Escherichia coli* and *Staphylococcus aureus* of 2 *versus* 6 μM (18, 19). Furthermore, tachyplesin interacts not only with anionic phospholipids of bacterial and mitochondria but also with neutral lipids of eukaryotic plasma membrane (4, 5, 18). Ellerby *et al.* (10) reported that their proapoptotic peptide inhibited proliferation with an EC_{50} of about 100 μg/ml for endothelial cells, whereas our results indicated that RGD-tachyplesin had a much stronger efficacy on proliferating

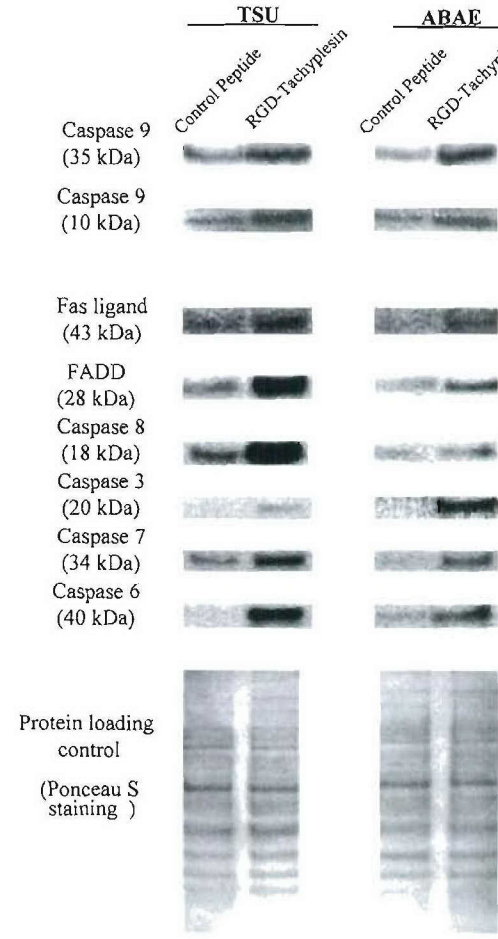

Fig. 3. Effect of RGD-tachyplesin on molecules involved in the apoptosis cascade. Twenty μg of lysate from TSU and ABAE cells treated with 100 μg/ml control peptide or RGD-tachyplesin were loaded onto a 4–12% BT NuPAGE gel, electrophoresed, and transferred to a nitrocellulose membrane. The loading and transfer of equal amounts of protein were confirmed by staining with a Ponceau S solution. After blocking with 5% nonfat milk, the membranes were incubated for 1 h with 1 μg/ml antibodies to caspase 9, Fas ligand, FADD, caspase 8, caspase 3, caspase 7, and caspase 6 followed by horseradish peroxidase-conjugated antirabbit IgG and enhanced chemiluminescence substrate and finally exposed to Hyperfilm MP.

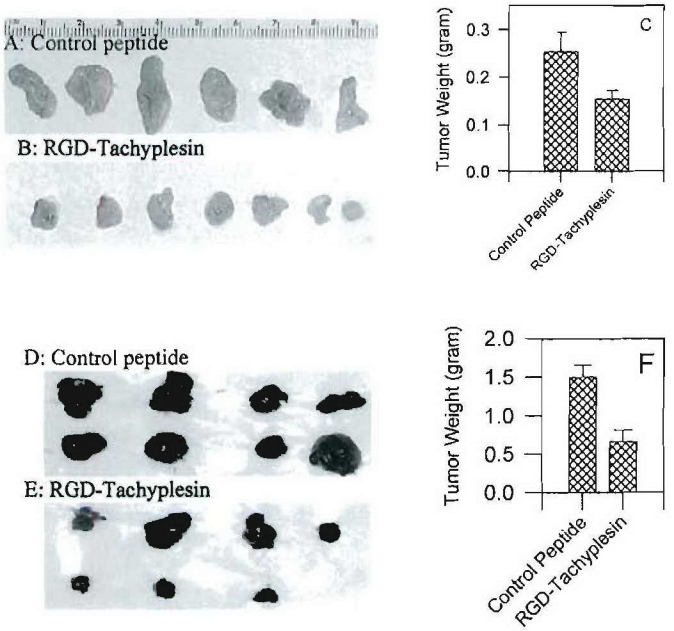

Fig. 4. Effect of RGD-tachyplesin on tumor growth *in vivo*. *A–C*, effect of RGD-tachyplesin on the TSU xenografts on CAM. TSU cells (2×10^6) were mixed with either control peptide or RGD-tachyplesin (100 μg) and immediately placed on top of the CAM of 10-day-old chicken embryos and incubated at 37.8°C. Every other day, additional peptides were applied tropically to the TSU xenografts. Five days later, the xenografts were removed from the CAM, photographed, and weighed. The TSU xenografts treated with RGD-tachyplesin were significantly smaller than those treated with the control peptide ($P < 0.01$). *D–F*, effect of RGD-tachyplesin on tumor growth in the mouse model. B16 melanoma cells (5×10^5) were injected s.c. into the flank of C57BL/6 mice and allowed to establish themselves for 2 days. Every other day after that, 250 μg of control peptide or RGD-tachyplesin were injected i.p. into the mice. At the end of 2 weeks, the mice were sacrificed, and the xenografts were removed, photographed, and weighed. The B16 xenografts from animals treated with RGD-tachyplesin were significantly smaller than those from animals treated with the control peptide ($P < 0.01$).

endothelial cells, with an EC_{50} of about 35 μg/ml. Furthermore, RGD-tachyplesin acts not only on proliferating endothelial cells but also on tumor cells. This dual effect of RGD-tachyplesin will enhance its antitumor function.

In conclusion, this study demonstrates that RGD-tachyplesin can be used as an antitumor agent. By disrupting vital membranes and inducing apoptosis, it inhibits all of the tumor cells tested. Further study of RGD-tachyplesin and its analogues may lead to finding a new category of antitumor drug.

Acknowledgments

The animal protocols were reviewed and approved by the Animal Care and Use Committee of Georgetown University.

References

1. Kokryakov, V. N., Harwig, S. S., Panyutich, E. A., Shevchenko, A. A., Aleshina, G. M., Shamova, O. V., Korneva, H. A., and Lehrer, R. I. Protegrins. Leukocyte anti-microbial peptides that combine features of corticostatic defensins and tachyplesins. FEBS Lett., *327:* 231–236, 1993.
2. Shigenaga, T., Muta, T., Toh, Y., Tokunaga, F., and Iwanaga, S. Anti-microbial tachyplesin peptide precursor. cDNA cloning and cellular localization in the horseshoe crab (*Tachypleus tridentatus*). J. Biol. Chem., *265:* 21350–21354, 1990.
3. Nakamura, T., Furunaka, H., Miyata, T., Tokunaga, F., Muta, T., Iwanaga, S., Niwa, M., Takao, T., and Shimonishi, Y. Tachyplesin, a class of anti-microbial peptide from the hemocytes of the horseshoe crab (*Tachypleus tridentatus*). Isolation and chemical structure. J. Biol. Chem., *263:* 16709–16713, 1988.
4. Park, N. G., Lee, S., Oishi, O., Aoyagi, H., Iwanaga, S., Yamashita, S., and Ohno, M. Conformation of tachyplesin I from *Tachypleus tridentatus* when interacting with lipid matrices. Biochemistry, *31:* 12241–12247, 1992.
5. Katsu, T., Nakao, S., and Iwanaga, S. Mode of action of an anti-microbial peptide, tachyplesin I, on biomembranes. Biol. Pharm. Bull., *16:* 178–181, 1993.
6. Gray, M. W., Burger, G., and Lang, B. F. Mitochondrial evolution. Science (Washington DC), *283:* 1476–1481, 1999.
7. Brenner, C., and Kroemer, G. Mitochondria: the death signal integrators. Science (Washington DC), *289:* 1150–1151, 2000.
8. Li, H., Kolluri, S. K., Gu, J., Dawson, M. I., Cao, X., Hobbs, P. D., Lin, B., Chen, G., Lu, J., Lin, F., Xie, Z., Fontana, J. A., Reed, J. C., and Zhang, X. Cytochrome *c* release and apoptosis induced by mitochondrial targeting of nuclear orphan receptor TR3. Science (Washington DC), *289:* 1159–1164, 2000.
9. Du, C., Fang, M., Li, Y., Li, L., and Wang, X. Smac, a mitochondrial protein that promotes cytochrome *c*-dependent caspase activation by eliminating IAP inhibition. Cell, *102:* 33–42, 2000.
10. Ellerby, H. M., Arap, W., Ellerby, L. M., Kain, R., Andrusiak, R., Rio, G. D., Krajewski, S., Lombardo, C. R., Rao, R., Ruoslahti, E., Bredesen, D. E., and Pasqualini, R. Anti-cancer activity of targeted pro-apoptotic peptides. Nat. Med., *5:* 1032–1038, 1999.
11. Arap, W., Pasqualini, R., and Ruoslahti, E. Cancer treatment by targeted drug delivery to tumor vasculature in a mouse model. Science (Washington DC), *279:* 377–380, 1998.
12. Brooks, P. C., Clark, R. A. F., and Cheresh, D. A. Requirement of vascular integrin $\alpha_v\beta_3$ for angiogenesis. Science (Washington DC), *264:* 569–571, 1994.
13. Kaufmann, S. H., and Earnshaw, W. C. Induction of apoptosis by cancer chemotherapy. Exp. Cell Res., *256:* 42–49, 2000.
14. Brooks, P. C., Silletti, S., von Schalscha, T. L., Friedlander, M., and Cheresh, D. A. Disruption of angiogenesis by PEX, a noncatalytic metalloproteinase fragment with integrin binding activity. Cell, *92:* 391–400, 1998.
15. Liu, X., Kim, C. N., Yang, J., Jemmerson, R., and Wang, X. Induction of apoptotic program in cell-free extracts: requirement for dATP and cytochrome *c*. Cell, *86:* 147–157, 1996.
16. Desagher, S., Osen-Sand, A., Nichols, A., Eskes, R., Montessuit, S., Lauper, S., Maundrell, K., Antonsson, A., and Martinou, J. C. Bid-induced conformational change of Bax is responsible for mitochondrial cytochrome *c* release during apoptosis. J. Cell Biol., *144:* 891–901, 1999.
17. Slee, E. A., Harte, M. T., Kluck, R. M., Wolf, B. B., Casiano, C. A., Newmeyer, D. D., Wang, H-G. Reed, J. C., Nicholson, D. W., Alnemri, E. S., Green, D. R., and Martin, S. J. Ordering the cytochrome *c*-initiated caspase cascade: hierarchical activation of caspases-2, -3, -7, -8, and -10 in a caspase-9-dependent manner. J. Cell Biol., *144:* 281–292, 1999.
18. Matsuzaki, K. Why and how are peptide-lipid interactions utilized for self-defense? Magainins and tachyplesins as archetypes. Biochim. Biophys. Acta, *1462:* 1–10, 1999.
19. Javadpour, M. M., Juban, M. M., Lo, W. C., Bishop, S. M., Alberty, J. B., Cowell, S. M., Becker, C. L., and McLaughlin, M. L. *De novo* anti-microbial peptides with low mammalian cell toxicity. J. Med. Chem., *39:* 3107–3113, 1996.

[CANCER RESEARCH 63, 5685–5690, September 15, 2003]

Advances in Brief

A Peptide with Three Hyaluronan Binding Motifs Inhibits Tumor Growth and Induces Apoptosis[1]

Xue-Ming Xu,[2] Yixin Chen,[3] Jinguo Chen, Shanmin Yang, Feng Gao,[4] Charles B. Underhill, Karen Creswell, and Lurong Zhang[5]

Department of Oncology, Lombardi Cancer Center, Georgetown University Medical School, Washington, DC 20057

Abstract

A number of hyaluronan (HA) binding proteins such as soluble CD44, receptor for hyaluronan-mediated motility (RHAMM), and metastatin inhibit tumor growth and metastasis. To determine whether the HA binding motif is the element responsible for the antitumor effect of this family of proteins, we examined the biological activity of a 42-amino acid peptide (designated as BH-P) that contains three HA binding motifs [B(X_7)B] from human brain HA binding protein. In initial experiments with cultured cells, we found that synthetic BH-P inhibited the proliferation and colony formation of tumor cells. It also blocked the growth of tumors on the chorioallantoic membranes of 10-day chicken embryos. In addition, MDA-435 melanoma cells that had been transfected with an expression vector for BH-P grew at a slower rate in nude mice than the vector-alone transfectants. Final studies revealed that the BH-P could activate caspase-8, caspase-3, and poly(ADP-ribose) polymerase and trigger the apoptosis of tumor cells. Taken together, these results suggest that the HA binding motif that is present in HA binding proteins may be responsible for the antitumor effect exerted by the members of this family.

Introduction

The members of the family of HA[6] binding proteins (HABPs) can be divided into two major groups: membrane-bound forms, such as soluble CD44 (1) and receptor for HA-mediated motility (2); and extracellular forms, such as aggrecan (3) and link protein (4). These HABPs have been implicated in a number of cellular functions such as migration, adhesion (5), growth, differentiation, and apoptosis (6–8). Many of these functions are important in tumor progression (6, 9, 10).

In contrast to membrane-bound HA receptors, the truncated soluble forms of HA receptors have been found to possess antitumor activity (11–13). For example, a soluble recombinant CD44 disrupted the interaction between CD44 and HA and inhibited tumor formation and metastasis (11, 12). Similarly, a soluble form of RHAMM blocked the ability of tumor cells to form lung metastases (13). Importantly, clinical data have demonstrated that a high level of soluble CD44 in the serum was associated with a favorable clinical outcome in ovarian cancer (14). Conversely, low serum levels of soluble CD44 variant 6 were associated with poor prognosis of patients with pancreatic carcinoma (15). These findings suggest that soluble HA receptors shed from tumor cells might trigger a signaling pathway to block tumor cell growth.

In addition, the extracellular forms of HABPs also exhibit antitumor activity. The most notable example is cartilage, which contains particularly large amounts of HABPs (16). Because cartilage is an avascular tissue and relatively tumor resistant (17), thousands of cancer patients have taken oral preparations of cartilage as an alternative medicine, based on a belief that it contains natural antitumor substances. Although the therapeutic value of this approach is still controversial (18, 19), in some patients, cartilage does exhibit an anticancer activity (20–23). Indeed, several proteins and peptides isolated from cartilage have been found to have both antitumor and antiangiogenic activity (24–27). Along these lines, we have purified HABPs from bovine cartilage by affinity chromatography and found that it inhibits tumor growth and angiogenesis (28).

Because several different members of the HABP family have inhibitory effects on tumor growth, metastasis, and angiogenesis (20–28), it is possible that the commonly shared HA binding motif B(X_7)B of HABPs is responsible for these effects. B(X_7)B is the minimal amino acid composition required for HA binding and consists of two basic amino acids (either arginine or lysine) flanking a sequence of seven amino acids (29). It is highly conserved in members of the HABP family, and each member contains several such motifs. We speculate that the peptide that contains HA binding motifs might also exert antitumor activity.

To test this hypothesis, we synthesized or expressed BH-P containing 42 amino acids with three HA binding motifs derived from human brain HABP and examined its antitumor activity both *in vitro* and *in vivo*. The results suggest that the peptide enriched in HA binding motifs possesses an antitumor activity that may be mediated by the induction of apoptosis.

Materials and Methods

Synthesis of BH-P. BH-P (CNGRCGGRRAVLGSPRVKWTFLSRGRG-GRGVRVKVNEAYRFR) contains three HA binding motifs from the NH_2 terminus of the human brain HABP (GenBank accession number AY007241). It has a molecular mass of 4,736 and an isoelectric point of 12.01. The control peptide (control-P) consists of the same amino acids with a scrambled sequence. To impede enzymatic degradation, the NH_2 terminus of the synthetic peptides was acetylated, and the COOH terminus was amidated. Before use, the peptides were dissolved in dimethylformamide and 1% acetate acid, diluted with saline to a concentration of 1 mg/ml, and sterilized by boiling for 15 min.

HA Binding Assay. Fifty μg of BH-P or control-P in 100 μl of PBS were mixed with 20 μl of [^{3}H]HA (5×10^5 cpm/μg, 490 μg/ml; Ref. 30) in the presence and absence of 50-fold excess of cold HA, incubated for 1 h, and then applied to nitrocellulose membranes on a dot blot apparatus. The free [^{3}H]HA

Received 4/26/03; revised 7/8/03; accepted 7/30/03.

The costs of publication of this article were defrayed in part by the payment of page charges. This article must therefore be hereby marked *advertisement* in accordance with 18 U.S.C. Section 1734 solely to indicate this fact.

[1] This work was supported by United States Army Medical Research and Materiel Command Contracts DAMD17-00-1-0081 and DAMD17-01-1-0708 and National Cancer Institute/NIH Grant R29 CA71545 (to L. Z.). Y. C. was a recipient of a Visiting Scholar Award from the Key Laboratory of China Education Ministry on Cell Biology and Tumor Cell Engineering, Xiamen University, Fujian, People's Republic of China.

[2] Present address: NIH/National Cancer Institute, 9000 Rockville Pike, Bethesda, MD 20892.

[3] The Key Laboratory of China Education Ministry on Cell Biology and Tumor Cell Engineering, Xiamen University, Fujian, P.R.C.

[4] Dept. of Laboratory Medicine, No. 6 People's Hospital of Jiaotong University Medical School, Shanghai, P.R.C.

[5] To whom requests for reprints should be addressed, at Department of Oncology, Georgetown University Medical Center, 3970 Reservoir Road, NW, Washington, DC 20007. Phone: (202) 687-6397; Fax: (202) 687-7505; E-mail: zhangl@georgetown.edu.

[6] The abbreviations used are: HA, hyaluronan; HABP, HA binding protein; RHAMM, receptor for HA-mediated motility; Z-VAD-FMK, benzyloxycarbonyl-Val-Ala-Asp-fluoromethyl ketone; Z-VDVAD-FMK, benzyloxycarbonyl-Val-Asp-Val-Ala-Asp-fluoromethyl ketone; CAM, chorioallantoic membrane; PARP, poly(ADP-ribose) polymerase.

was washed away with PBS, and each dot was cut out individually and counted for radioactivity.

Cell Proliferation Assay. Aliquots of complete medium containing 5,000 MDA-435 melanoma cells were distributed into a 96-well tissue culture plate. On the following day, the medium in each well was replaced with 160 μl of fresh medium and 40 μl of solution containing different concentrations of the peptides. One day later, 0.3 μCi of [^{3}H]thymidine in 30 μl of serum-free medium were added to each well. After 8 h, the cells were harvested, and the amount of incorporated [^{3}H]thymidine was determined with a beta counter. In some cases, 200 μg/ml of HA (Lifecore, Chaska, MN), 20 units/ml of testicular hyaluronidase (H4272; Sigma, St. Louis, MO), 40 μM Z-VAD-FMK (a pan-caspase inhibitor), or 20 μM Z-VDVAD-FMK (an inhibitor for caspase-2, -3, and -7) was added with the peptides to determine whether the effects of BH-P could be blocked.

Colony Formation Assay. Twenty thousand MDA-435 cells were suspended in 1 ml of 0.36% agarose in complete medium containing 100 μg/ml (21 μM) of control-P or BH-P, and then the cells were placed immediately on the top layer of 0.6% solid agarose in complete medium in 6-well plates. Two weeks later, the number of colonies >60 μm in diameter was determined using an Omnicon Image Analysis System (Imaging Products International, Inc., Chantilly, VA).

Tumor Growth on the Chicken CAM. Three million MDA-435 cells or one million B16 melanoma cells were placed on top of the CAMs of 10-day-old chicken embryos (15 eggs/group) and incubated at 37.8°C for 2 days to allow the tumors to become established. Then, 200 μg of control-P or BH-P in 200 μl of PBS were either i.v. injected into the CAMs once (in the B16 model) or tropically administrated onto the tumor xenografts (in MDA-435 model) on the CAMs on a daily basis. Five days later, the xenografts were dissected from the membrane, photographed, and weighed.

Construction of Expression Vector of BH-P and Transfection of MDA-435 Cells. The BH-P amino acid sequence was back-translated into a cDNA sequence (5′-TGC AAC GGT CGT TGC GGT GGT CGT CGT GCT GTT CTG GGT TCC CCG CGT GTT AAA TGG ACC TTC CTG TCC CGT GGT CGT GGT GGT CGT GGT GTT CGT GTT AAA GTT AAC GAA GCT TAC CGT TTC CGT TAA-3′) using the GCG-Lite - Protein Sequence Analysis of NIH online software. Two oligo DNAs of either forward or reverse direction of BH-P cDNA with 15-bp overlap were synthesized, annealed to each other, and extended using Pwo DNA polymerase (Roche). The extended full-length BH-P DNA was used as template for its amplification using PCR and two primers from each end of BH-P cDNA. The PCR products were inserted into the pSecTag vector, which has a cytomegalovirus promoter and Igκ signal peptide for secretion (Invitrogen, Carlsbad, CA). The correct reading frame of BH-P cDNA in the pSecTag vector was confirmed by DNA sequencing. The pSecTag-BH-P or vector alone was transfected into MDA-435 cells using the calcium precipitation method. The control or BH-P transfectants that survived in 800 μg/ml of G418 and were positive for the expression of BH-P, as detected by RT-PCR, were pooled and expanded for further *in vivo* studies.

Tumor Growth in Nude Mice. Transfected MDA-435 cells (3×10^6) were injected into the mammary fat pads of nude mice. The size of the tumor xenografts was measured twice a week, and the tumor volumes were calculated from the following formula: (length × width^2)/0.52. Two months later, the mice were sacrificed, and the tumors were harvested and weighed. The tumor xenografts formed by pSecTag-BH-P transfected cells were compared with those formed by the cells transfected with the control vector. The animal protocols were reviewed and approved by the Animal Care and Use Committee of Georgetown University.

Cell Binding Assay. FITC-BH-P (1 μg/ml), with or without 100-fold excess BH-P, was added to MDA-435 cells cultured on cover slips and incubated at 4°C for 30 min. The cells were washed with cold PBS and fixed with freshly prepared, buffered 4% formaldehyde and then examined with a confocal microscope.

Cell Surface HA Binding Assay. MDA-435 or TSU tumor cells were harvested with EDTA-PBS and pretreated with 50 units/ml of testicular hyaluronidase at 37°C for 30 min and then mixed with FITC-BH-P (1 μg/ml) with or without a 100-fold excess of HA at 4°C for 30 min. The binding of FITC-BH-P to the cell surface was analyzed by flow cytometry.

FITC-Dextran Staining. To determine whether BH-P damaged the plasma membrane, we probed the cells with FITC-dextran. MDA-435 cells at ~80% confluence were treated with 100 μg/ml of control-P or BH-P overnight, harvested with 5 mM EDTA in PBS, washed, and resuspended in 10% calf serum, 90% DMEM and incubated for 1 h to allow the cells to recover from possible damage during harvesting. The cells were then treated with 5 μg/ml of FITC-dextran (Molecular Probes, Eugene, OR) for 10 min at room temperature, fixed with 4% paraformaldehyde, and subjected to flow cytometry analysis.

Western Blotting. Both cultured MDA-435 cells and tumor xenografts formed by MDA-435 transfected cells were analyzed for apoptosis-related molecules. Cultures of MDA-435 cells at ~80% confluence were treated with 100 μg/ml of either control-P or BH-P overnight and then harvested with 1.0 ml of lysis buffer (1% Triton X-100, 0.5% sodium deoxycholate, 0.5 mg/ml leupeptin, 1 mM EDTA, 1 mg/ml pepstatin, and 0.2 mM phenylmethylsulfonyl fluoride). The tumors (25–30 mg) formed by MDA-435 transfectants in nude mice were immersed in liquid nitrogen, homogenized, and lysed in 1.0 ml of lysis buffer. The concentration of protein in cell lysate was determined with the BCA reagent (Pierce, Rockford, IL), and 20 μg of protein from each lysate were loaded onto a 4–12% BT NuPAGE gel, electrophoresed, and transferred to a nitrocellulose membrane. The membranes were blocked with 5% nonfat milk in PBS for 30 min and then incubated for 1 h with 1 μg/ml primary antibodies against caspase-8, caspase-3, PARP, and α-tubulin and followed by peroxidase-labeled secondary antibodies and Super-signal Western reagents (Pierce).

Detection of DNA Fragmentation. MDA-435 cells and TSU human bladder cancer cells were cultured with either 100 μg/ml control-P or BH-P for 24 h, harvested with 10 mM EDTA, and washed once with PBS. The cell pellets were suspended in 1 ml of buffer (150 mM NaCl, 50 mM EDTA, pH 8.0, 1% SDS, and 0.5 mg/ml of proteinase K) and incubated at 55°C for 16 h. After extraction with phenol and chloroform, the genomic DNA was precipitated with ethanol. The DNA pellets were dissolved in 100 μl of TE buffer [10 mM Tris (pH 8)-1 mM EDTA], and then 15 μl of samples were electrophoresed in a 1.5% agarose gel, stained with ethidium bromide, and photographed.

Statistical Analysis. The mean and SE were calculated from the raw data and then subjected to Student's *t* test. $P < 0.05$ was regarded as statistically significant.

Results

Synthetic BH-P Binds to HA. In initial experiments, we tested the synthetic BH-P for its ability to bind to HA. As shown in Fig. 1*A*, BH-P had significant [^{3}H]HA binding activity that could be blocked by a 50-fold excess of cold HA. In contrast, the control-P showed little or no binding to [^{3}H]HA, indicating that the binding of BH-P to HA was specific.

BH-P Inhibits the Growth of Tumor Cells *in Vitro*. When BH-P was added to the medium of cultured MDA-435 cells for 18–24 h, it caused the cells to become rounded and detached, whereas the control peptide had no such effect (data not shown). To quantitatively measure the extent of this inhibitory effect, the cells were subjected to a [^{3}H]thymidine incorporation assay. Figure 1*B* shows that the proliferation of MDA-435 tumor cells was inhibited by BH-P in a dose-dependent manner with an EC_{50} of ~100 μg/ml. In contrast, control-P had no effect, even at a concentration of 200 μg/ml (Fig. 1*B*, *first column*). In addition, BH-P also inhibited the colony formation of these tumor cells under anchorage-independent conditions on soft agar (Fig. 1*C*).

When BH-P was tested on a panel of cultured cells, its effects varied depending on the cell type. BH-P appeared to have a greater effect on tumor cells than on the relatively normal cell lines Cos-7 (green monkey kidney cells) and NIH-3T3 (fibroblast cells; data not shown).

BH-P Inhibits Tumor Growth *in Vivo*. In view of these *in vitro* results, we then examined the effects of BH-P *in vivo* in two different model systems.

In the first model system, BH-P was directly injected into a vein of chicken embryo CAMs on which tumor xenografts were growing. As

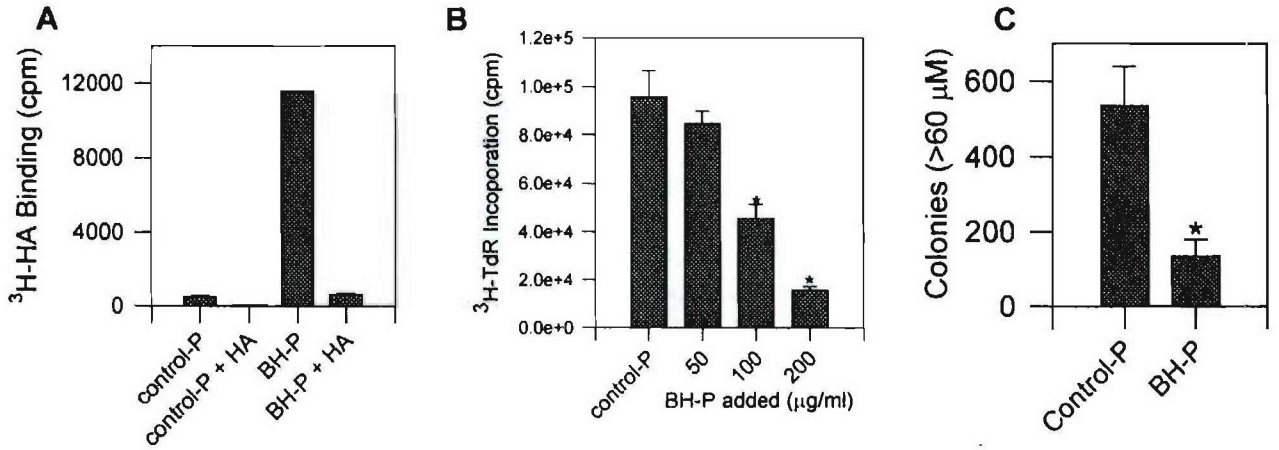

Fig. 1. Binding of BH-P to HA and the inhibitory effects of BH-P on the growth of tumor cells. *A*, binding of BH-P to HA. Fifty μg of BH-P or control-P in 100 μl of PBS were mixed with 20 μl of [^{3}H]HA without or with a 50-fold excess of cold HA for 1 h and then were transferred to a nitrocellulose membrane on a dot blot apparatus. After washing, the complex of [^{3}H]HA and BH-P that had bound to the filter was counted for radioactivity. BH-P binds to [^{3}H]HA, which could be abolished by an excess of HA. *B*, BH-P inhibited the proliferation of MDA-435 tumor cells in a dose-dependent manner. *TdR*, thymidine. *C*, BH-P reduced the ability of MDA-435 cells to form colonies on soft agar. The results represent the mean (n = 3) of a representative experiment; *bars*, SE. Each experiment was repeated at least three times with similar results. *, $P < 0.05$.

shown in Fig. 2*A*, the sizes of tumor xenografts formed by B16 melanoma cells that had been i.v. injected with BH-P were much smaller than those injected with control-P. Similar results were obtained with MDA-435 cells in the same model (Fig. 2*B*). Furthermore, the difference in the tumor weights between the test and control groups was statistically significant (Fig. 2, *C* and *D*). The fact that BH-P demonstrated an inhibitory effect on the growth of both B16 melanoma and MDA-435 cells suggested that the antitumor effect of BH-P was not limited to one cell line and was likely to be universal.

The second model system consisted of gene transfection, which has the following advantages: (*a*) it results in a high concentration of BH-P in the tumors, which could not be achieved by systemic administration of synthetic BH-P; (*b*) BH-P should be evenly distributed in the tumors; and (*c*) a consistent level of BH-P could be maintained in

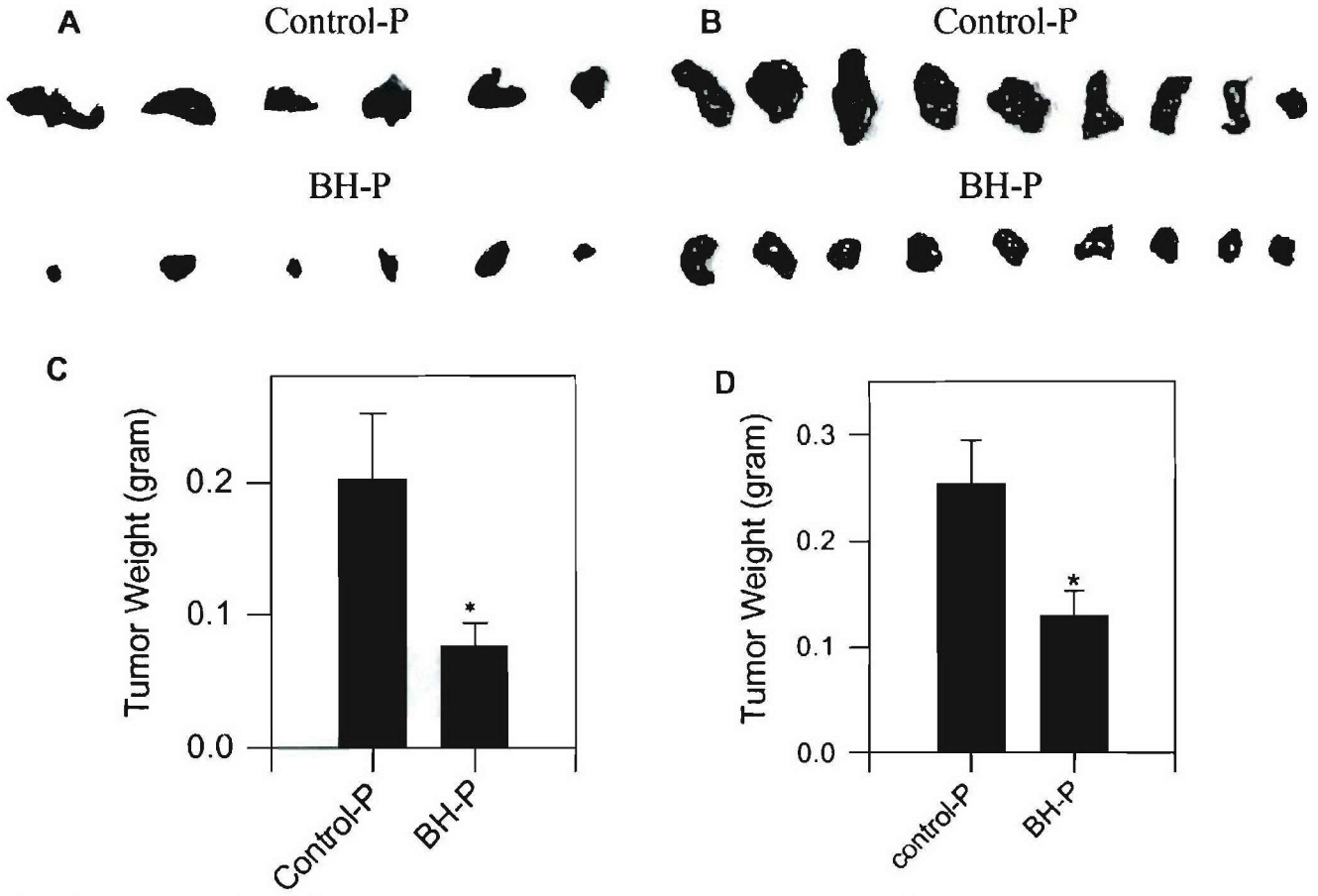

Fig. 2. Inhibition of tumor growth on CAM. Two days after B16 melanoma cells (1×10^6) or MDA-435 cells (3×10^6) were placed on top of the CAMs of 10-day-old chicken embryos, 200 μg of control-P or BH-P in 200 μl of PBS were either i.v. injected into the CAMs once or tropically administrated onto the tumor xenografts on a daily basis. Five days later, the tumors were harvested, photographed (*A* and *B*), and weighed (*C* and *D*). Compared with the control-P, the tumors treated with BH-P were smaller ($P < 0.05$). *Bars*, SE.

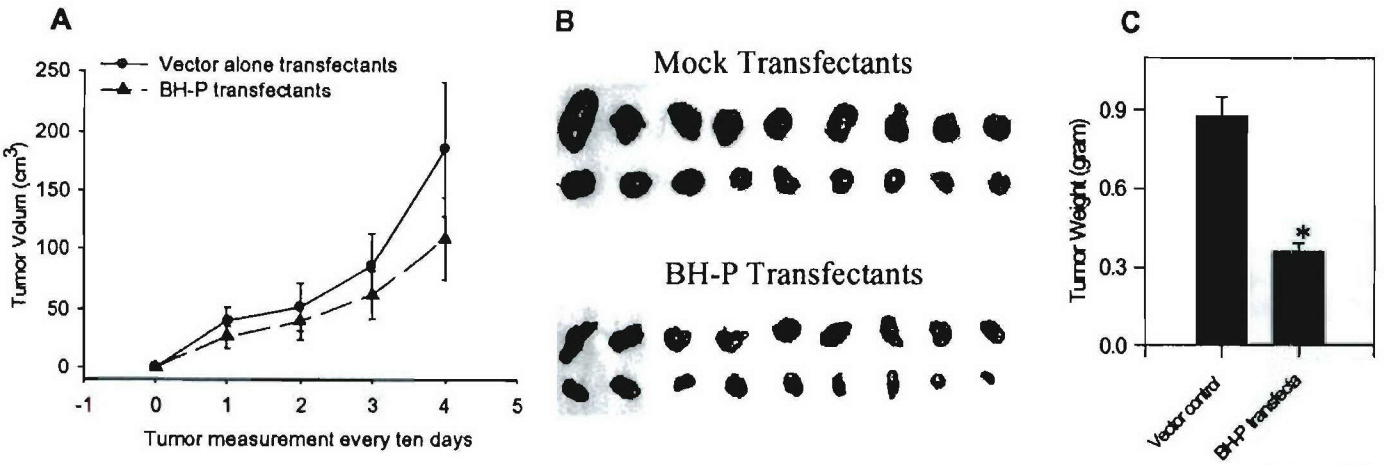

Fig. 3. Inhibitory effect of BH-P on tumor growth of its transfectants. MDA-435 cells (3×10^6), transfected with expression vector for BH-P, were injected into the mammary fat pads of nude mice, and tumor growth was monitored. *A*, tumor xenografts of cells transfected with BH-P grew slower than those of control cells after 20 days. *Bars*, SE. *B*, BH-P transfectants formed smaller tumor xenografts. *C*, the mean tumor weight of BH-P transfectants was less than the control group ($P < 0.01$). *Bars*, SE.

the tumors. For this approach, the cDNA sequence coding for BH-P was obtained by back-translation and then inserted into a pSecTag vector that had a cytomegalovirus promoter and an Igκ signal peptide for secretion. The MDA-435 cells were transfected with either a pSecTag empty vector or a BH-P-pSecTag expression vector. To avoid clonal variation, the transfectants that survived in G418 selection medium and expressed BH-P were first pooled and then injected into the mammary fat pads of nude mice. Fig. 3*A* shows that the growth curve of the MDA-435 cells transfected with BH-P was below that of the mock-transfected cells. Forty-two days after inoculation, the average size of tumor xenografts in the BH-P group was smaller than that in the control group (Fig. 3*B*), and the difference in tumor weight between the two groups was statistically significant (Fig. 3*C*; $P < 0.05$).

Thus, the results from two different experimental models were consistent with each other, strongly indicating that BH-P could inhibit tumor growth *in vivo*. Importantly, when BH-P was administered at a concentration that inhibited tumor growth, there was no notable side effect on either the chicken embryos or mice with regard to animal body weight and activity assessed at the end of each experiment (data not shown).

BH-P Binds to the Plasma Membrane and Causes an Increased Permeability. To determine whether there was a physical association of BH-P with the targeted cells, a binding assay was preformed. MDA-435 cells were incubated with FITC-BH-P at 4°C for 30 min and examined under a confocal microscope. Green fluorescence clearly outlined the tumor cells, suggesting that FITC-BH-P bound to the plasma membranes (Fig. 4*A*). This could be blocked by a 100-fold excess of BH-P, indicating that the BH-P specifically bound to the cell surface.

Presumably, BH-P was binding to HA or other glycosaminoglycans on the cell surface. To test for this, we preincubated the tumor cells with testicular hyaluronidase to digest HA and chondroitin sulfate on the cell surface, or added an excess HA to FITC-BH-P to block its ability to bind to HA, and then examined the alterations in BH-P binding on the cell surface and the interference of its function. Indeed, an excess of HA or pretreatment of hyaluronidase prevented the binding of FITC-BH-P to the cell surface (Fig. 4*B*) and reversed the inhibitory effect of BH-P on cell proliferation, as measured by thymidine incorporation (data not shown). This indicates that at least some of the inhibitory activity of BH-P was a result of its ability to bind the cell surface HA or chondroitin sulfate.

Next, we wanted to determine whether BH-P damaged the plasma membrane. To address this issue, we used high molecular weight FITC-dextran (40,000), which is normally excluded from the cytoplasm of cells with intact plasma membranes. However, when MDA-435 cells were treated with 100 μg/ml of BH-P, the percentage of cells that stained positively for FITC-dextran increased from 12% in control-P-treated cells to 37% in those treated with BH-P (Fig. 4*C*), indicating that the permeability of the plasma membrane was increased with the BH-P treatment.

BH-P Triggers Apoptosis. To determine whether BH-P triggered apoptosis, both MDA-435 and TSU tumors cells were treated with BH-P or control-P, and then the DNA was extracted and electrophoresed on a 1.5% agarose gel. Fig. 4*D* shows DNA laddering in BH-P-treated tumor cells but not in the control-P-treated cells, suggesting that BH-P could trigger apoptosis.

We then examined the activation of molecules that are part of the apoptotic pathway by Western blotting. Fig. 4*E* shows that caspase-8, caspase-3, and PARP were activated in both tumors formed by cells transfected with BH-P expression vectors in nude mice and in cultured tumor cells as compared with their control counterparts. To determine whether blocking apoptosis could prevent the inhibitory effects of BH-P on tumor cells, Z-VAD-FMK (40 μM; a pan-caspase inhibitor) and Z-VDVAD-FMK (20 μM; an inhibitor for caspase-2, -3, and -7) were added to tumor cells treated with (as test) or without (as control) BH-P. The result demonstrated that although the caspase inhibitors alone did not have any effect on the cell proliferation, the inhibitory effect of BH-P on tumor cells could be blocked by the addition of Z-VAD-FMK or Z-VDVAD-FMK (data not shown), which strongly suggests that the BH-P inhibition of tumor growth is associated with caspase-related apoptosis.

Discussion

The results of this study demonstrate that BH-P, a peptide enriched with $B(X_7)B$ motifs that bind to HA, can exert antitumor effects as indicated by the following: (*a*) BH-P inhibits the proliferation of tumor cells growing under both anchorage-dependent and -independent conditions; and (*b*) BH-P inhibits tumor growth *in vivo* in both the chicken embryo CAM and nude mice xenograft models. This inhibitory effect of BH-P was tested with MDA-435 human melanoma cancer cells, B16 melanoma cells, and TSU human bladder cancer cells. In each case, BH-P exerted a similar inhibitory effect, suggesting that the effect of BH-P is not cell line specific but is a universal phenomenon. Notably, there were no obvious side effects on either the development of the chicken embryos or on the body weights of the

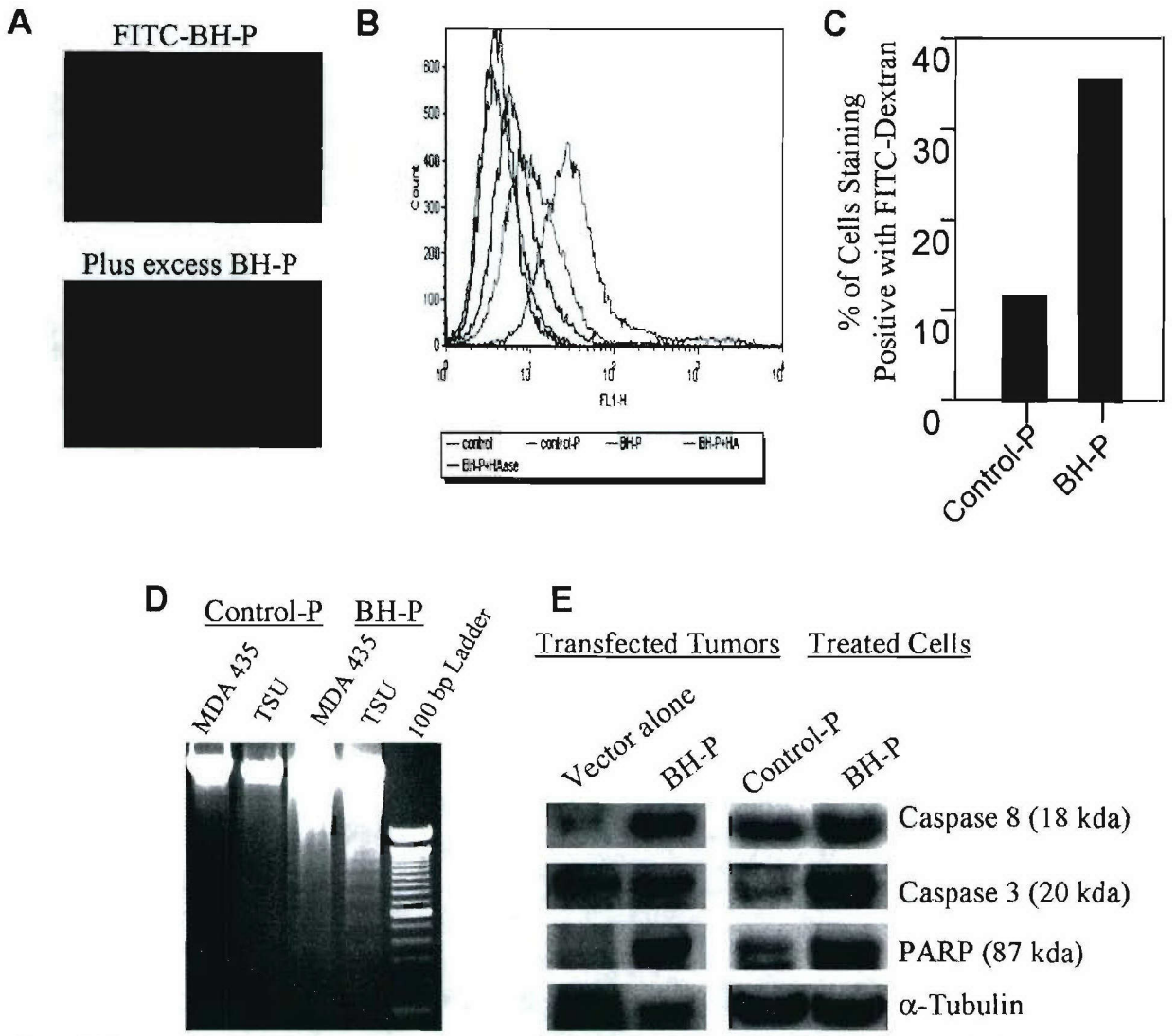

Fig. 4. Effect of BH-P on apoptosis-related molecules. *A*, confocal microscopy shows the binding of FITC-BH-P to the surface of MDA-435 cells (*top*), which could be blocked by excess of BH-P (*bottom*). *B*, flow cytometry shows that the binding of FITC-BH-P to the cell surface was blocked by an excess of HA or preincubation with hyaluronidase. *C*, flow cytometry shows that treatment with BH-P resulted in an increased permeability of FITC-dextran, suggesting that the plasma membrane was damaged. *D*, analysis of DNA from MDA-435 and TSU cells indicates that treatment with BH-P results in laddering. *E*, Western blot analysis indicated that caspase-8, caspase-3, and PARP were activated in both tumors formed by BH-P transfectants and in cultured tumor cells treated with BH-P.

mice, suggesting that BH-P spares normal cells and preferentially blocks the growth of malignant tumor cells.

BH-P appears to exert its antitumor activity through its ability to induce apoptosis. The first step in this process is the binding of BH-P to the cell surface, which was suggested by confocal analysis with FITC-BH-P (Fig. 4*A*). This binding presumably involves HA or its related molecules (chondroitin sulfate), as indicated by flow cytometry analysis in which the treatment with excess HA or hyaluronidase blocked the binding of FITC-BH-P to the cell surface (Fig. 4*B*). Importantly, the interference of BH-P binding to cell surface HA reversed its effects on cell proliferation, suggesting that HA binding on the cell surface is necessary for the effect of BH-P. After binding and internalization, BH-P appears to trigger the apoptosis cascade, as indicated by the activation of critical molecules in the apoptosis pathway, such as caspase-8, caspase-3 and PARP, eventually resulting in the fragmentation of DNA. Indeed, the fact that several caspase inhibitors reversed the inhibitory effects of BH-P on cell proliferation strongly suggested that its effect was related to the induction of apoptosis. The increased permeability of the plasma membrane upon the treatment with BH-P could result from either direct damage caused by the binding of BH-P to the cell surface or as a consequence of intracellular apoptosis on the membrane. At present, the initial target of BH-P is unclear.

Although this is the first report regarding a peptide enriched in HA binding motifs having an antitumor activity, other biological effects have been attributed to HA binding peptides. For example, Mummert *et al.* (31) have reported that a 12-mer HA binding peptide, obtained from a screen of a peptide library with a phage display technique, could block HA-mediated leukocyte trafficking and inhibit inflammatory reactions. This 12-mer peptide has only one HA binding motif. In separate experiments, we found that a single HA binding motif is not sufficient to induce an antitumor effect (data not shown). According to our results, three HA binding motifs appear to be required to impart antitumor activity. We believe that the numbers of HA binding motifs in the peptides may determine their function. To block the HA-CD44 interaction that mediates the leukocyte migration, one HA binding motif seems sufficient (31). However, to trigger apoptosis in tumor cells, it seems to require a peptide that has more than one $B(X_7)B$ motif to simultaneously act on more than one site or more than one molecule on the cell surface.

Recently, it has been reported that the binding of HA to CD44 could block apoptosis induced by antibodies to Fas (32). Directly, CD44 could physiologically trigger the up-regulation of Fas (33), and the activated T cells could use CD44 to undergo apoptosis (34). To weaken apoptosis, the Fas-triggering cells appeared to shed CD44 (35). These studies suggest that the HABP in conjunction with Fas sends a negative signal that could result in apoptosis. The ability of BH-P to activate caspase-8 (Fig. 4, *D* and *E*), a critical molecule in the Fas pathway, implies BH-P may function in a fashion similar to CD44 to trigger apoptosis.

The identification of the basic structural element responsible for antitumor activity has a number of practical implications: (*a*) a small functional peptide is easy to prepare, compared with macromolecular proteins; (*b*) its small size allows it to better penetrate tumors, which helps to promote its antitumor activity; and (*c*) it should be easy to identify similar compounds to mimic antitumor activity of HABPs and peptides. The interruption of physiological function of native HABPs could result in an impairment in cell migration, invasion, and activation of apoptosis. In conclusion, basic research on the function of HA binding peptides may lead to the identification of other novel agents to trigger apoptosis and block tumor progression.

References

1. Aruffo, A., Stamenkovic, I., Melnick, M., Underhill, C. B., and Seed, B. CD44 is the principal cell surface receptor for hyaluronate. Cell, *61:* 1303–1301, 1990.
2. Cheung, W. F., Cruz, T. F., and Turley, E. A. Receptor for hyaluronan-mediated motility (RHAMM), a hyaladherin that regulates cell responses to growth factors. Biochem. Soc. Trans., *27:* 135–142, 1999.
3. Watanabe, H., Cheung, S. C., Itano, N., Kimata, K., and Yamada, Y. Identification of hyaluronan-binding domains of aggrecan. J. Biol. Chem., *272:* 28057–28065, 1997.
4. Dudhia, J., Hardingham, T. E. The primary structure of human cartilage link protein. Nucleic Acids Res., *18:* 2214, 1990.
5. Isacke, C. M., and Yarwood, H. The hyaluronan receptor, CD44. Int. J. Biochem. Cell Biol., *34:* 718–721, 2002.
6. Bartolazzi, A., Peach, R., Aruffo, A., and Stamenkovic, I. Interaction between CD44 and hyaluronate is directly implicated in the regulation of tumor development. J. Exp. Med., *180:* 53–66, 1994.
7. Charrad, R. S., Li, Y., Delpech, B., Balitrand, N., Clay, D., Jasmin, C., Chomienne, C., and Smadja-Joffe, F. Ligation of the CD44 adhesion molecule reverses blockage of differentiation in human acute myeloid leukemia. Nat. Med., *5:* 669–676, 1999.
8. Yu, Q., Toole, B. P., and Stamenkovic, I. Induction of apoptosis of metastatic mammary carcinoma cells *in vivo* by disruption of tumor cell surface CD44 function. J. Exp. Med., *186:* 1985–1996, 1997.
9. Zhang, L., Underhill, C. B., and Chen, L. Hyaluronan on the surface of tumor cells is correlated with metastatic behavior. Cancer Res., *55:* 428–433, 1995.
10. Zahalka, M. A., Okon, E., Gosslar, U., Holzmann, B., and Naor, D. Lymph node (but not spleen) invasion by murine lymphoma is both CD44- and hyaluronate-dependent. J. Immunol., *154:* 5345–5355, 1995.
11. Guo, Y. J., Liu, G., Wang, X., Jin, D., Wu, M., Ma, J., and Sy, M. S. Potential use of soluble CD44 in serum as indicator of tumor burden and metastasis in patients with gastric or colon cancer. Cancer Res., *54:* 422–426, 1994.
12. Sy, M. S., Guo, Y. J., and Stamenkovic, I. Inhibition of tumor growth *in vivo* with a soluble CD44-immunoglobulin fusion protein. J. Exp. Med., *176:* 623–627, 1992.
13. Mohapatra, S., Yang, X., Wright, J. A., Turley, E. A., and Greenberg, A. H. Soluble hyaluronan receptor RHAMM induces mitotic arrest by suppressing Cdc2 and cyclin B1 expression. J. Exp. Med., *183:* 1663–1668, 1996.
14. Zeimet, A. G., Widschwendter, M., Uhl-Steidl, M., Muller-Holzner, E., Daxenbichler, G., Marth, C., and Dapunt, O. High serum levels of soluble CD44 variant isoform v5 are associated with favourable clinical outcome in ovarian cancer. Br. J. Cancer, *76:* 1646–1651, 1997.
15. Gansauge, F., Gansauge, S., Rau, B., Scheiblich, A., Poch, B., Schoenberg, M. H., and Beger, H. G. Low serum levels of soluble CD44 variant 6 are significantly associated with poor prognosis in patients with pancreatic carcinoma. Cancer (Phila.), *80:* 1733–1739, 1997.
16. Underhill, C. B., and Zhang, L. Analysis of hyaluronan using biotinylated hyaluronan-binding proteins. Methods Mol. Biol., *137:* 441–447, 2000.
17. Lee, A., and Langer, R. Shark cartilage contains inhibitors of tumor angiogenesis. Science, *221:* 1185–1187, 1983.
18. Blackadar, C. B. Skeptics of oral administration of shark cartilage. J. Natl. Cancer Inst., *85:* 1961–1962, 1993.
19. Ernst, E. Shark cartilage for cancer? Lancet, *24; 351:* 298, 1998.
20. Horsman, M. R., Alsner, J., and Overgaard, J. The effect of shark cartilage extracts on the growth and metastatic spread of the SCCVII carcinoma. Acta Oncol., *37:* 441–445, 1998.
21. Gonzalez, R. P., Leyva, A., and Moraes, M. O. Shark cartilage as source of antiangiogenic compounds: from basic to clinical research. Biol. Pharm. Bull., *24:* 1097–1101, 2001.
22. Gingras, D., Renaud, A., Mousseau, N., and Beliveau, R. Shark cartilage extracts as antiangiogenic agents: smart drinks or bitter pills? Cancer Metastasis Rev., *19:* 83–86, 2000.
23. Falardeau, P., Champagne, P., Poyet, P., Hariton, C., and Dupont, E. Neovastat, a naturally occurring multifunctional antiangiogenic drug, in phase III clinical trials. Semin. Oncol., *28:* 620–625, 2001.
24. Langer, R., Brem, H., Falterman, K., Klein, M., and Folkman, J. Isolations of a cartilage factor that inhibits tumor neovascularization. Science (Wash. DC), *193:* 70–72, 1976.
25. Moses, M. A., Sudhalter, J., and Langer, R. Identification of an inhibitor of neovascularization from cartilage. Science, *248:* 1408–1410, 1990.
26. Moses, M. A., Sudhalter, J., and Langer, R. Isolation and characterization of an inhibitor of neovascularization from scapular chondrocytes. J. Cell Biol., *119:* 475–482, 1992.
27. Liang, J. H., and Wong, K. P. The characterization of angiogenesis inhibitor from shark cartilage. Adv. Exp. Med. Biol., *476:* 209–223, 2000.
28. Liu, N., Lapcevich, R. K., Underhill, C. B., Han, Z., Gao, F., Swartz, G., Plum, S. M., Zhang, L., and Gree, S. J. Metastatin: a hyaluronan-binding complex from cartilage that inhibits tumor growth. Cancer Res., *61:* 1022–1028, 2001.
29. Yang, B., Yang, B. L., Savani, R. C., and Turley, E. A. Identification of a common hyaluronan binding motif in the hyaluronan binding proteins RHAMM, CD44 and link protein. EMBO J., *13:* 286–296, 1994.
30. Culty, M., Shizari, M., Thompson, E. W., and Underhill, C. B. Binding and degradation of hyaluronan by human breast cancer cell lines expressing different forms of CD44: correlation with invasive potential. J. Cell Physiol., *160:* 275–286, 1994.
31. Mummert, M. E., Mohamadzadeh, M., Mummert, D. I., Mizumoto, N., and Takashima, A. Development of a peptide inhibitor of hyaluronan-mediated leukocyte trafficking. J. Exp. Med., *192:* 769–779, 2000.
32. Lisignoli, G., Grassi, F., Zini, N., Toneguzzi, S., Piacentini, A., Guidolin, D., Bevilacqua, C., and Facchini, A. Anti-Fas-induced apoptosis in chondrocytes reduced by hyaluronan: evidence for CD44 and CD54 (intercellular adhesion molecule 1) involvement. Arthritis Rheum., *44:* 1800–1807, 2001.
33. Fujii, K., Fujii, Y., Hubscher, S., and Tanaka, Y. CD44 is the physiological trigger of Fas up-regulation on rheumatoid synovial cells. J. Immunol., *167:* 1198–1203, 2001.
34. Chen, D., McKallip, R. J., Zeytun, A., Do, Y., Lombard, C., Robertson, J. L., Mak, T. W., Nagarkatti, P. S., and Nagarkatti, M. CD44-deficient mice exhibit enhanced hepatitis after concanavalin A injection: evidence for involvement of CD44 in activation-induced cell death. J. Immunol., *166:* 5889–5897, 2001.
35. Gunthert, A. R., Strater, J., von Reyher, U., Henne, C., Joos, S., Koretz, K., Moldenhauer, G., Krammer, P. H., and Moller, P. Early detachment of colon carcinoma cells during CD95(APO-1/Fas)-mediated apoptosis. I. De-adhesion from hyaluronate by shedding of CD44. J. Cell Biol., *134:* 1089–1096, 1996.

Int. J. Cancer: **109,** 49–57 (2004)

Publication of the International Union Against Cancer

HYALURONAN-BINDING PEPTIDE CAN INHIBIT TUMOR GROWTH BY INTERACTING WITH Bcl-2

Ninfei LIU, Xue-Ming XU, Jinguo CHEN, Luping WANG, Shanmin YANG, Charles B. UNDERHILL and Lurong ZHANG*

Department of Oncology, Georgetown University Medical Center, Washington DC, USA

Previous studies have indicated that proteins that bind hyaluronan can also inhibit the growth of tumor cells. To determine if synthetic peptides also possessed these properties, we tested a series of polypeptides containing structural motifs from different proteins for their ability to bind [^{3}H]hyaluronan, and identified one compound termed P4 that had a particularly strong interaction. Further studies revealed that P4 also inhibited the growth of tumor cells in tissue culture as well as on the chorioallantoic membranes of chicken embryos. In addition, expression vectors for P4 caused tumor cells to grow slower in nude mice and reduced their vascularization. The P4 peptide also inhibited VEGF-induced angiogenesis in the chorioallantoic membranes of chicken embryos. Studies on cultured cells indicated that P4 induced apoptosis, which was blocked by a pan-caspase inhibitor. Confocal microscopy revealed that shortly after its uptake, P4 became associated with mitochondria. Immunoprecipitation indicated that P4 could bind to Bcl-2 and Bcl-x_L, which are associated with mitochondria and regulate apoptosis. This was also supported by the fact that P4 induced the release of cytochrome c from preparations of mitochondria. Taken together, these results suggest that P4 binds to Bcl-2 and related proteins and this activates the apoptotic cascade.

Key words: *apoptosis; angiogenesis; cytochrome c; mitochondria; caspases*

A number of proteins that can bind to hyaluronan also have antitumor properties.[1–7] Indeed, we have previously described a complex of proteins termed metastatin that was isolated from cartilage by affinity chromatography on hyaluronan-Sepharose.[1] Metastatin consists of a fragment of aggrecan and the link protein that binds to hyaluronan with high affinity and specificity. We found that metastatin could inhibit the growth of tumor cells in several model systems. For example, in mice that previously had been inoculated with either B16 melanoma or Lewis lung carcinoma cells, multiple *i.p.* injections of metastatin reduced the number of tumor nodules that formed in the lungs. Similarly, in chicken embryos, a single injection of metastatin inhibited the growth of B16 and TSU tumor cells on the chorioallantoic membrane. Significantly, in each case this antitumor activity was blocked if the preparation of metastatin was premixed with an excess of hyaluronan, suggesting that a free binding site was critical for its activity. Additional experiments indicated that metastatin acted by blocking tumor angiogenesis. In particular, when VEGF-induced angiogenesis was tested in the chicken chorioallantoic membrane system, metastatin significantly reduced the number and density of the blood vessels. Experiments with endothelial cells growing in tissue culture also indicated that metastatin was able to induce apoptosis in these cells. Based on these results, we postulated that metastatin was able to target proliferating endothelial cells that were involved in tumor neovascularization.

In addition to metastatin, a number of other hyaluronan binding proteins also have antitumor activity. For example, a recombinant version of CD44 fused with an immunoglobulin chain that can bind to hyaluronan also inhibited the growth of human mammary carcinoma and lymphoma cells in nude mice.[2,3] A second example is the RHAMM protein which is a cell surface receptor for hyaluronan and regulates cell mobility. Mohapata *et al.*[4] found that a soluble version of this protein will arrest the growth of cultured tumor cells in the G_2/M transition, and this appears to be due to the down regulation of Cdc2/Cyclin B1. Another example is the factor TSG-6, which is secreted by a variety of cells after stimulation with inflammatory cytokines. This factor is able to both bind hyaluronan and block tumor cell growth.[5] A final example is endostatin, a 20 kDa fragment of the C-terminal of collagen XVIII that inhibits angiogenesis and as a result inhibits the growth of tumors.[6] Endostatin also appears to be able to bind hyaluronan as suggested by the presence of specific structural motifs and a basic region formed by 11 arginine residues.[7]

These previous findings prompted us to examine synthetic peptides for both hyaluronan binding activity and for antitumor properties. To accomplish this, we designed a series of peptides containing the motif B[X_7]B (2 basic amino acids flanking a sequence of 7 amino acids), which is common to many hyaluronan binding proteins as originally described by Yang *et al.*[8] The peptides contained 1 or more of these motifs derived from a variety of different proteins. When these peptides were tested for their ability to bind [^{3}H] hyaluronan, 1 particular peptide termed P4 was identified that had a particularly strong interaction. We then examined P4 with regard to antitumor activity and found that it also inhibited the growth of tumor cells on the chorioallantoic membranes of chicken embryos and that tumor cells transfected with P4 expression vectors grew slower in nude mice. Further studies suggested that the P4 peptide rapidly entered the cytoplasm of cells where it interacted with members of the Bcl-2 family of proteins to induce apoptosis. These results suggest that proteins or peptides that can bind to hyaluronan may represent a new category of compounds with antitumor activity.

MATERIAL AND METHODS

Synthesis of peptides

A series of peptides were designed that contained the hyaluronan-binding motif B[X7]B from a variety of different proteins (Table I). In some cases these domains were coupled together using a series of VVV or GG residues to provide flexible linkages.

Abbreviations: FITC-P4, fluorescein isothiocyanate labeled P4 peptide; GFP, green fluorescence protein; PBS-A, phosphate-buffered saline without calcium or magnesium; PMSF, phenyl methyl sulfonyl fluoride.

Grant sponsor: U.S. Army Med. Res. and Mat. Command; Grant numbers: DAMD17-00-1-0081, DAMD17-01-1-0708; Grant sponsor: NCI/NIH; Grant number: R29 CA71545 The first two authors share senior authorship. Dr. Liu's current address is: Department of Plastic Surgery, No. 9 People's Hospital, Shanghai Second Medical University, Shanghai, P. R. China. Dr. Xu' current address is: NIH/NCI, 9000 Rockville Pike, Bethesda, MD 20892.

*Correspondence to: Department of Oncology, Georgetown University Medical Center, 3970 Reservoir Road, NW, Washington DC 20007, USA. Fax: +202-687-7505;
E-mail: zhangl@georgetown.edu or underhic@georgetown.edu

Received 10 June 2003; Revised 17 September 2003; Accepted 24 September 2003

DOI 10.1002/ijc.11636
Published online 11 December 2003 in Wiley InterScience (www.interscience.wiley.com).

TABLE 1 - HYALURONAN-BINDING ACTIVITY OF SELECTED PROTEINS AND PEPTIDES

Protein/peptide designation	Structure	Amino Acids	Source	Specific binding CPM ± range
Bovine Serum albumin		—	Negative control	80 ± 31
Cartilage Proteoglycan		—	Positive control	17,894 ± 160
P1	CNGRCGGKQKIKHVVKLK	18	RHAMM[9]	−41 ± 16
P2	CNGRCGGKLKSQLVKRK	17	RHAMM[9]	8 ± 15
P3	CNGRCGGRRRKKIQGRSKR	19	Hyaluronidase[10]	−19 ± 5
P4	CNGRCGGKQKIKHVVKLKVVVKLKSQLVKRKVVVRRRKKIQGRSKR	46	RHAMM/HAase[9, 10]	6,566 ± 147
P5	CNGRCGGKIRIKWTKLTSDYLKQGKKTYGGYQGRVFLK	40	Link protein[11]	692 ± 39
P6	CNGRCGGRLLVQGSLRGGRIMGITLVSKKGGRISPNPKCGK	41	LYVE[12]	−179 ± 191
P7	CNGRCGGRAVGLAGTFRAPLSSRLGGRHPTWPQK	34	Endostatin[13]	57 ± 99
P8	RRAVGLAGTFCNGRCGGAPLSSLGGHPTWPQRRK	34	Random	−114 ± 12

To improve the targeting of the peptide to tumor and endothelial cells, the N-terminus consisted of a CNGRG sequence that acts as a ligand for CD13.[14] Finally, to impede enzymatic degradation, the N-terminals of the peptides were acetylated, and the C-terminals were amidated. The peptides were synthesized by Genemed (San Francisco, CA) and dissolved in a small amount of dimethylformamide and 1% acetate acid, diluted with saline to a concentration of 1 mg/ml and sterilized by placing in a boiling water bath for 15 min.

Hyaluronan binding assay

To assay for the binding of the peptide to hyaluronan, we took advantage of the fact that hyaluronan does not adhere to nitrocellulose by itself but will do so in the presence of proteins or peptides that bind to it. The [^{3}H]hyaluronan (1.35×10^5 cpm/μg) was prepared from the medium of rat fibrosarcoma cells cultured in the presence of [^{3}H]acetate as previously described.[15] For the binding assay, 2 μg [^{3}H]hyaluronan was mixed with 2 μg of the peptide (or protein) in a final volume of 50 μl of phosphate-buffered saline (PBS-A). For each sample, the background was determined by including an excess of nonlabeled hyaluronan (40 μg). After incubating 20 min, 2 20 μl aliquots were applied to a sheet of nitrocellulose using a dot blot apparatus, allowed to soak in for 20 min before wells were washed with PBS-A (3 times, 100 μl/well) under vacuum. The individual dots were cut out and assayed for radioactivity in a scintillation counter. The specific binding was calculated by subtracting the background (*i.e.*, with an excess of nonlabeled hyaluronan) from the total binding.

Cell culture

The MDA-435 (human breast cancer), TSU (human bladder cancer), B16 (mouse melanoma), Cos-7, NIH-3T3, 293T cells and ABAE (adult bovine aortic endothelial) cells were maintained in 10% calf serum and 90% DMEM except as otherwise indicated. HUVEC (human umbilical veins endothelial cells) were cultured in 20% fetal bovine serum and 80% DMEM containing 10 ng/ml fibroblast growth factor 2 and vascular endothelial growth factor.

Cell proliferation assay

Approximately 5,000 cells were distributed into 96-well tissue culture plates and the following day the media was replaced with 160 μl of fresh media and 40 μl of a solution containing different concentrations of either the P4 or the random peptide as a control. One day later, 30 μl of 0.3 μCi of [^{3}H]thymidine in serum-free media was added to each well, and after approximately 8 hr the cells were harvested and the amount of incorporated [^{3}H]thymidine was determined with a beta counter.

Growth of tumor xenografts on the chicken chorioallantoic membrane

Rapidly growing cultures of B16 cells were harvested, washed, centrifuged and pellets containing $2–3 \times 10^6$ cells were placed on the chorioallantoic membranes of 10-day-old chicken embryos (15 eggs/group) incubated at 37.8°C. After 2 days, 100 μl of PBS containing 100 μg of P4 or random peptide were injected into blood vessels in the CAM. Five days later, the xenografts as well as the chicken embryos were harvested.

Transfection of cultured cells with expression vectors

The sequence of P4 was back-translated into a cDNA sequence, which was synthesized and inserted into a p-Igκ/hygro vector (Invitrogen, Carlsbad, CA). This vector was then used to transfect MDA-435 and TSU tumor cells which were selected with 800 μg/ml hygromycin and the resulting clones were pooled. The expression of P4 by these cells was determine by Western blotting with a polyclonal antibody generated against the P4 (Genemed).

Angiogenesis assay

Disks of filter paper (0.5 cm diameter) containing 10 ng/ml of both VEGF and FGF-2 (Repro, Rocky Hill, NJ) were placed on the CAMs of 7-day-old chicken embryos, which were then injected

with either P4 or a random peptide (100 μg in 0.2 ml).[16] Four days later, the CAMs immediately adjacent to the filter paper were fixed and examined by computerized image analysis. An Optimas 5 program was used to calculate the vessel area index, which corresponds to area occupied by the blood vessels normalized to the total area examined.

Analysis of apoptosis

MDA-435 cell were cultured in the presence of P4 or the random peptide (100 μg/ml) for 24 hr, harvested, washed with PBS and the cell pellets were digested with 0.5 mg/ml proteinase K in 1% SDS, 150 mM NaCl, 50 mM EDTA, pH 8.0, at 55°C for 16 hr. The resulting digest was extracted with phenol and chloroform, and the genomic DNA was precipitated with isopropanol. DNA pellets were dissolved in TE buffer (10 mM Tris, 1 mM EDTA, pH 7.4) and were electrophoresed on a 1.5% agarose gel.[17]

Confocal microscopy

In some experiments, MDA-435 cells growing on cover slips were incubated with 1 μg/ml of FITC-P4 (N-terminal labeled, Genemed) for 1 hr, either alone (as test) or in the presence of 50 μg of nonlabeled P4 (as control). For the double-label experiments, the cells were incubated with FITC-P4 at 37°C for 20 min followed by 25 nM of MitoTracker (Molecular Probes, Eugene, OR). In each case, the cells were washed, fixed and then examined under a confocal microscope.

Flow cytometry

To analyze cells for early stages of apoptosis, we used annexin V and propidium iodide staining.[18] Cultures of MDA-435 and ABAE cells were treated overnight with P4 or the random peptide, harvested with 5 mM EDTA in PBS, washed and resuspended in complete medium and allowed to recover. The cells were then suspended in 100 μl of binding buffer (140 mM NaCl, 10 mM HEPES and 2.5 mM $CaCl_2$, pH 7.4) and mixed with 5 μl of FITC-annexin V and 2.5 μl of 0.1% propidium iodide (Molecular Probes, Eugene, OR). After 15 min at room temperature, 300 μl of binding buffer was added, and the samples were analyzed by flow cytometry. The percentage of cells with green staining of FITC-annexin V (apoptotic cells) but not red staining of propidium iodide (dead cells) was calculated.[18]

To analyze the integrity of mitochondria, cells were stained with JC-1 (Molecular Probes), which gives a high red fluorescence signal for cells with healthy, functional mitochondria and shifts to a high green fluorescence and low red fluorescence for those with mitochondria with a decreased membrane potential.[17] Suspensions of MDA-435 and ABAE cells were prepared as described and then incubated with 10 μg/ml of JC-1 for 10 min at room temperature and then subjected to flow cytometry analysis for both green fluorescence and red fluorescence (Molecular Probes).

Western blotting

Cultured cells were treated with the peptides and extracted in lysis buffer (1% triton X-100, 0.5% sodium deoxycholate, 0.5 mg/ml leupetin, 1 mM EDTA, 1 mg/ml pepstatin and 0.2 mM phenylmethyl-sulfonyl fluoride). Samples containing 20 μg of protein were loaded onto 4–12% BT NuPAGE gel (Novex, San Diego, CA), electrophoresed and transferred to a nitrocellulose membrane. The membranes were blocked with 5% nonfat milk in PBS for 30 min and then incubated for 1 hr with 1 μg/ml antibodies against caspase 9, caspase 3, PARP or α-tubulin (Santa Cruz Biotechnologies, Santa Cruz, CA). After washing, the membrane was incubated for 1 hr with 0.2 μg/ml of peroxidase-labeled antirabbit IgG followed by an enhanced chemoluminescent substrate (Pierce, Rockford, IL).

ELISA for protein binding

The wells of ELISA plates (marician-treated to facilitate peptide binding) were incubated with 200 μl of 5 μg/ml P4 or random peptide at room temperature overnight. After blocking, purified human recombinant Bcl-2 protein (Santa Cruz Biotechnologies, Santa Cruz, CA) at different concentrations (100 μl of 0–1.0 μg /ml) was added to plate, incubated for 1 or 2 hr. After washing, a solution containing 0.5 μg/ml of antibodies to Bcl-2 was added for 1 hr followed by peroxidase-labeled secondary antibody and finally a peroxidase substrate consisting of 2,2′-azino-bis(3-ethylbenz-thiazoline-6-sulfonic acid) and H_2O_2. The OD_{405} was determined with an ELISA reader

Immunoprecipitation

The 293T cells were transiently transfected with pCMV vector containing Bcl-2 or Bcl-x_L cDNA fused at N-terminal to GFP or containing GFP alone as a control. Twelve hours later, the cells were incubated with biotin-P4 for 3 hr and harvested in 1.5 ml of lysis buffer (0.5% nonidet P-40, 150 mM NaCl, 1 mM EDTA, 20 mM Tris, pH 8.0, 10 μg/ml aprotinin, 10 μg/ml leupeptin and 1 mM PMSF). One milliliter of the cell lysates was mixed with streptavidin-beads overnight at 4°C. The beads were washed and extracted in 30 μl of Laemmli sample buffer, and 10 μl samples were analyzed by Western blotting using antibodies to GFP (Santa Cruz Biotechnologies).

Release of cytochrome c

A cell-free preparation of mitochondria was prepared from MDA-435 cells by differential centrifugation.[19] For this, 5×10^7 cells were washed with PBS, re-suspended in 5 vol of CFS buffer (220 mM mannitol, 68 mM sucrose, 2 mM NaCl, 2.5 mM KH_2PO_4, 0.5 mM EGTA, 2 mM MgCl2, 5 mM pyruvate, 0.1 mM PMSF and 10 mM HEPES-NaOH, pH 7.4) and swollen on ice for 20 min. The cells were then disrupted by 10–15 aspirations through a 22-gauge needle and centrifuged at 750*g* for 5 min at 4°C to remove the nuclei. The supernatant was centrifuged again (15,000*g*, 15 min, 4°C) to recover the mitochondrial fraction. The resulting pellet was resuspended in a buffer consisting of 250 mM sucrose, 20 mM Hepes, pH 7.5, 10 mM KCl, 1.5 mM $MgCl_2$, 1 mM EDTA, 1 mM EGTA, 1 mM DTT and 0.1 mM PMSF and divided into 3 equal fractions. One fraction was treated with vehicle alone, another was mixed with 50 μg/ml of the control peptide and the third with P4. After 1 hr at 25°C, the tubes were centrifuged (15,000*g* for 15 min) to pellet the mitochondria. The supernatants (containing the released cytochrome c) and the pellets (containing the mitochondria) were collected and analyzed for cytochrome c by Western blotting (antibody from Santa Cruz).

RESULTS

Design of the hyaluronan binding peptide

In initial studies, we designed a series of peptides containing hyaluronan-binding motifs derived from different proteins (Table I). These were then tested for their ability to bind to [^{3}H]hyaluronan by using an assay that took advantage of the fact that hyaluronan by itself does not bind to nitrocellulose but does so in the presence of hyaluronan-binding peptides or proteins. The validity of this assay was demonstrated by the fact that a cartilage proteoglycan (a complex of aggrecan and link protein) that is known to bind hyaluronan demonstrated a significant specific binding of [^{3}H]hyaluronan to nitrocellulose but not the nonbinding protein bovine serum albumin.

Among these peptides examined, one designated P4 stood out with regard to its ability to bind hyaluronan (Table I). The P4 peptide consisted of 3 B[X_7]B motifs: 2 from RHAMM and 1 from hyaluronidase as well as 2 VVV linkers between these domains. In contrast, P1 through P3, which contained the individual hyaluronan-binding motifs, did not display significant activity. It appears that multiple motifs are required to observe significant binding activity. It should also be mentioned that a CNGR motif was placed on the N-terminus to target the peptides to CD13 that is present on both tumor and endothelial cells.[14] However, subsequence experiments revealed that removal of this sequence had no effect on its ability to inhibit the proliferation of cultured cells.

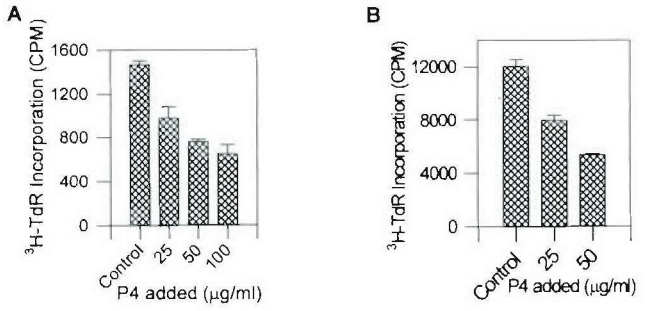

FIGURE 1 – Effect of P4 on the growth of cultured cells: (*a*, *b*) MDA-435 and ABAE cells were cultured in the presence of varying concentrations of the P4 peptide and 100 μg/ml of the random peptide (control). After 24 hr, [^{3}H]thymidine was added to the cultures for an additional 10 hr and then the cells were harvested and the amount of incorporated [^{3}H]thymidine was determined. The P4 peptide inhibited the growth of both cell types in a dose-dependent fashion, while the control samples containing the random peptides had little or no effect.

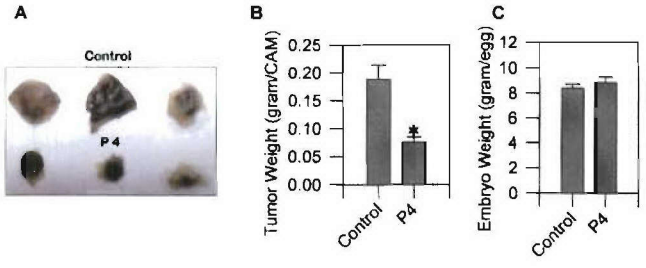

FIGURE 2 – Effect of P4 on the growth of tumor xenografts on the CAM of chicken embryos: B16 cells were applied to the CAMs of 10-day-old chicken embryos and allowed to grow for 2 days. At this point the embryos were injected with 100 μg of P4 or the random peptide and 5 days later the xenografts were harvested, photographed and weighed. (*a*,*b*) Injection of P4 resulted in a significant reduction in the size of the xenografts as compared to the random peptide ($p<0.01$). (*c*) The weights of the chicken embryos in the 2 groups were similar, indicating that the P4 peptide did not inhibit their development.

The interaction of P4 with [^{3}H]hyaluronan could also be inhibited by both chondroitin sulfate and heparin suggesting that the interaction was of an ionic nature. For a control in subsequent experiments, we used the P8 peptide that did not demonstrate significant binding activity towards hyaluronan. This peptide was a randomized version of P7.

Effect of P4 on the growth of tumor cells

Next, we examined the effects of P4 and the random peptide on the growth of cultured cells as judged by thymidine incorporation. When different concentrations of P4 were added to cultures of MDA-435 (human breast cancer) or ABAE (bovine endothelial) cells, their proliferation was inhibited as compared to those treated with the random peptide (Fig. 1*a*,*b*). Furthermore, when P4 was added to MDA-435 cells suspended in soft agar, the subsequent formation of colonies was greatly reduced (data not shown). However, P4 had little or no effect on the proliferation of relatively normal cells, such as Cos 7 (kidney epithelium) and NIH-3T3. Thus, the effects of P4 vary depending upon the cell type, with tumor and endothelial cells being particularly sensitive.

The P4 peptide had a similar effect on B16 cells growing on the CAM of chicken embryos. When P4 was injected *i.v.* into the CAMs of chicken embryos containing B16 tumor xenografts, the tumor growth was significantly reduced as compared to those from CAMs injected with the random peptide ($p<0.01$, Fig. 2*a*,*b*).

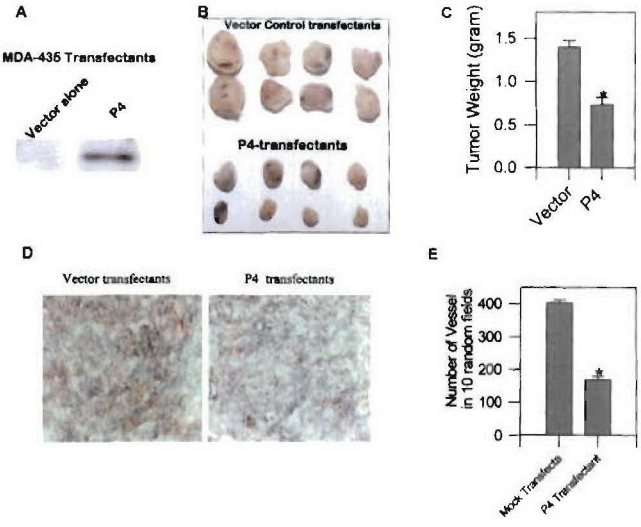

FIGURE 3 – The growth of tumor cells transfected with an expression vector for P4: (*a*) MDA-435 cells transfected with either an empty expression vector or one containing P4 cDNA were extracted, subjected to Western blotting and probed with a rabbit antibody to P4. The expression of P4 is apparent in cells transfected with the P4 expression vector but not in those transfected with the vector alone. (*b*,*c*) Both control and P4 transfected tumor cells were inoculated into nude mice and 3 weeks later, the tumor xenografts were harvested, photographed and weighed. Both the size and the weights of the P4 expressing xenografts were significantly smaller than the control counterparts ($p<0.05$). (*d*) Frozen sections were prepared from the tumor xenografts and stained with an antibody against CD31 to identify endothelial cells (in red). Representative views show that the xenografts formed from control cells (*i.e.*, vector transfectants) were more highly vascularized than those formed by P4 transfectants. (*e*) The number of blood vessels in 10 random fields also demonstrated that the xenografts of cells transfected with the P4 expression vector were less vascularized than those formed by control cells.

Significantly, the P4 had no apparent toxic effect on the embryos as judged by their final weights (Fig. 2*c*).

We then examined the effects of P4 on the growth of tumor cells in mice following transfection with an expression vector to achieve a high local concentration of P4 in the tumor cells. For this experiment, the amino acid sequence of P4 was back-translated into a cDNA sequence, inserted into an expression vector and then transfected into MDA-435 cells. The resulting transfected cells expressed the P4 protein based on Western blotting with an antibody against P4 (Fig. 3*a*). When the cells were injected into nude mice, the tumor xenografts formed by the P4 transfectants were much smaller than those formed by those transfected with a control (empty) vector (Fig. 3*b*,*c*). A similar inhibition of cell growth was also obtained with transfected TSU cells (data not shown).

To determine whether the difference in the size of the xenografts could have been due to vascularization, we examined the blood vessel density by staining histological sections with antibodies to CD31, a marker for endothelial cells. As shown in Fig. 3*d*, the density of blood vessels in xenografts formed by the cells transfected with P4 was much less than that of the control xenografts and this was confirmed by computerized image analysis (Fig. 3*e*).

Inhibition of vascularization

The fact that tumor xenografts expressing P4 had fewer blood vessels than their control counterparts suggested that P4 may be acting on vascularization. To further test this possibility, we used an angiogenesis assay in which filter papers containing VEGF and FGF-2 were placed on the CAMs of chicken eggs, and then P4 or the random peptide were injected into veins of the CAMs. Four days later, the blood vessels in the CAMs adjacent to the paper disk

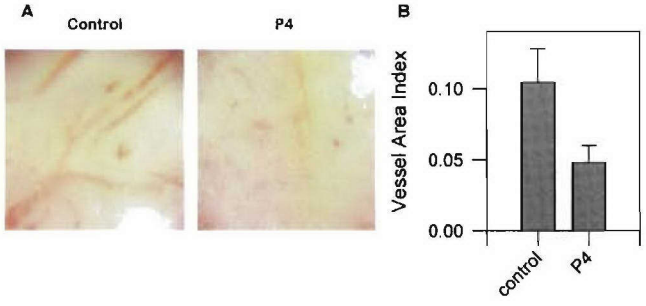

FIGURE 4 – The effect of P4 on angiogenesis in the chicken CAM: For the angiogenesis assay, disks of filter paper containing both VEGF and FGF-2 were placed on the CAMs of 7-day-old chicken embryos, which were also injected with either P4 or random peptide. Four days later, the CAM immediately adjacent to the filter paper were fixed and subjected to computerized image analysis. (*a*) Representative images of the CAMs show that in the P4 injected samples, there was significant reduction in the number of blood vessels as compared to those injected with the random peptide. (*b*) Computerized image analysis of the samples showed that injection of P4 resulted in a 50% reduction in the vessel area index as compared to those injected with the random peptide.

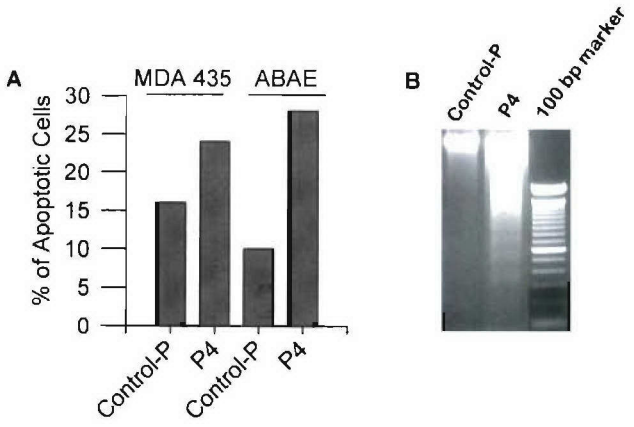

FIGURE 5 – Induction of apoptosis by P4: The effect of the peptides on the induction of apoptosis was tested using 2 different assays. (*a*) In the first assay, MDA-435 and ABAE cells were incubated overnight with the P4 or random peptides (50 μg/ml), stained with annexin V and propidium iodide and then analyzed by flow cytometry. A greater proportion of the cells treated with P4 stained with annexin V than those treated with the control peptide, indicating that apoptosis was stimulated by P4. (*b*) In the second assay, TSU cells were cultured in the presence of the peptides (100 μg/ml) for 24 hr and then the DNA was extracted and analyzed by agarose gel electrophoresis. Laddering of the DNA was clearly apparent in cells treated with P4 but not in those treated with the random peptide, indicating that P4 can induce apoptosis.

was were examined by computerized image analysis and the degree of vascularization was expressed as the ratio of the area of blood vessels normalized to the total area viewed under the microscope (vessel area index). Figure 4 shows that P4 inhibited the vascularization of the CAM as compared to the random peptide and is consistent with the possibility that P4 inhibits the growth of newly forming blood vessels that are necessary for growing tumors.

Induction of apoptosis

One possible mechanism by which P4 could be acting is by inducing apoptosis in either endothelial or tumor cells. To test this possibility, we examined the effects of P4 on several markers of apoptosis. First, we used flow cytometry to examine staining with annexin V which binds to phosphatidylserine residues that become exposed on the outer leaflet of the plasma membrane during the early stages of apoptosis.[18] As shown in Fig. 5*a*, when either MDA-435 or ABAE cells were exposed to P4 overnight, there was a significant increase in the fraction of cells demonstrating positive annexin staining as compared to equivalent cells that had been treated with the random peptide. This suggests that P4 can induce apoptosis in both tumor and endothelial cells.

Another marker of apoptosis is DNA fragmentation that occurs later in the process.[17] To assay for this, TSU tumor cells were treated with either P4 or the random peptide, and the DNA was extracted from these cells and subjected to agarose gel electrophoresis. As shown in Figure 5*b*, the DNA from the tumor cells treated with P4 exhibited clear evidence of laddering indicative of apoptosis, while the similar cultures treated with the random peptide did not.

We then examined the effect of P4 on enzymes associated with the apoptotic pathway.[20] For this, MDA-435 cells were treated with either P4 or the random peptide and then analyzed by Western blotting for caspase 9, caspase 3, PARP and tubulin. Figure 6*a* shows that treatment with P4 resulted in the activation of caspase 9 and 3 and the cleavage of PARP, whereas no difference was apparent in the α-tubulin used as a loading control. This again suggests that P4 can trigger apoptosis.

To further test the role of caspases in P4-induced cell death, we examined the effect of Z-VAD-FMK a pan-caspase inhibitor.[21] As shown in Figure 6*b*, Z-VAD-FMK partially reversed the inhibitory effects of P4 on the [^{3}H]thymidine incorporation in ABAE cells. Thus, P4 appears to be acting through a caspase dependent pathway.

Taken together, these results suggest that P4 can induce apoptosis in tumor and endothelial cells and this may be responsible for its antitumor activity.

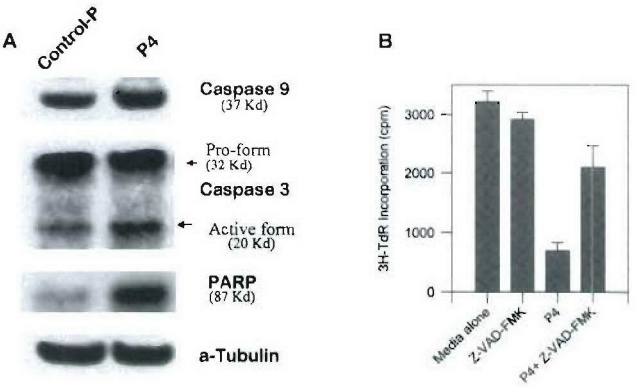

FIGURE 6 – Effect of peptides on members of the apoptotic cascade: Two different techniques were used to determine the effect of P4 on the apoptotic cascade; Western blotting and effect of a caspase inhibitor. (*a*) MDA-435 cells were treated with either random (control-P) peptides or P4 (50 μg/ml) for 8 hr, extracted with detergents and analyzed by Western blotting using antibodies to caspase 9, caspase 3, PARP and α-tubulin (as a loading control). The figure shows that P4 appears to enhance the levels of activated caspase 9 and caspase 3 as well as promote the levels of cleaved PARP, one of the down-stream targets of the caspase cascade. This indicates that P4 can induce apoptosis in cultured tumor cells. (*b*) ABAE cells were cultured in the presence of the pan-caspase inhibitor Z-VAD-FMK, the P4 peptide and a combination of the 2. After 24 hr, the incorporation of [^{3}H]thymidine was examined. Whereas Z-VAD-FMK by itself had little or no effect on cell proliferation, it partially blocked the inhibitory effects of P4, suggesting that the effects of P4 are at least partially mediated through the caspase cascade.

Internalization and localization of P4 in cells

To determine the mechanism by which P4 induces apoptosis, we examined the interaction of P4 with various subcellular organelles. To accomplish this, cells were treated with FITC-P4 and the distribution of the fluorescent label was followed with a confocal microscope. In initial experiments, we found that when both tumor

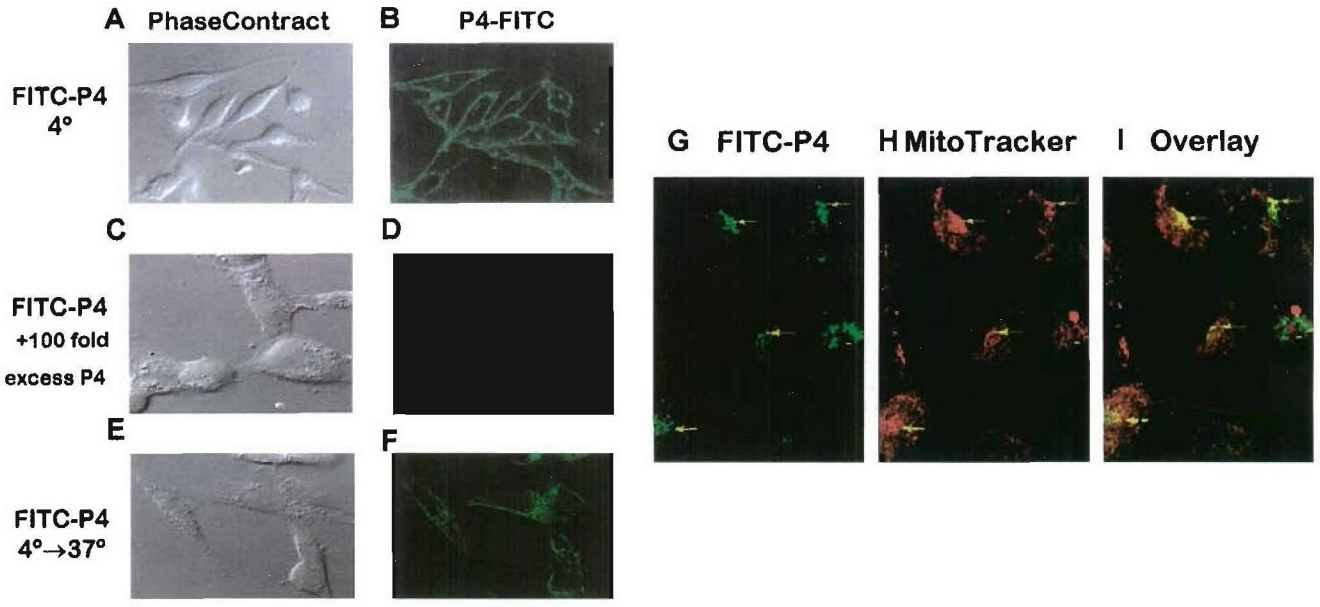

FIGURE 7 – Internalization of FITC-P4: To follow the uptake of the P4 peptide, MDA-435 cells were cultured with 1 μg/ml of FITC-P4 in the presence and absence of unlabeled P4 for 1 hr at 4°C, fixed and examined microscopically. (*a–d*) Phase and confocal fluorescent microscopic views of the cells indicated that under these conditions the FITC-P4 became associated with the plasma membrane and this was blocked by an excess of nonlabeled P4 peptide. (*e,f*) When the temperature was raised to 37°C, the FITC-P4 was internalized by the cells, and appeared to accumulate in the perinuclear region. (*g,h*) To trace the cellular location of P4 in greater detail, cells were incubated with FITC-P4 at 4°C for 1 hr, at which point MitoTracker was added and the cells were further incubated at 37°C for 20 min. Then the cells were fixed and examined under a confocal microscope. The intracellular FITC-P4 (in green, *g*) colocalized with MitoTracker (in red, *h*) shown in the overlay image (in yellow, *i*), indicating that P4 was transported to mitochondria, a central organelle in the apoptotic pathway.

and endothelial cells were maintained at 4°C, the FITC-P4 bound to their surfaces and could be competed off by an excess of nonlabeled P4 (Fig. 7*a–d*). In subsequent experiments, we found that when the temperature was raised to 37°C, the MDA-435 cells rapidly internalized the FITC-P4, which became associated with small particles located next to the nucleus (Fig. 7*e,f*). To determine if FITC-P4 interacted with the mitochondria, we carried out a double-label experiment with both FITC-P4 and MitoTracker, a marker for mitochondria. Figure 7*g* shows that the intracellular FITC-P4 (in green, Fig. 7*g*) did indeed co-localized with MitoTracker (in red, Fig. 6*h*), as indicated by the overly imaging (in yellow, Fig. 7*i*), indicating that P4 was transported to mitochondria, a central organelle in the apoptosis pathway.

The association between P4 and the mitochondria suggested that it might also alter the function of this organelle. In particular, it could inhibit the membrane potential of the mitochondria that is essential for respiration. To test this possibility, MDA-435 and ABAE cells were treated with the fluorescent dye JC-1 that changes its spectrum depending upon the membrane potential of the mitochondria.[17] As shown in Figure 8, we found that treatment with P4 caused an increase in the fraction of cells having depolarized mitochondrial membranes. Taken together, these results suggest that shortly after P4 is taken up by the cells, it becomes associated with the mitochondria and alters their membrane potential.

P4 binds to anti-apoptotic bcl-2 and Bcl-x_L

The mitochondria play a central role in regulating apoptosis. Indeed, several members of the Bcl-2 family interact with the mitochondria to control its function as well as the apoptotic cascade.[22] Thus, it is possible that P4 interacts with Bcl-2 or related proteins on the mitochondria. To test this possibility, we examined the binding between P4 and Bcl-2 using an ELISA. For this, immobilized P4 was probed with varying concentrations of purified Bcl-2 followed by an antibody to Bcl-2. As shown in Figure 9, the Bcl-2 bound to the P4 in a dose-dependent fashion but demonstrated little or no binding to the random peptide or to wells coated with vehicle alone.

We further examined the interaction between P4 and Bcl-2 by immunoprecipitation. For this, 293T cells were transiently transfected with an expression vector coding for Bcl-2 or Bcl-x_L fused to green fluorescence protein (GFP) or with GFP alone as a control (Fig. 9*b*, lanes 1–3). The cells were then incubated with biotin-P4, extracted and mixed with streptavidin-Sepharose beads. The bound material was then analyzed by Western blotting using an antibody to GFP. Figure 9*b* shows that P4 could pull down both Bcl-2-GFP and Bcl-x_L-GFP (lanes 5 and 6) but had no effect on GFP alone (lanes 4), indicating that the interaction occurs between Bcl-2/Bcl-x_L and P4. Similar results were obtained with MCF-7 cells transfected with a Bcl-2 expression vector (data not shown).

If P4 exerts its effects by blocking Bcl-2-induced apoptosis, then the overexpression of Bcl-2 should block this process. To test this possibility, MCF-7 cells were transfected with an expression vector for Bcl-2 or an empty vector and then tested for their response to P4 by thymidine incorporation. When the parental MCF-7 cells were treated with P4 overnight, they detached from the substratum, became rounded and condensed, whereas this did not occur with their counterparts treated with the random peptide. However, when the MCF-7 cells that over-expressed Bcl-2 were treated with P4, they were much less susceptible to cell damage compared to the vector transfected cells (46% of Bcl-2 high expressing cells *vs.* 70% of control cells). Thus, excess levels of Bcl-2 appears to reduce the toxic effects of P4, which again suggests that Bcl-2 is the target of P4.

Release of cytochrome c

To determine if P4 initiated apoptosis by destabilizing the mitochondria, we performed an *in vitro* assay to detect the release of cytochrome c. A crude preparation of mitochondria was isolated from MDA-435 cells by differential centrifugation and divided into 3 fractions that were treated with vehicle alone, a random peptide and P4, respectively. The 3 samples were centrifuged to

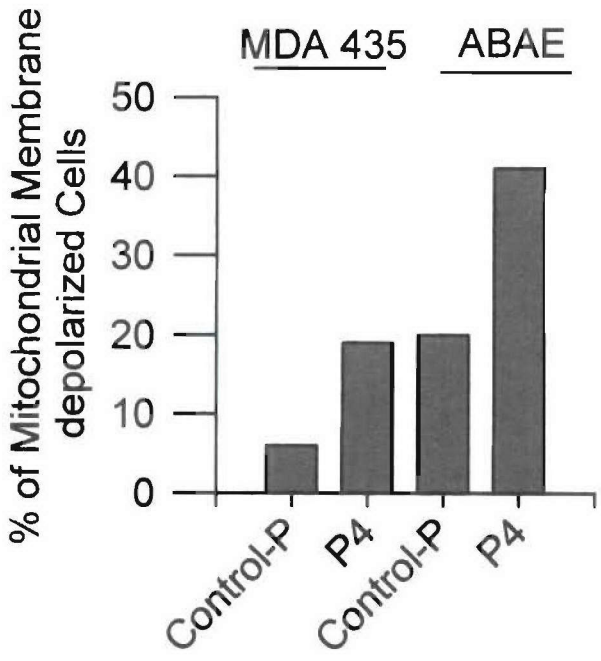

FIGURE 8 – Depolarization of mitochondria membranes: MDA-435 and ABAE cells were treated with 50 μg/ml of a random peptide (control-P) or P4 overnight, stained with JC-1 and analyzed by flow cytometry to distinguish those with a high-green and low-red fluorescence (indicative of depolarized mitochondria). A higher percentage of the P4-treated cells had depolarized mitochondria as compared to cells treated with the random peptide.

separate the pellets containing the particulate fraction from the supernatants containing the soluble components. All of the resulting fractions were then analyzed by Western blotting for cytochrome c. Figure 10 shows that increased cytochrome c was detected in the supernatant of samples treated with P4 (lane 3) but not in those treated with either the random peptide or vehicle alone (lane 1 and 2).

DISCUSSION

Based on the results of our study, we propose the following multistep model to account for the effects of P4 on tumor growth: 1) P4 bind to hyaluronan or other glycosaminoglycans on the surfaces of tumor and endothelial cells and is taken up into the cytoplasm, 2) the peptide then binds to Bcl-2 and related proteins on mitochondria, 3) this interaction inhibits the membrane potential of the mitochondria and leads to the release of cytochrome c into the cytoplasm, 4) the free cytochrome c activates caspase 9 that initiates the cascade of downstream effectors, and 5) this induces apoptosis in the target cells that results in the inhibition of tumor growth. The evidence for each of these steps will summarized as follows.

The first step of our model is that P4 preferentially targets the surfaces of tumor and endothelial cells. We believe that this preference is due to ability of P4 to bind to hyaluronan and other glycosaminoglycans, which was the basis of its initial selection. A number of studies have shown that hyaluronan is up-regulated on rapidly proliferating cells including both tumor and endothelial cells and this could account for the relatively selective activity of the P4 against proliferating as opposed to not-nonproliferating cells.[23,24] The results of confocal microscopic studies have indicated that once P4 had bound to the cell surfaces, it was quickly internalized. Perhaps the uptake of the P4 is mediated by CD44 which is responsible for the uptake of hyaluronan into endosomes and lysosomes.[25] Presumably, the P4 could then enter the cytoplasm by either passive leakage or by active transport as has been shown to be the case with vacuoles.[26]

In the second step of this model, P4 becomes associated with Bcl-2 and related proteins on the mitochondrial membrane. Direct evidence from both ELISA and immunoprecipitation experiments have indicated that P4 binds to Bcl-2 and Bcl-x_L. More indirect evidence is provided by confocal microscopy experiments that show that FITC-P4 becomes associated with the mitochondria that have both Bcl-2 and Bcl-x_L on their surfaces. Finally, experiments have shown that cells that overexpress Bcl-2 are relatively resistant to the P4-induced apoptosis. Again, this is consistent with our postulate that P4 interacts with Bcl-2 and related proteins. Presumably, the physical association of P4 with Bcl-2 and Bcl-x_L alters the activity of these molecules.

In the next step of our model, we postulate that P4 inhibits the function of the mitochondria and causes the release of cytochrome c. This situation is consistent with other studies showing that the Bcl-2 and related molecules control the stability of the mitochondria.[22] In particular, the anti-apoptotic Bcl-2 family members are believed to be anchored to the mitochondrial membranes and form a large macromolecular lattice structure that also includes Apaf-1, an adaptor for caspase 9. When these proteins bind to pro-apoptotic member of the Bcl-2 family, the lattice conformation is altered, forming ion-conducting channels and releasing Apaf-1 and cytochrome c into the cytosol.[20] In our study, flow cytometry experiments have shown that shortly after exposure to P4, the spectrum of JC-1 is altered, suggesting that the membrane potential of mitochondria is inhibited. At the same time, P4 also appears to cause the release of cytochrome c, which was demonstrated with the mitochondrial preparations. Presumably, the binding of P4 to Bcl-2 alters the integrity of the mitochondria and this leads to the release of cytochrome c.

In the fourth step of our model, the cytochrome c released by the mitochondria activates the caspase cascade leading to apoptosis. Again, this is supported by several lines of evidence. For example, Western blotting has shown that exposure of cells to P4 results in the activation of caspase 9 as would be expected from the interaction between cytochrome c and Apaf-1. Similarly, other downstream members of the apoptotic cascade such as caspase 3 and PARP were also activated. The induction of apoptosis in the target cells was clearly demonstrated by increased staining with annexin V, an early marker of apoptosis, as well as by DNA fragmentation that occurs during later stages.[17,18] A final piece of evidence that caspases are involved in mediating the P4-induced apoptosis is that the pan-caspase inhibitor Z-VAD-FMK blocked the effects of P4 on tumor cells.

In the final step of our working model, the apoptosis of the target cells inhibits the growth of tumors. This was supported by the fact that injection of P4 peptide inhibited the growth of tumor cells on the CAM of chicken embryos and that transfection of tumor cells with P4 expression vectors inhibited their growth in mice. It is important to note that the P4 peptide did not appear to be toxic to the host tissue since it had no effect on the growth or development of the chicken embryos or the weight of the mice.

The P4 peptide may be inhibiting tumor growth by both direct and indirect mechanisms. The direct mechanism involves the tumor cells themselves as suggested by the fact that P4 inhibits tumor cells growing in tissue culture. The indirect mechanism involves the endothelial cells that are responsible for neovascularization of the tumors. When the P4 peptide was applied to the chicken CAM it inhibited the vascularization induced by VEGF and FGF-2. In addition, histological analysis of the xenografts formed by tumor cells expressing P4 in nude mice revealed that there was a decreased density of blood vessels as compared to control xenografts. Thus, P4 appears to be acting both at the level of tumor cells as well as on endothelial cells that are responsible for neovascularization of the tumors. This may be similar to the situation with several other chemotherapeutic agents that have been shown to target both tumor as well as endothelial cells.[27]

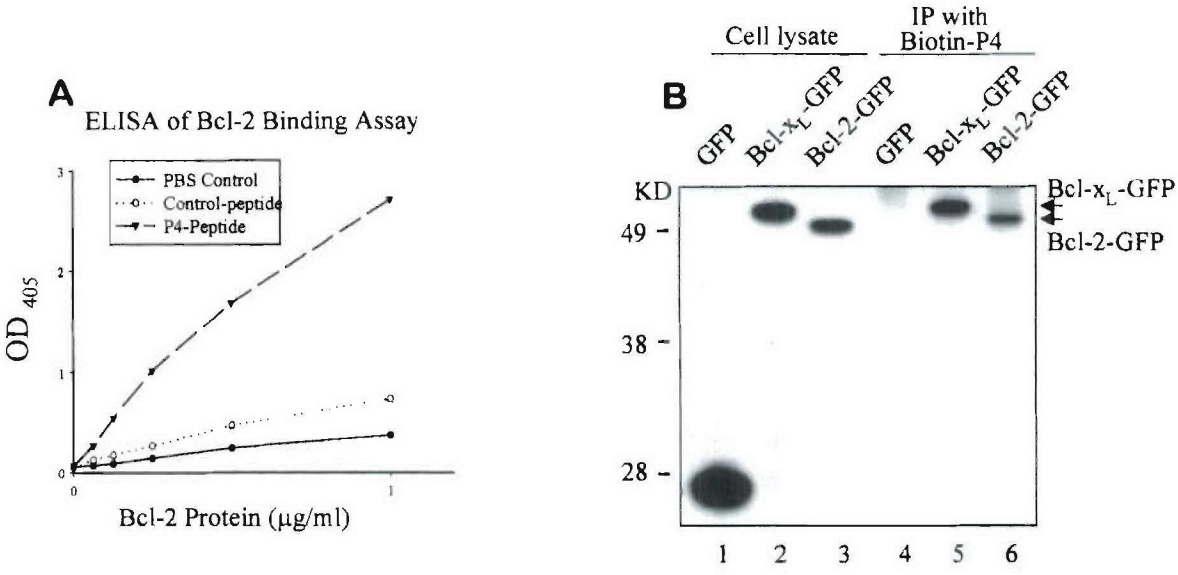

FIGURE 9 – Binding of P4 to Bcl-2 and Bcl-x_L. The interaction between P4 and Bcl-2 was examined with an ELISA and by immunoprecipitation. (*a*) For the ELISA, varying concentrations of Bcl-2 were added to the wells of an ELISA plates that had been coated with either P4, a random peptide or saline. After blocking, the wells were incubated sequentially with antibodies directed against Bcl-2, peroxidase-labeled secondary antibodies and finally a peroxidase substrate. The OD_{405} was determined using an ELISA reader and showed that Bcl-2 bound to wells coated with the P4 peptide but not to those coated with the random peptide or uncoated (saline). (*b*) For the immunoprecipitation assay, 293T cells were transiently transfected with expression vectors for GFP alone (control) and for Bcl-2 and Bcl-x_L fused to GFP. As shown in lanes 1 through 3, the transfected cells expressed each of these proteins as determined by Western blotting with antibodies to GFP. The cells were then extracted in a detergent solution, mixed with biotinylated P4, precipitated with streptavidin-Sepharose and analyzed by Western blotting. Lanes 4 through 6 show the P4 brought down both the Bcl-x_L-GFP and Bcl-2-GFP but not GFP itself. These results suggest that P4 binds to Bcl-2 and Bcl-x_L.

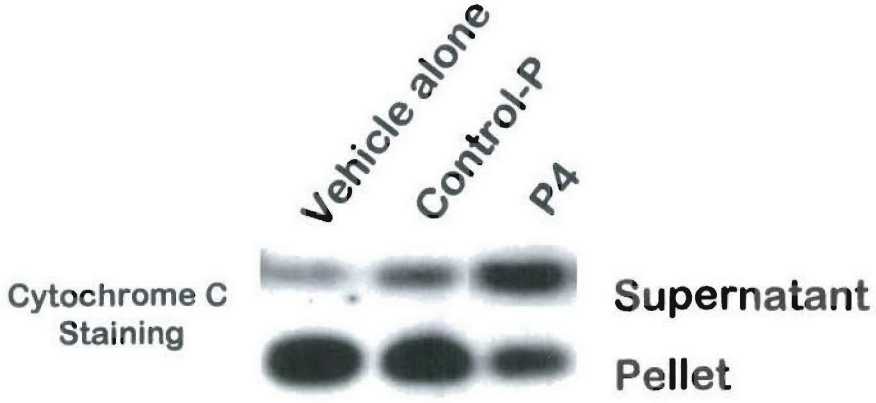

FIGURE 10 – Effect of P4 on the release of cytochrome c. A crude preparation of mitochondria was isolated from MDA-435 cells by differential centrifugation and divided into 3 equal fractions. One fraction was treated with vehicle alone, another with a random peptide (control-P) and the third with P4. The samples were then centrifuged (15,000*g*) to pellet the mitochondria. The supernatants (containing the released cytochrome c) and the pellets (containing the mitochondria) were collected and analyzed by Western blotting with antibodies to cytochrome c. In the 2 control samples (lanes 1 and 2), most of the cytochrome c was present in pellet, whereas in the samples treated with P4 (lane 3) most of the cytochrome c was in the soluble supernatant.

P4 appears to be structurally unrelated to other peptides that can interact with Bcl-2. Most proteins in the Bcl-2 family contain a BH3 domain that mediates the interaction with other family members and helps regulate the induction of apoptosis. Given its importance, a number of studies have attempted to identify peptides that interact with Bcl-2 or Bcl-x_L and antagonize their function. For example, Sattler synthesized peptides containing the BH3 domains of several Bcl-2 family members and found that many of them could bind to Bcl-x_L.[28] Synthetic BH3 peptides from pro-apoptotic members of the Bcl-2 family have an apoptosis-inducing activity.[29] However, when we compared the structures of the peptides with that of P4, we were unable to identify any similarity.

On the other hand, P4 does exhibit some structural similarity to other biologically active peptides. For example, Mummert *et al.*[30] used phage display to identify a peptide consisting of 12 amino acids that binds specifically to hyaluronan. This peptide contains 2 basic amino acids separated by a sequence of 8 amino acids similar to that found in P4. However, in contrast to P4, the peptide describe by Mummert *et al.*[30] binds specifically to hyaluronan and not to chondroitin sulfate. This peptide blocked the interaction between lymphocytes and hyaluronan, which inhibited a number of inflammatory reactions. Another biologically active peptide was described by Ellerby *et al.*[31] that appears to target mitochondria and trigger apoptosis. This peptide also has a high positive charge similar to that found in P4; however it is not clear whether it can bind to hyaluronan. Finally, tachyplesin is a small peptide found in the hemocytes of horseshoe crabs that has antibiotic activity.[32] Recently, we have reported that this compound can induce apoptosis in cultured cells and block tumor growth. This peptide also has a high positive charge similar to that of P4. Based on our results, we speculate that the antitumor activity of these latter 2 compounds may be mediated by a mechanism similar to that described here for P4.

There are a number of issues that should be addressed concerning the potential use of P4 or related compounds for the treatment of cancer. First, it is important to note that relatively high concentrations of the peptide are required to achieve antitumor activity both *in vivo* and *in vitro*. While P4 appears to be relatively nontoxic to normal tissues, the high concentrations needed make administration cumbersome. Secondly, since the peptide is small, its half-life in circulation is relatively short. Again, this necessitates the use of large amounts of material over frequent intervals. However, it may be possible to design related peptides that overcome these limitations. For example, it may be possible to produce recombinant versions of the peptide containing a greater number of basic motifs that results in a higher affinity for both hyaluronan and for Bcl-2. At the same time, the increased size of the compounds could prolong their half-life in circulation. Such compounds may demonstrate superior antitumor activity while minimizing their negative side effect.

ACKNOWLEDGEMENTS

This work was supported by U. S. Army Med. Res. and Mat. Command (DAMD17-00-1-0081 and DAMD17-01-1-0708) and NCI/NIH (R29 CA71545) to L.Z. The animal protocols were reviewed and approved by the Animal Care and Use Committee of Georgetown University.

REFERENCES

1. Liu N, Lapcevich RK, Underhill CB, Han Z, Gao G, Swartz G, Plumb SM, Zhang L, Green SJ. Metastatin: a hyaluronan binding complex for cartilage that inhibits tumor growth. Cancer Res 2001;61:1022–8.
2. Sy MS, Guo YJ, Stamenkovic I. Inhibition of tumor growth in vivo with a soluble CD44-immunoglobulin fusion protein. J Exp Med 1992;176:623–7.
3. Yu Q, Toole BP, Stamenkov I. Induction of apoptosis of metastatic mammary carcinoma cells in vivo by disruption of tumor cell surface CD44 function. J Exp Med 1997;186:1985–96.
4. Mohapatra S, Yang X, Wright JA, Turley EA, Greenberg AH. Soluble hyaluronan receptor RHAMM induces mitotic arrest by suppressing Cdc2 and cyclin B1 expression. J Exp Med 1996;183:1663–8.
5. Wisniewski HG, Hua J-C, Poppers DM, Naime D, Vilcek J, Cronstein BN. TSG-6, a glycoprotein associated with arthritis, and its ligand hyaluronan exert opposite effects in a murine model of inflammation. J Immunol 1996;156:1609–15.
6. O'Reilly MS, Boehm T, Shing Y, Fuka N, Wasios G, Lane WS, Flynn E, Birkhead JR, Olsen BR, Folkman J. Endostatin: an endogenous inhibitor of angiogenesis and tumor growth. Cell 1997;88:277–85.
7. Hohenester E, Sasaki T, Olsen BR, Timpl R. Crystal structure of the angiogenesis inhibitor endostatin at 1.5 A resolution. EMBO J 1998; 17:1656–64.
8. Yang B, Yang BL, Savani RC, Turley EA. Identification of a common hyaluronan binding motif in the hyaluronan binding proteins RHAMM, CD44 and link protein. EMBO J 1994;13:286–96.
9. Yang B, Zhang L, Turley EA. Identification of two hyaluronan-binding domains in the hyaluronan receptor RHAMM. J Biol Chem 1993;268:8617–23.
10. Hope TJ, Zhu L, Parslow TG, Yang B, Stern M, Turley EA, Stern R. Partial sequence of porcine liver hyaluronidase: identification of a hemoplexin and two putative HA-binding domains. J Cell Biochem Suppl 1993;17E:175 (abstract).
11. Goetinck PF, Stirpe NS, Tsonis PA, Carlone D. The tandemly repeated sequences of cartilage link protein contain the sites for interaction with hyaluronic acid. J Cell Biol 1987;105:2403–08.
12. Banerji S, Ni J, Wang SX, Clasper S, Su J, Tammi R, Jones M, Jackson DG. LYVE-1, a new homologue of the CD44 glycoprotein, is a lymph-specific receptor for hyaluronan. J Cell Biol 1999;144:789–801.
13. Saarela J, Ylikarppa R, Rehn M, Purmonen S, Pihlajaniemi T. Complete primary structure of two variant forms of human type XVIII collagen and tissue-specific differences in the expression of the corresponding transcripts. Matrix Biol 1998;16:319–28.
14. Arap W, Pasqualini R, Ruoslahti E. Cancer treatment by targeted drug delivery to tumor vasculature in a mouse model. Science 1998;279: 377–80.
15. Culty M, Shizari M, Thompson EW, Underhill CB. Binding and degradation of hyaluronan by human breast cancer cell lines expressing different forms of CD44: correlation with invasive potential. J Cell Phys 1994;160:275–86.
16. Brooks PC, Silletti S, von Schalscha TL, Friedlander M, Cheresh DA. Disruption of angiogenesis by PEX, a noncatalytic metalloproteinase fragment with integrin binding activity. Cell 1998;92:391–400.
17. Cossarizza A, Kalashnikova G, Grassilli E, Chiapelli R, Salvioli S, Capri M, Barbieri D, Troiano L, Rfanceschi C. Mitochondrial modification during rat thymocyte apoptosis: a study at the single cell level. Exp Cell Res 1994;214:23–330.
18. Vermes I, Haanen C, Steffens-Nakken H, Reutelingsperger C. A novel assay of apoptosis: flow cytometric detection of phosphatidylserine expression on early apoptotic cells using fluorescein labelled Annexin V. J Immunol Meth 1995;184:39–51.
19. Pedersen PL, Greenawalt JW, Reynafarje B, Hullihen J, Decker GL, Soper JW, Bustamente E. Preparation and characterization of mitochondria and submitochondrial particles of rat liver and liver-derived tissues. Meth Cell Biol 1978;20:411–81.
20. Green DR, Reed JC. Mitochondria and apoptosis. Science 1998;281: 1309–12.
21. McColl KS, He H, Xhong H, Whitacre CM, Berger NA, Distelhorst CW. Apoptosis induction by the glucocorticoid hormone dexamethasone and the calcium-ATPase inhibitor thapsigargin involves Bcl-2 regulated caspase activation. Molec Cell Endocrinol 1998;139:229–38.
22. Adams JM, Cory S. The Bcl-2 protein family: arbiters of cell survival. Science 1998;181:1322–26.
23. Matuoka K, Namba M, Mitsui Y Hyaluronate synthetase inhibition by normal and transformed human fibroblasts during growth reduction. J Cell Biol 1987;104:1105–15.
24. Mohamadzadeh M, DeGrendele H, Arizpe H, Estess P, Siegelman M. Proinflammatory stimuli regulate endothelial hyaluronan expression and CD44/HA-dependent primary adhesion. J Clin Invest 1998;101 97–108.
25. Culty M, Nguyen NA, Underhill CB. The hyaluronan receptor (CD44) participates in the uptake and degradation of hyaluronan. J Cell Biol 1992;116:1055–62.
26. Kovacsovics-Bankowski M, Rock KL. A phagosome-to-cytosol pathway for exogenous antigens presented on MHC class I molecules. Science 1995;267:243–6.
27. Browder T, Butterfield CE, Kraling NM, Blair NS, O'Reilly MS, Folkman J. Antiangiogenic scheduling of chemotherapy improves efficacy against experimental drug-resistant cancer. Cancer Res 2000; 60:1878–86.
28. Sattler M, Liang H, Nettesheim D, Meadows RP, Harlan JE, Eberstadt M, Yoon HS, Shuker SB, Chang BS, Minn AJ, Thompson CB, Fesik SW. Structure of Bcl-x_L-Bak peptide complex: recognition between regulators of apoptosis. Science 1997;275:983–6.
29. Wang JL, Zhang ZJ, Choksi S, Shan S, Lu Z, Croce CM, Alnemri ES, Korngold R, Huang Z. Cell permeable Bcl-2 binding peptides: a chemical approach to apoptosis induction in tumor cells. Cancer Res 2000;60:1498–502.
30. Mummert ME, Mohamadzadeh M, Mummert SI, Mizumoto N, Takashima A. Development of a peptide inhibitor of hyaluronan-mediated leukocyte trafficking. J Exp Med 2000;192:769–79.
31. Ellerby HM, Apap W, Ellerby LM, Kain R, Andrusiak R, Rio GD, Krajewski S, Lombardo CR, Rao R, Ruoslahti E, Bredesen DE, Pasqualini R. Anti-cancer activity of targeted pro-apoptotic peptides. Nat Med 1999;5:1032–38.
32. Chen, Y, Xu X, Chen JN, Underhill CB, Creswell K, Hong S, Zhang L. Anti-tumor effects of RGD-tachyplesin. Cancer Res. 2001;61: 2434–38.

Tachyplesin Activates the Classic Complement Pathway to Kill Tumor Cells

Jinguo Chen,[1] Xue-Ming Xu,[2] Charles B. Underhill,[1] Shanmin Yang,[3] Luping Wang,[4] Yixin Chen,[5] Shuigen Hong,[5] Karen Creswell,[1] and Lurong Zhang[3]

[1]Department of Oncology, Lombardi Comprehensive Cancer Center, Georgetown University Medical Center, Washington, District of Columbia; [2]National Cancer Institute, NIH, Bethesda, Maryland; [3]Department of Radiation Oncology, University of Rochester Medical Center, Rochester, New York; [4]Department of Pathology, Beijing General Hospital, Beijing, PR China; and [5]Key Laboratory of China Education Ministry on Cell Biology and Tumor Cell Engineering, Xiamen University, Fujian, PR China

Abstract

Tachyplesin is a small, cationic peptide that possesses antitumor properties. However, little is known about its action mechanism. We used phage display to identify a protein that interacted with tachyplesin and isolated a sequence corresponding to the collagen-like domain of C1q, a key component in the complement pathway. Their interaction was subsequently confirmed by both ELISA and affinity precipitation. Tachyplesin seemed to activate the classic complement cascade because it triggered several downstream events, including the cleavage and deposition of C4 and C3 and the formation of C5b-9. When TSU tumor cells were treated with tachyplesin in the presence of serum, activated C4b and C3b could be detected on tumor cells by flow cytometry, Western blotting, and confocal microscopy. However, this effect was blocked when the tumor cells were treated with hyaluronidase or a large excess of hyaluronan, indicating that hyaluronan or related glycosaminoglycans were involved in this process. Treatment of cells with tachyplesin and serum increased in membrane permeability as indicated by the ability of FITC-dextran to enter the cytoplasm. Finally, the combination of tachyplesin and human serum markedly inhibited the proliferation and caused death of TSU cells, and these effects were attenuated if the serum was heat-inactivated or if hyaluronidase was added. Taken together, these observations suggest that tachyplesin binds to both hyaluronan on the cell surface and C1q in the serum and activates the classic complement cascade, which damages the integrity of the membranes of the tumor cells resulting in their death. (Cancer Res 2005; 65(11): 4614-22)

Introduction

Small peptides represent a promising new group of compounds in the fight against cancer (1–3). Of particular interests are naturally occurring peptides that have antimicrobial activity, many of which also have antitumor activity (4–6). To date, >100 antibiotic peptides have been described and these can be arbitrarily classified into three major groups based on their structure: linear peptides, disulfide-linked peptides (such as defensins and tachyplesins; refs. 7–9), and those containing posttranslationally modified amino acids. In most cases, these peptides contain cationic amino acids that can interact electrostatically with the anionic head groups of phospholipids found in negatively charged membranes. Once these peptides bind to the membrane, their amphipathic helices can distort the lipid bilayer (with or without the formation of pores), resulting in the loss of membrane integrity. For example, polyphemusin I, a cationic antimicrobial peptide obtained from the horseshoe crab, has been shown to bind lipopolysaccharide coat of bacteria and permeabilize the outer membrane. However, it did not have any affinity for neutral lipids (10). The membranes of both prokaryotic cells and the mitochondria of eukaryotic cells maintain a large transmembrane potential and have a high content of anionic phospholipids, reflecting their common ancestry. In contrast, the plasma membranes of eukaryotic cells generally have a low potential and are composed almost exclusively of zwitterionic phospholipids (11). Many antibacterial peptides, therefore, preferentially disrupt prokaryotic and mitochondrial membranes (12, 13).

Tachyplesin, a small peptide composed of 17 amino acids, is isolated from the horseshoe crab (14). It has an amphipathic structure conferred by two antiparallel β-sheets held rigidly in place by two disulfide bonds. This structure seems to be critical for its antimicrobial activity (15). Previously, we found that a synthetic version of tachyplesin conjugated to the integrin homing domain RGD blocked the growth of tumor cells both *in vitro* and *in vivo* (5). RGD-tachyplesin inhibited the proliferation of both cultured tumor and endothelial cells and reduced the colony formation of TSU cancer cells. Importantly, *in vivo*, it could inhibit the growth of tumors via induction of apoptosis in both tumor and endothelial cells evidenced by activation of several caspases in both the mitochondrial and Fas-dependent pathways. More recently, we found that tachyplesin by itself (i.e., without the RGD domain) could inhibit tumor growth in the presence of normal serum even against cells that overexpress the multiple-drug resistant gene (data not shown).

However, little is known about the action mechanism of tachyplesin and it is unclear how it affects the plasma membranes of eukaryotic cells. The present study was to elucidate the mechanism by which tachyplesin was able to inhibit the growth of tumor and endothelial cells. Using the T7 phage display technique, we identified the C1q subcomponent of human complement 1 as a potential target of tachyplesin. The interaction between C1q and tachyplesin was confirmed by an ELISA and by affinity precipitation. The binding of tachyplesin to C1q seems to trigger the activation of the classic complement pathway and leads to the killing of TSU tumor cells. Interestingly, this effect was blocked if the target cells were pretreated with hyaluronidase or an excess of hyaluronan. This indicates that tachyplesin may initially

Note: J. Chen and X-M. Xu share senior authorship. L. Zhang was a recipient of a Visiting Scholar Award from the Key Laboratory of China Education Ministry on Cell Biology and Tumor Cell Engineering, Xiamen University, Fujian, PR China.

Requests for reprints: Lurong Zhang, Department of Radiation Oncology, University of Rochester Medical Center, 601 Elmwood Avenue, Rochester, NY 14642-8647. Phone: 585-275-2985; Fax: 585-275-6337; E-mail: Lurong_Zhang@urmc.rochester.edu.

target hyaluronan and related compounds on the cell surface and subsequently bind to C1q in the serum to activate the complement pathway. This represents a new mechanism for an antitumor agent.

Materials and Methods

Peptides and reagents. Two peptides were chemically synthesized: tachyplesin that consists of the sequence KWCFRVCYRGICYRRCR and a control peptide that contained the same amino acids but in a scrambled sequence. To impede enzymatic degradation of these peptides, the NH_2 terminals were acetylated and the COOH terminals were amidated.

Normal human sera were obtained from healthy volunteers. In some experiments, the serum was incubated at 56°C for 30 minutes to inactivate the complement system.

Reduction, alkylation, and acetylation of tachyplesin. The derivatization of the peptides was done as described by Prohaszka (7). A 1 mg/mL solution of tachyplesin in PBS was incubated with 20 mmol/L DTT at 37°C for 3 hours, followed by the addition of 60 mmol/L iodoacetamide at 4°C for 1 hour, which resulted in the complete reduction of disulfide bonds and the alkylation of the free -SH groups. The peptides were then dialyzed (molecular weight cutoff 1,000; Spectro/Pro) against water. Aliquots of the resulting peptides were further acetylated with acetic anhydride overnight. The reduced, alkylated, and acetylated peptides were thoroughly dialyzed against water, concentrated, and kept at −20°C until use.

Phage display. A T7 phage library of cDNA sequences from human breast tumor cells (T7 Select) containing 1.6×10^7 recombinants was purchased from Novagen (Madison, WI). Tachyplesin or control peptide (5 μg/mL) was coated onto Microtiter wells (Micro Membranes, Inc., Newark, NJ) overnight at 4°C and blocked with 1% bovine serum albumin. After washing, 2×10^9 plaque-forming units of the library were added to each well and incubated overnight at 4°C. The wells were then washed five times with 0.1% Tween 20 in TBS. The bound phages were recovered with 4 mol/L urea, diluted with TBS, and amplified in *Escherichia coli* in top agarose gel. After 3-hour incubation, the phage plagues were harvested for the next round of screening. This procedure was repeated four to five times until the plagues recovered in tachyplesin-coated wells outnumbered those in control peptide wells by 100-fold. Ten positive colonies were picked randomly and the DNA fragments encoding the binding protein were amplified by PCR using T7 Select Primer Up/Down pair and subjected to dideoxy sequencing. Eight of ten plaques gave an identical sequence. The deduced amino acid sequence was then used to search for their molecular identities and homologies using BLASTN 2.2.6 from Genbank + European Molecular Biology Laboratory + DNA Data Bank of Japan + Protein Data Bank sequence databases.

ELISA. In most cases, microtiter plates were coated overnight with human C1q protein or peptide diluted in coating buffer [0.1 mol/L Na_2CO_3/$NaHCO_3$ (pH 9.6)] and then blocked with 2% bovine serum albumin for 2 hours at room temperature. All subsequent steps were done in 1% gelatin in veronal-buffered saline (VBS) consisting of 5 mmol/L sodium barbital, 150 mmol/L NaCl, 0.15 mmol/L $CaCl_2$, and 1 mmol/L $MgCl_2$ unless otherwise indicated, and each step was followed by three washes with 0.1% Tween 20 in PBS. The enzymatic activity of peroxidase was assessed by the addition of 2,2′-azino-bis(3-ethylbenzthiazoline-6-sulfonic acid (ABTS, Sigma, St. Louis, MO) and H_2O_2. The plate was read at a wavelength of 405 nm.

To confirm the binding of tachyplesin to C1q, two assays were done. First, the purified C1q (Sigma) were coated onto microtiter plates and the biotinylated tachyplesin was added at room temperature for 2 hours followed by peroxidase-conjugated streptavidin and ABTS substrate. Second, in reverse, the tachyplesin or the control peptide was coated and then C1q or normal human serum was added to the plate. The bound C1q was determined with a polyclonal rabbit antibody to C1q (1:1,000 dilution, DAKO, Carpinteria, CA) followed by a peroxidase-conjugated antirabbit IgG.

To detect the activation of the classic complement pathway, ELISA-based assays were done on plates coated with peptides (10 μg/mL) that were incubated with normal human serum diluted in VBS (C4b 1:2 for 30 minutes, C3b 1:2 for 20 minutes, and C5b-9 1:20 for 60 minutes) at room temperature according to their turnover rate (16, 17). The activated components were assessed using goat polyclonal antibodies to C4 (ICN, Aurora, OH) and to C3 and a rabbit polyclonal antibody to C5b-9 complex (Calbiochem, San Diego, CA).

Affinity precipitation and Western blotting. The serum samples (200 μL) were preabsorbed with 50 μL of streptavidin-Sepharose beads (Amersham, Piscataway, NJ) and then incubated with biotinylated tachyplesin (20 μg) and streptavidin-Sepharose beads (50 μL) overnight at 4°C. After washing, the bound proteins were eluted from the beads with 60 μL of Laemmli sample buffer (under reducing conditions) and electrophoresed on a 10% SDS-PAGE gel. After transfer to sheet of hydrophilic polyvinylidene fluoride (PVDF), the blot was immunostained with polyclonal antibodies to C1q (1:1,000) or to C4 (1:5,000) followed by a peroxidase-conjugated secondary antibody. The immunopositive bands were detected using Super Signal West Pico Chemiluminescent substrate (Pierce, Rockford, IL).

For the analysis of C3b deposition, TSU cells were incubated in 10% normal human serum along with tachyplesin or control peptide at 37°C for 60 minutes. After washing, the cells were harvested in lysis buffer (1% Triton X-100, 0.5% sodium deoxycholate, 1 mmol/L EDTA, 0.5 mg/mL leupeptin, 1 mg/mL pepstatin, and 0.2 mmol/L phenylmethylsulfonyl fluoride). The protein concentration of the cell lysates was determined with the BCA reagent (Pierce). Twenty micrograms of protein from each lysate were electrophoresed on a 10% SDS-PAGE gel and then transferred to sheet of PVDF. The sheet was blocked in 5% nonfat milk and incubated with a polyclonal antibody to C3 (1 μg/mL) overnight at 4°C followed by a peroxidase-labeled secondary antibody and a chemiluminescent substrate as described above.

Fluorescence-activated cell sorting analysis. To analyze the attachment of tachyplesin to the cell surface, TSU tumor cells were harvested with 10 mmol/L EDTA and incubated in the presence or absence of 0.1 mg/mL testicular hyaluronidase (H4272, Sigma) for 1 hour at 37°C. FITC-tachyplesin (1 μg/mL) with or without 200 μg/mL of hyaluronan (Lifecore, Chaska, MN) was then added to the TSU cells and incubated at 4°C for 30 minutes followed by fixation with freshly prepared formaldehyde. The binding of FITC-tachyplesin to the cell surface was analyzed by flow cytometry.

For analysis of deposition of complement components on cell surface, TSU tumor cells were again harvested with EDTA and incubated in the presence or absence of 0.1 mg/mL testicular hyaluronidase for 1 hour at 37°C. Then, 100 μg/mL of the peptides dissolved in VBS was added to the cell cultures in the presence or absence of 10% normal human serum and the cells were incubated for 20 minutes at room temperature. The cells were washed, incubated sequentially with goat polyclonal antibody to human C4 or C3 (20 μg/mL, 30 minutes at 4°C), FITC-conjugated donkey anti-goat antibody (1:200, 30 minutes, at 4°C), and finally propidium iodide. The cells were analyzed by fluorescence-activated cell sorting (FACS) within 1 hour.

The permeability of the plasma membrane was analyzed by staining with FITC-dextran (M_r 40,000, Molecular Probes, Eugene, OR). For this, TSU cells grown to 80% confluence were incubated with tachyplesin (50 μg/mL) in the presence of 10% human serum overnight. After harvesting, the cells were incubated with 5 μg/mL of FITC-dextran for 30 minutes and then subjected to flow cytometry analysis.

Confocal microscopy. All cells were maintained in improved MEM medium supplemented with 10% FCS, 2 mmol/L L-glutamine, and antibiotics in 5% CO_2/95% air. For analysis of deposition of complement components on cell surface, TSU cells were seeded on coverlids at 50% to 60% confluence 18 to 24 hours before treatment and then incubated with tachyplesin (50 μg/mL) in the presence of 10% normal human serum for 20 minutes. After washing, a polyclonal antibody to C3 (1:200) was added to the cells at 4°C for 30 minutes followed by a FITC-labeled secondary antibody (1:200). After fixation in 4% formaldehyde, the coverslips were mounted using Prolong Antifade kit (Molecular Probes) and analyzed with a confocal microscopy.

To detect binding of tachyplesin to the cell surface, TSU tumor cells cultured on coverslips were incubated with FITC-tachyplesin (1 μg/mL) at

4°C for 30 minutes. After washing and fixating with 4% formaldehyde, the cells were examined with a confocal microscopy.

[^{3}H]Hyaluronan binding assay. The [^{3}H]hyaluronan (5×10^5 cpm/μg, 490 μg/mL) was isolated from the medium of rat fibrosarcoma cells grown in the presence of ^{3}H-labeled acetate as described previously (18, 19). Tachyplesin (50 μg) in 100 μL of PBS was mixed at room temperature for 2 hours with 20 μL of [^{3}H]hyaluronan in the presence or absence of a 100-fold excess of nonlabeled hyaluronan and then spotted onto a nitrocellulose membrane. The free [^{3}H]hyaluronan was washed away with PBS and the complex of [^{3}H]hyaluronan and tachyplesin that retained on the filter membrane was processed for scintillation counting.

Cell proliferation assay. The [^{3}H]thymidine incorporation assay was carried out as described previously (5, 20). Aliquots of complete medium containing ~10,000 cells were distributed into a 96-well tissue culture plate. On the next day, the media was replaced with fresh media without serum, peptide, and normal human serum or heat-inactivated serum. In some experiments, testicular hyaluronidase was added to fresh media before the addition of peptide and serum. One day later, 0.3 μCi of [^{3}H]thymidine in serum-free media were added to each well; after another 8 hours, the cells were harvested and the amount of incorporated [^{3}H]thymidine was determined with a β counter.

Trypan blue absorbance assay. To determine the extent of cell death, we used the trypan blue absorbance assay according to the method described by Uliasz and Hewett (21). For this, TSU tumor cells were subcultured into 24-well plates (1×10^5 cells/well) in 1 mL of 10% fetal bovine serum-90% DMEM. On the following day, the media was removed and cells were exposed to different concentrations of tachyplesin or control peptide in the presence of either native or heated-inactivated human serum. After 18 hours, a 0.4% solution of trypan blue was added to each well to a final concentration of 0.05% and further incubated at 37°C for 15 minutes. Next, media was removed and the cells were gently washed with ice-cold PBS (3×750 μL). The cells were then lysed with 200 μL of 1% SDS and gently triturated. Finally, 175 μL of the SDS/trypan blue solution was transferred to a 96-well plate and read spectrophotometrically at 590 nm. The background absorbance value was obtained from sham-treated cultures and was subtracted from all experimental values to obtain specific absorbance for each condition. All samples were assayed in triplicates.

Results

Isolation and characterization of tachyplesin-binding phages. To identify molecules that bind to tachyplesin, we screened a phage-displayed library of some 1.6×10^7 unique clones expressing sequences from breast cancer cells ranging in size from 300 to 3,000 bp in length fused to the *T7* gene 10 capsid protein. Phage particles expressing tachyplesin-binding proteins/peptides were affinity purified on the wells of a microtiter plate coated with tachyplesin or control peptide. After four or five rounds of biopanning, the number of phages from the tachyplesin-coated plates was ~100-fold greater than that from control peptide plates. Ten plaques were then selected and amplified by PCR. Eight had the same-size PCR products and some of these were then sequenced. The deduced amino acid sequences were then subjected to a blast analysis, which repeatedly identified human C1q. The region of C1q binding to tacyplesin was located around the first 400 bp of complement C1q B chain open reading frame (Genbank accession no. NM_000491), corresponding to the NH_2-terminal collagen-like domain of C1q (5, 22).

Binding of the C1q to tachyplesin. To further test the possibility that tachyplesin binds to C1q, we examined the interaction between these two proteins using an ELISA-like system. In the first assay, plates were coated with tachyplesin or the control peptide, probed with C1q, and then the amount of bound C1q was detected with anti-C1q. As shown in Fig. 1*A*, C1q binds to immobilized tachyplesin in a dose-dependent manner, but not to the control peptide. Similar results were obtained when the plates were precoated with C1q and then probed with biotinylated tachyplesin (Fig. 1*B*). However, this interaction was significantly reduced if the tachyplesin was denatured by reduction and alkylation of the disulfide bonds and further acetylation of the charged side chains (Fig. 1*C*), which suggests that the interaction between tachyplesin and C1q depends on the secondary structure of tachyplesin.

The binding of tachyplesin to C1q was also dependent on the NaCl concentration used in the assay buffer (Fig. 1*D*). The maximum binding occurred at 0.15 mol/L NaCl, the normal physiologic salt concentration. Both increasing and decreasing the ionic strength in the assay drastically reduced the binding.

The interaction between tachyplesin and C1q was further examined by affinity precipitation and Western blotting of normal human serum. For this, a biotinylated tachyplesin was incubated with normal human serum, followed by streptavidin-Sepharose. The immobilized proteins were then eluted and analyzed by Western blotting. As shown in Fig. 2, probing the blot with a polyclonal antibody revealed three bands corresponding to three chains of the C1q complex (*A*: 27.5 kDa, *B*: 25.2 kDa, and *C*: 23.8 kDa, respectively) in the tachyplesin-treated sample, but not in the samples without the peptide or with the control peptide. Not surprisingly, only a small portion of C1q from the serum was pulled down because serum contains a relatively high concentration of this protein (80 μg/mL; ref. 23). Taken together, these results suggests that C1q binds to both immobilized (surface-bound) and free (liquid-phase) tachyplesin, and tachyplesin binds to both purified and serum C1q, which confirms that there is true interaction between these two molecules.

Activation of the classic complement pathway by tachyplesin. To determine if tachyplesin could activate the complement pathway, we used ELISAs with tachyplesin-coated microplates. Normal serum was diluted with VBS (containing Ca^{2+}) and applied to wells coated with tachyplesin or the control peptide, washed, and then probed with antibodies against C4, C3, and C5b-9. As shown in Fig. 3*A*, significant amounts of activated fragments of C4b, C3b, and C5b-9 complex were bound to the immobilized tachyplesin but not to the immobilized control peptide. Furthermore, when the same fresh serum was heat-inactivated (56°C, 30 minutes) before use, then the amount of C4b, C3b, and C5b-9 complex was greatly reduced. These results show that tachyplesin is able to trigger the activation of whole classic complement cascade, which is characterized by the appearance of C4b, C3b, and C5b-9 complex.

To further test for the presence of activated C4b fragments, Western blotting was done. For this, normal fresh human serum was mixed with the biotinylated tachyplesin or control peptide, affinity-precipitated with streptavidin-Sepharose, and then subjected to SDS-PAGE and Western blotting using antibodies to C4. Figure 3*B* shows that the three peptide chains of C4b (α 97 kDa, β 75 kDa, and γ 33 kDa, respectively) were affinity-precipitated in the tachyplesin-treated sample, but not in those treated with the control peptide or in the absence of peptide. This is consistent with the results obtained from ELISA and further supports the conclusion that tachyplesin can activate the classic complement cascade. Whereas it is possible that tachyplesin binds directly to C4b, the phage display results suggest that this is not the case. Tachyplesin seems to initially and mainly bind to C1q and then to C4b.

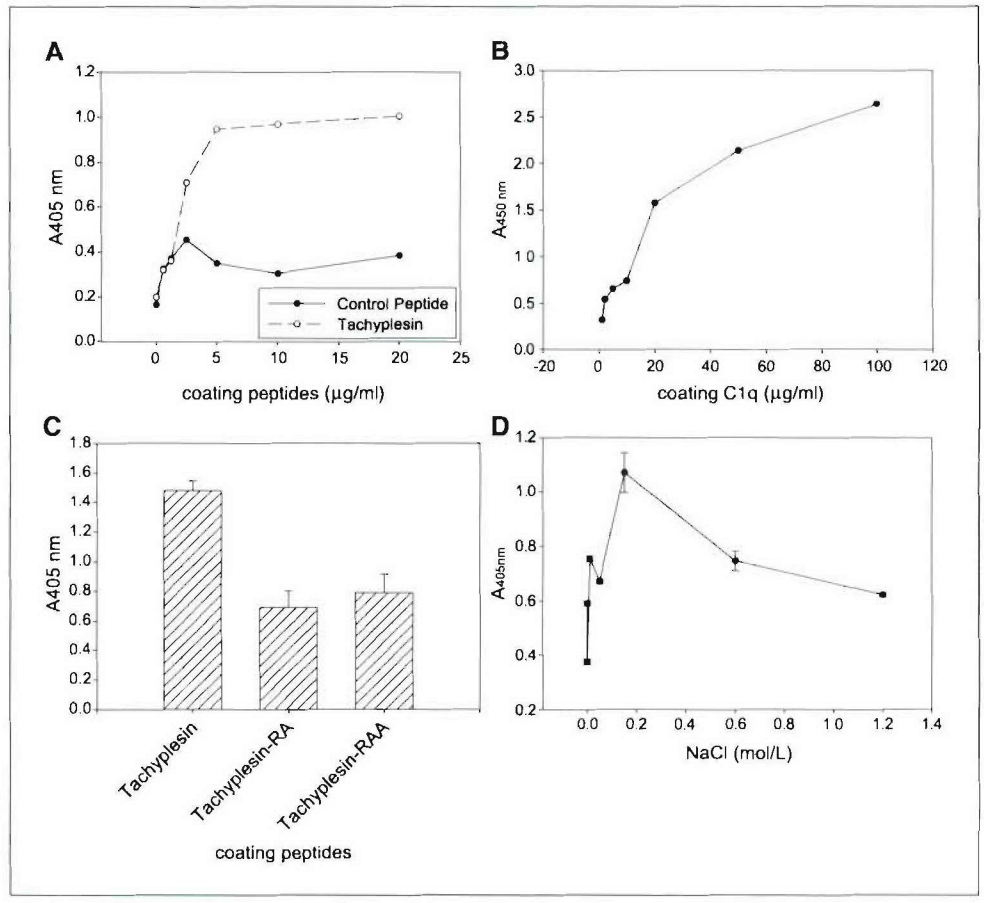

Figure 1. The interaction between tachyplesin and the C1q subcomponent of complement 1. *A*, ELISA plates were coated with varying concentrations of either tachyplesin or the control peptide and then incubated with 1 μg of C1q that was then detected with anti-C1q and peroxidase-conjugated detection system. The C1q bound to the plate coated with tachyplesin but not to that coated with the control peptide. *B*, plates were coated with varying concentrations of purified C1q, probed with biotinylated tachyplesin (1 μg/mL), and then assessed with the streptavidin-conjugated peroxidase and substrate system. Again, the tachyplesin bound to the immobilized C1q. *C*, similar amounts (10 μg/mL) of native, reduced, or alkylated (*RA*), and reduced, alkylated, and acetylated (*RAA*) tachyplesin replaced the tachyplesin in the above (*A*) binding system. The binding of C1q to native tachyplesin was significantly greater than either of the denatured peptides. *D*, to test the effect of ionic strength on the interaction, ELISA plate was coated with 10 μg/mL of C1q and then incubated with 0.1 μg/mL of biotinylated tachyplesin in VBS buffer of variable ionic strength. The maximum binding corresponded to physiologic ionic strength of 0.15 mol/L NaCl.

Role of hyaluronan in the deposition of C4b and C3b on tumor cells. Because tachyplesin contains a hyaluronan-binding motif [$B(X)_7B$; ref. 20], we investigated the possibility that tachyplesin can bind to hyaluronan (both free and cell associated). We took advantage of the fact that hyaluronan by itself does not bind to nitrocellulose but will do so in the presence proteins or peptides that bind to it (19). In the assay, tachyplesin was mixed with [^{3}H]hyaluronan and then applied to a nitrocellulose membrane. The free [^{3}H]hyaluronan was washed away and the complex of [^{3}H]hyaluronan-tachyplesin retained on the filter membrane was analyzed. Figure 4*A* shows that tachyplesin binds strongly to hyaluronan and this could be abolished by a 100-fold excess of unlabeled hyaluronan. In contrast, the control peptide showed little or no binding to [^{3}H]hyaluronan, indicating that the binding of tachyplesin to hyaluronan was specific.

We then examined the binding of FITC-tachyplesin to TSU cells that express large amounts of hyaluronan on their surfaces (20, 24). As shown in Fig. 4*B*, tachyplesin was distributed on the surface of the cells. This binding was significantly reduced by the addition of an excess of free hyaluronan on pretreatment with hyaluronidase (Fig. 4*C*) as shown by flow cytometry analysis. These results suggest that hyaluronan or related molecules, such as chondroitin sulfate (25), act as targets for tachyplesin on the cell surface.

In the classic pathway of complement activation, 4- to 5-fold more C3b than C4b is deposited on the surfaces of target cells (17). In addition, C3 contains a thioester moiety that can form covalent bonds with nearby molecules in the transition from C3 to C3b. Thus, C3b deposition represents an index of complement activation. For this reason, we tested whether tachyplesin could induce the deposition of C3b on tumor cells. TSU cells were incubated in a mixture of normal serum and tachyplesin, stained with antibodies to C3, then examined by confocal microscopy. As shown in Fig. 5*A* and *B*, C3b was indeed deposited on the surfaces of TSU cells.

The presence of activated C3b was also shown by Western blotting of TSU cells following treatment with serum and tachyplesin. Figure 5*C* shows that in the samples treated with

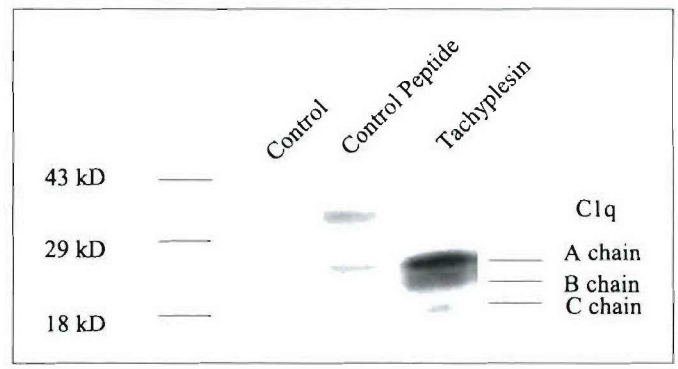

Figure 2. Affinity precipitation of serum C1q with tachyplesin. Normal human serum was incubated without or with biotinylated tachyplesin and control peptide, along with streptavidin-Sepharose in VSB buffer at 4°C overnight. After washing, the beads were extracted in Laemmli sample buffer (reducing conditions) and subjected to SDS-PAGE and Western blotting with anti-C1q antibody. Three bands representing the A, B, C chains of C1q (27,550, 25,200, 23,800 Da, respectively) were apparent in the sample incubated with biotinylated tachyplesin but not detected in the absence of peptide or in the control peptide. The results are representative of three different experiments.

tachyplesin, two subunits of C3b (α 115 kDa and β 75 kDa) and possibly degraded iC3b (? band for α1). Significantly, a high molecular weight band (*HMW* in Fig. 5*C*) was found with Western blotting under reducing conditions, indicating a covalent linkage to large membrane constituents. Scans of these Western blots revealed that the majority of deposited C3b (70-80%) was present in this high molecular weight form. This is consistent with the fact that in the transition from C3 to C3b, a thioester moiety, can form covalent bonds with nearby molecules. FACS analysis of cells treated with tachyplesin and serum (Fig. 5*D*) showed that there was a significant increase in FITC-tagged antibody to C3, indicating that C3b was deposited on the tumor cells, which did not occur with cells treated with the control peptide. These results are consistent with those from confocal microscopy and Western blotting.

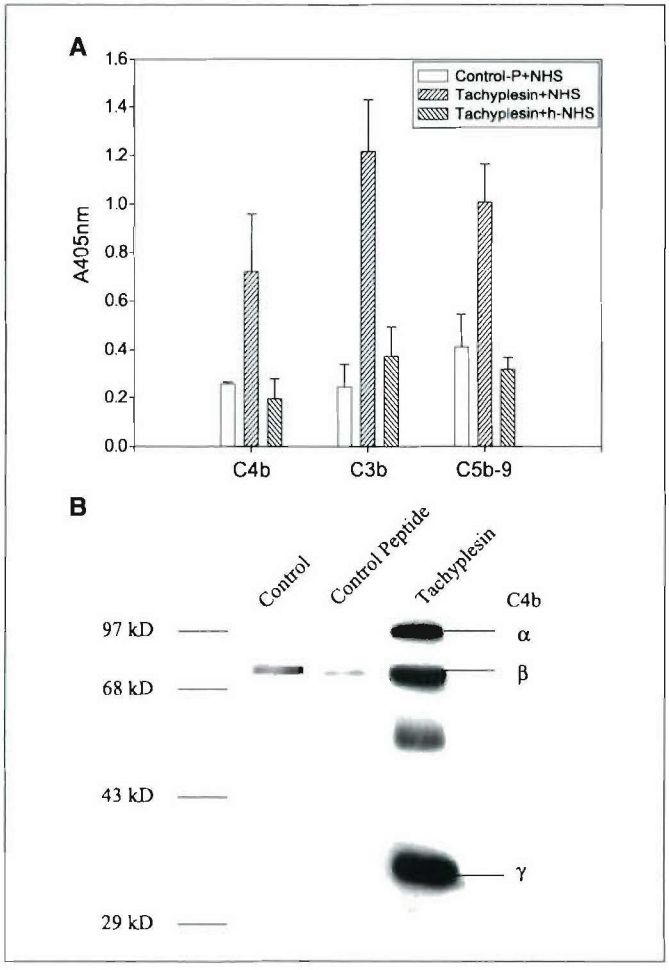

Figure 3. Determination of tachyplesin-mediated activation of the classic complement pathway by ELISA and affinity precipitation. *A*, microtiter plates were coated with either tachyplesin of the control peptide (10 μg/mL) incubated with normal human serum (*NHS*) without or with heat inactivation (*h-NHS*). The serum was diluted with VBS (1:2 for C4b, C3b and 1:20 for C5b-9). Complement activation was then assessed using polyclonal antibodies against C4, C3 and a polyclonal antibody to C5b-9. There was a significant amount of immobilized C4b, C3b and C5b-9 detected in the wells that were coated with tachyplesin and incubated with normal human serum compared with those coated with the control peptide or incubated with heat-inactivated serum. *B*, for affinity precipitation and Western blotting, normal human serum was treated without peptide or biotinylated control peptide or biotinylated tachyplesin. Streptavidin-Sepharose beads were added to the mixture, washed thoroughly, and processed for SDS-PAGE and Western blotting with antibodies to C4b. The bands α, β, γ chains of C4 (M_r 97, 75, and 33 kDa, respectively) were apparent in the samples treated with tachyplesin, but not with the control peptide or in the absence of peptide.

Because tachyplesin can bind to hyaluronan, we investigated the possibility that membrane-bound hyaluronan plays a role the binding of tachyplesin-mediated activation of complement on the surface of tumor cells. Suspensions of TSU cells were pretreated with hyaluronidase before the addition of tachyplesin and human serum; the presence of C3b was detected by immunostaining followed by FACS analysis. As shown in Fig. 5*D*, hyaluronidase pretreatment markedly reduced the intensity of fluorescence, indicating a reduction in C3b deposition. Thus, hyaluronan or related glycosaminoglycans seems to play a key role in the activation of complement on the cell surface by tachyplesin.

Effect of tachyplesin on tumor cells. The complement membrane attack complex (MAC, C5b-9) can damage the cell membrane, which results in the killing of the target cells. The possibility that tachyplesin can trigger the deposition of complement and the formation of C5b-9 on the surfaces of tumor cells via the classic pathway suggests that it might kill cells by disrupting the integrity of the plasma membrane. To test this possibility, we examined the permeability of cell membrane with macromolecule FITC-dextran, which is excluded by the membranes of viable, healthy cells but can pass through the damaged plasma membrane of unhealthy cells (2). Figure 6*A* showed that when cells were treated with tachyplesin and human serum, the fluorescence spectrum shifted, indicating that more FITC-dextran had passed through the plasma membrane and entered the cytoplasm. Thus, it seems that treatment with tachyplesin disrupted the cell membrane and increased its permeability.

Finally, we examined the effect of tachyplesin and normal human serum on tumor cell proliferation as measured by thymidine incorporation and cell death as measured by trypan blue uptake. As indicated in Figs. 6*B* and 7, TSU cells treated with tachyplesin in the presence of complete human serum showed a marked inhibition of proliferation and an increased extent of cell death. Figure 6*B* also showed that treatment with hyaluronidase significantly reversed the effects, again suggesting that cell-surface hyaluronan plays a critical role in tachyplesin-induced inhibition of tumor cell growth. Significantly, heat-inactivated serum also attenuated the effects of tachyplesin, but to a lesser extent than hyaluronidase treatment. These results imply that tachyplesin may have multiple effects on the cells leading to both growth arrest and death.

Discussion

The results of this study suggests the following multistep model to account for the antitumor activity of tachyplesin. First, tachyplesin binds to hyaluronan (or closely related glycosaminoglycans) on the surfaces of the target cells. Second, this bound tachyplesin interacts with C1q in the blood. Third, the tachyplesin activates the classic complement pathway. Finally, the formation of the MAC disrupts the integrity of the plasma membrane and results in the death of the target cells.

In the first step of our model, tachyplesin binds to the hyaluronan or related molecules on the surface of the target cells, is supported by several lines of evidence: (*a*) tachyplesin directly binds to soluble [^{3}H]hyaluronan, which may be due to the presence of a $B(X)_7B$ sequence that is known to bind hyaluronan (20); (*b*) pretreatment of TSU cells with hyaluronidase (which degrades both hyaluronan and chondroitin sulfate) resulted in a decreased tachyplesin-mediated deposition of C3b on the cell surface, leading to a decreased cytotoxic effects of tachyplesin as indicated by reduced [^{3}H]thymidine incorporation. It seems that the binding of

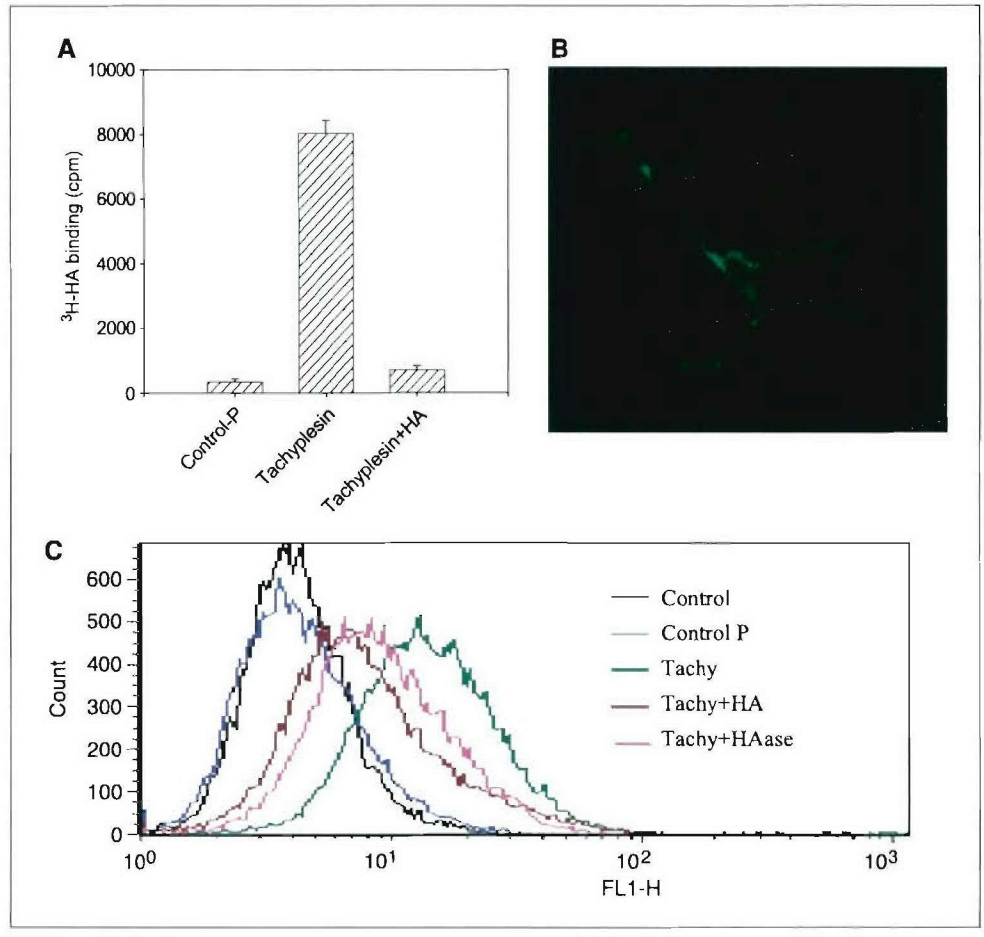

Figure 4. Hyaluronan-mediated attachment of tachyplesin to TSU tumor cells. *A*, to determine the binding of tachyplesin to hyaluronan, tachyplesin and the control peptide were mixed with [^{3}H]hyaluronan, applied to a sheet of nitrocellulose, and extensively washed. A significant amount of [^{3}H]hyaluronan bound to the nitrocellulose in the presence of tachyplesin but not in the control peptide or with an excess of unlabeled hyaluronan. *B*, 1×10^6 TSU tumor cells were incubated with 1 μg/mL of FITC-tachyplesin at 4°C for 30 minutes, fixed with freshly prepared 4% formaldehyde, and analyzed with confocal microscopy. Tachyplesin was associated with the surfaces of the cells. *C*, to determine the role of cell surface hyaluronan in the attachment of tachyplesin to tumor cells, the TSU cells were incubated with or without hyaluronidase (0.1 mg/mL) at 37°C for 1 hour. Then, 10 μg/mL of FITC-tachyplesin was added to the cells at 4°C for 30 minutes followed by fixation. Flow cytometry showed that the binding of FITC-tachyplesin to the cell surface was partially blocked by pretreatment with hyaluronidase or an excess of hyaluronan.

tachyplesin to cell surface hyaluronan is a critical first step in the subsequent induction of cytotoxicity. It is possible that in addition to hyaluronan, tachyplesin may also bind to chondroitin sulfate, which is also present on the surfaces of many cells (25) and is sensitive to digestion by testicular hyaluronidase. However, hyaluronan probably represents the major target because we had previously found that TSU cells have significant levels of cell surface hyaluronan (24).

The interaction between tachyplesin and hyaluronan could account for the relative specificity of antitumor activity of tachyplesin. Indeed, a body of studies has shown that many tumor cells (bladder, prostate, lung, colon, and breast) express high levels of hyaluronan whereas normal tissues express much less (26–28). In addition, studies have shown that endothelial cells involved in neovascularization express high levels of hyaluronan relative to those from established blood vessels (29). The fact that hyaluronan is preferentially expressed on the surfaces of tumors and endothelial cells involved in tumor vascularization could account for our previous observations that tachyplesin inhibits the growth of these cells relative to other nontumorigenic cells line that express less hyaluronan on their surfaces (5).

In the second step of our model, tachyplesin binds to C1q present in the serum. The phage display experiment reveals that tachyplesin binds to C1q, which is further confirmed by ELISA and affinity precipitation. The human C1q molecule (460 kDa) is a large complex composed of 18 polypeptide chains (6A, 6B, and 6C chains). As viewed under the electron microscope, the complex resembles a broccoli spear with common stalk that branches into six arms, each of which ends in globular head domains (22, 30). The phage display also reveals that tachyplesin binds to the stalk region of the B chain of C1q. This interaction seems ionic in nature because it was maximal under normal physiologic ionic strength and inhibited by either higher or lower ionic strength. However, the interaction clearly required the native configuration of tachyplesin that consists of a folded β-sheet stabilized by two disulfide bonds. When tachyplesin was reduced and alkylated, then the interaction with C1q was abrogated. In addition, the control peptide did not bind to C1q. Thus, whereas the interaction between tachyplesin and hyaluronan had an ionic component, the native structure of tachyplesin was essential for its activity.

In the next step of our model, the interaction of tachyplesin with C1q activates the classic complement pathway that consists of an enzyme cascade made up of numerous glycoproteins that under normal conditions exist in an inactive or proenzyme form. Activation of the complement system produces two major effects on the target cells: deposition of opsonic proteins (C3b and C4b) onto the cell surface and formation of C5b-9 (i.e., MAC). In this study, we have shown that the addition of fresh serum onto tachyplesin-coated plate results in the deposition of C1q downstream components C4b and C3b as well as the formation of C5b-9. In the case of C4b, this was confirmed by affinity precipitation followed by Western blotting. A similar process was found to occur on the cell surface. When TSU cells were treated with tachyplesin and serum, the C3b was deposited on their surfaces as determined by both fluorescent microscopy and

Western blotting. Importantly, heat inactivation of the serum, which destroys the complement system, also blocked many of the above processes, including the attachment of C4b, C3b, and C5b-9 on plastic plates coated with tachyplesin, and the deposition of C3b on the surfaces of TSU cells treated with tachyplesin. The ability of tachyplesin to induce the deposition of these downstream components strongly suggests the classic pathway of complement had been activated.

In the final step of our model, the formation of C5b-9 compromises the integrity of the plasma membrane leading to cell death. When cells were treated with tachyplesin and serum, there was an increased level of FITC-dextran entering the cytoplasm, suggesting the formation of large pores in the membrane, resulting in a decreased cell proliferation and viability. Significantly, this effect was diminished if the serum was heat-inactivated, again indicating that the activation of complement cascade was essential for cell damage effect of tachyplesin.

The formation of MAC is usually supposed to lyse the target cells. Indeed, several recent studies have indicated that activation of complement and the formation of the MAC can also result in apoptosis of target cells. For example, Nauta et al. (31) have shown that C5b-9 induces apoptosis through a caspase-dependent pathway that can be blocked by the inhibitor zVAD-fmk. Similarly, Cragg et al. (32) reported that activated complement results in DNA fragmentation, a characteristic of apoptosis. Our previous study showed that RGD-tachyplesin could induce apoptosis in a number of target cells (5) by increasing the Annexin V staining, activation of caspases 9, 8, and 3, and increase of the expression of the Fas ligand, Fas, caspase 7, and caspase 6. Based on these results, we had proposed that tachyplesin could activate apoptotic molecules involving both mitochondrial and Fas-dependent pathways. The results of the present study indicate that at least some of this apoptosis resulted from the compromising of the plasma membrane due to the tachyplesin-mediated activation of the classic complement cascade.

Whereas our model for the antitumor activity of tachyplesin is consistent with all of our previous data, it must be acknowledged that tachyplesin may have additional effects. We had found that even when the complement system was heat-inactivated, there was still some residual antitumor activity implying that other mechanisms may be involved. It is possible that even in the absence of the complement system, tachyplesin is able to directly compromise the plasma membrane, as it is believed to do with microbes.

Our results also indicate that tachyplesin is similar to other nonimmune activators of the classic complement pathway in that it binds to the stalk-like region of C1q, in contrast to the immune activators (IgG and IgM) that bind to the globular regions (30, 33, 34). It should be noted that simply binding to C1q is not sufficient to activate the complement cascade that is controlled at many levels as a safeguard against unintended activation by the

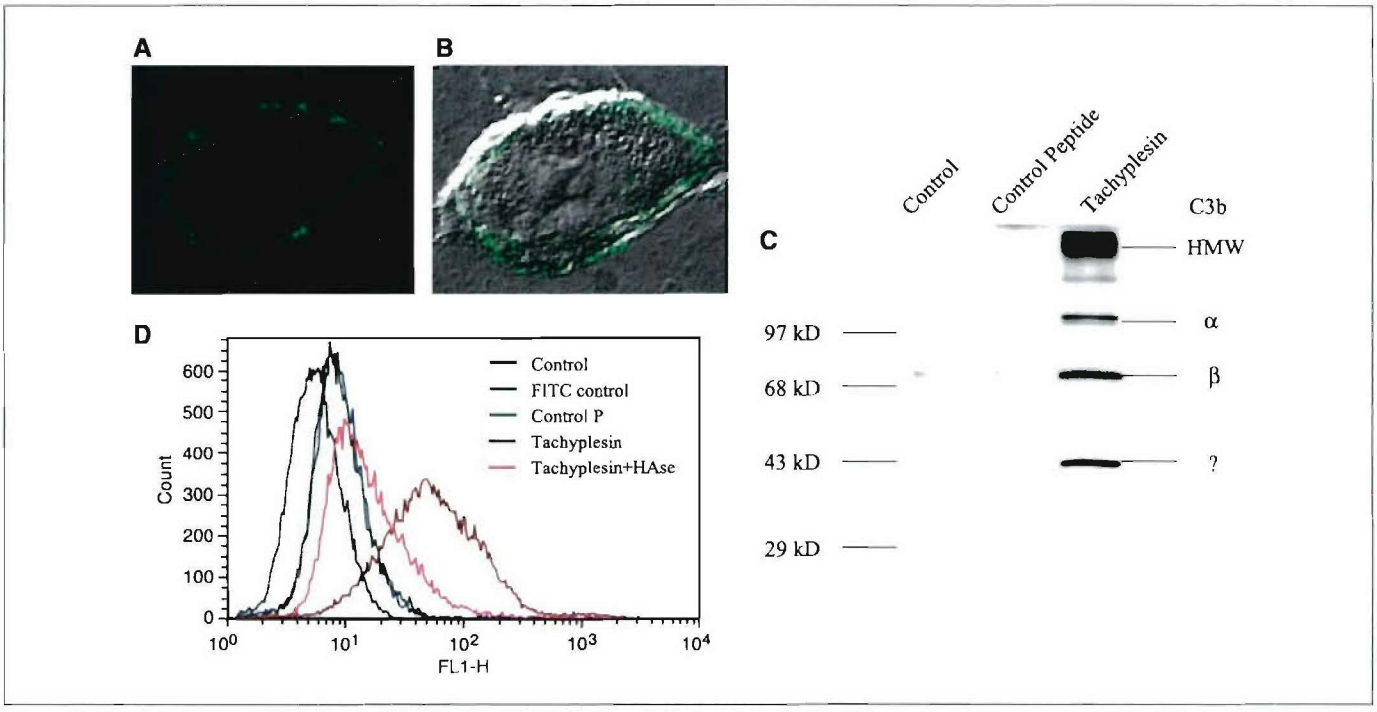

Figure 5. Effect of tachyplesin on the induction of complement on the surfaces of tumor cells. *A* and *B*, TSU cells were incubated with tachyplesin in the presence of 10% normal human serum for 20 minutes, washed, and then incubated with a polyclonal antibody to C3 (4°C for 30 minutes) followed by a FITC-secondary antibody and analysis by confocal microscopy. Both immunoflourescence alone and the merger of fluorescence and transmitted images are shown. *C*, to analyze complement activation by Western blotting, TSU cells were incubated in 10% normal human serum in the presence or absence of either tachyplesin or control peptide at 37°C for 60 minutes. After washing, the cell lysates were harvested and processed for Western blotting with antibodies to C3b. In the cells treated with tachyplesin, there were two bands corresponding to α and β subunits of C3b (115 and 75 kDa), as wells as a high molecular weight band representing C4b covalently bound to membrane constituents. These bands were reduced in cells treated without peptide or with the control peptide. *D*, to examine the role of cell surface hyaluronan in the deposition of complement, 100 μg/mL peptides were added to the cells culture in the presence of 10% normal human serum and incubated for 20 minutes at room temperature. The cells were then washed, incubated with a polyclonal antibody to human C3 (20 μg/mL) at 4°C for 30 minutes, followed by incubation with FITC-conjugated IgG (1:200) at 4°C for 30 minutes. The cells were finally stained with propidium iodide and analyzed with FACS. Preincubation with hyaluronidase abrogated the C3 deposition on TSU cell surfaces.

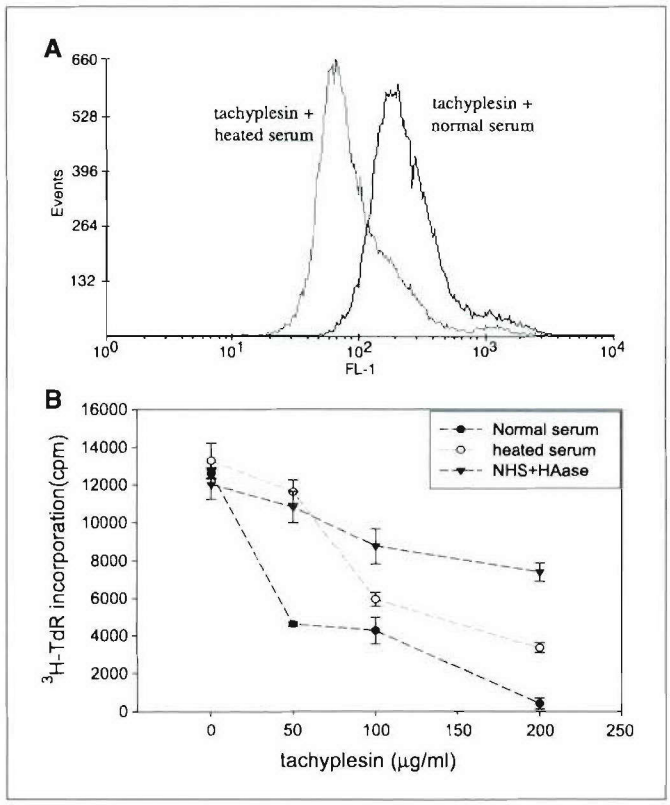

Figure 6. Biological effect of hyaluronidase on tachyplesin-mediated cytotoxicity of tumor cells. *A*, to determine whether tachyplesin damages the plasma membrane, TSU cells were incubated with tachyplesin plus heat-inactivated human serum or normal human serum overnight. After harvesting, the cells were incubated with 5 μg/mL of FITC-dextran (M_r 40,000) and subjected to flow cytometry. The amount of FITC-dextran taken up by the cells was significantly higher in those treated with tachyplesin than in the control cells, suggesting that tachyplesin disrupts the integrity of the plasma membrane. *B*, TSU tumor cells were treated with hyaluronidase (0.1 mg/mL) at 37°C for 1 hour. Then, tachyplesin and 2% normal human serum or heat-inactivated serum were added and incubated overnight followed by a [^{3}H]thymidine incorporation assay. The cytotoxic effects of tachyplesin in present of normal serum were reduced by either treatment with hyaluronidase or heat-inactivated serum ($P < 0.05$).

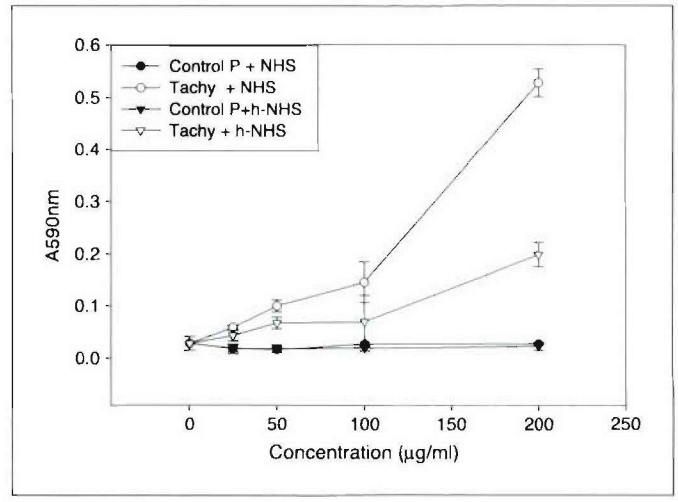

Figure 7. Cell death induced by tachyplesin and its activated complement TSU tumor cells were cultured in 24-well plates and then exposed for 18 hours to different concentrations of tachyplesin or control peptide (*Control P*) in the presence of either normal or heat-inactivated human serum. Then, a solution of 0.4% trypan blue was added to each well to a final concentration of 0.05%. The cells were incubated at 37°C for 15 minutes, washed, and lysed in 200 μL of 1% SDS. The amount of dye taken up by the cells was determined by reading the absorbance at A_{590}. All samples were assayed in triplicates. The cells treated with tachyplesin and normal human serum took up a significantly greater amount of dye compared with those treated with control peptide or heated-inactivated serum ($P < 0.05$).

body. Indeed, there are numerous modifiers in both the serum and on the cell surface that regulate the complement cascade (35, 36). Several studies have shown that *in situ* tumor cells overexpress some of these membrane-bound regulatory proteins, which may down-regulate an efficient local immune response, such as those induced by monoclonal antibody-mediated immunotherapy (37, 38). Tachyplesin seems to be able to bypass these "protective" mechanisms for tumor cells.

In conclusion, we believe that the model proposed for the antitumor activity for tachyplesin represents a new and promising avenue for targeting and attacking tumor cells. Previously, we had found that tachyplesin is capable of preventing tumor growth in both mice and chicken embryos without significant side effects (5). However, the concentration required to achieve a therapeutic effect was relatively high. If our proposed model is correct, then it may be possible to design other molecules with improved therapeutic effects in the way that one subdomain could be dedicated to the binding of hyaluronan and another to the binding and activation of C1q. At the same time, these peptides could be modified in such a way as to increase their stability and half-life in circulation. Such compounds could be effective as a new agent in a multipronged attach of tumor cells.

Acknowledgments

Received 6/24/2004; revised 2/11/2005; accepted 2/25/2005.

Grant support: U.S. Army Medical Research and Materiel Command grants DAMD17-00-1-0081 and DAMD17-01-1-0708; National Cancer Institute/NIH grant R29 CA71545; and Susan G. Komen Foundation (L. Zhang).

The costs of publication of this article were defrayed in part by the payment of page charges. This article must therefore be hereby marked *advertisement* in accordance with 18 U.S.C. Section 1734 solely to indicate this fact.

References

1. Gietema JA, de Vries EG. Clinical cancer research 2002: new agents and therapies. Drug Resist Updat 2002;5:192–203.
2. Papo N, Shahar M, Eisenbach L, Shai Y. A novel lytic peptide composed of D-amino acids selectively kills cancer cells in culture and in mice. J Biol Chem 2003;278:21018–23.
3. Ellerby HM, Arap W, Ellerby LM, et al. Anti-cancer activity of targeted pro-apoptotic peptides. Nat Med 1999;5:1032–8.
4. Shin SY, Lee SH, Yang ST, et al. Antibacterial, antitumor and hemolytic activities of α-helical antibiotic peptide, P18 and its analogs. J Pept Res 2001;58:504–14.
5. Chen Y, Xu X, Hong S, et al. RGD-Tachyplesin inhibits tumor growth. Cancer Res 2001;61:2434–8.
6. Yang N, Lejon T, Rekdal O. Antitumour activity and specificity as a function of substitutions in the lipophilic sector of helical lactoferrin-derived peptide. J Pept Sci 2003;9:300–11.
7. Prohaszka Z, Nemet K, Csermely P, Hudecz F, Mezo G, Fust G. Defensins purified from human granulocytes bind C1q and activate the classical complement pathway like the transmembrane glycoprotein gp41 of HIV-1. Mol Immunol 1997;34:809–16.
8. van den Berg RH, Faber-Krol MC, van Wetering S, Hiemstra PS, Daha MR. Inhibition of activation of the classical pathway of complement by human neutrophil defensins. Blood 1998;92:3898–903.
9. Panyutich AV, Szold O, Poon PH, Tseng Y, Ganz T. Identification of defensin binding to C1 complement. FEBS Lett 1994;356:169–73.
10. Zhang L, Scott MG, Yan H, Mayer LD, Hancock RE. Interaction of polyphemusin I and structural analogs

with bacterial membranes, lipopolysaccharide, and lipid monolayers. Biochemistry 2000;39:14504–14.
11. de Kroon AI, Dolis D, Mayer A, Lill R, de Kruijff B. Phospholipid composition of highly purified mitochondrial outer membranes of rat liver and *Neurospora crassa*. Is cardiolipin present in the mitochondrial outer membrane? Biochim Biophys Acta 1997;1325:108–16.
12. Chan SC, Yau WL, Wang W, Smith DK, Sheu FS, Chen HM. Microscopic observations of the different morphological changes caused by anti-bacterial peptides on *Klebsiella pneumoniae* and HL-60 leukemia cells. J Pept Sci 1998;4:413–25.
13. Risso A, Braidot E, Sordano MC, et al. BMAP-28, an antibiotic peptide of innate immunity, induces cell death through opening of the mitochondrial permeability transition pore. Mol Cell Biol 2002;22:1926–35.
14. Nakamura T, Furunaka H, Miyata T, et al. Tachyplesin, a class of antimicrobial peptide from the hemocytes of the horseshoe crab (*Tachypleus tridentatus*). Isolation and chemical structure. J Biol Chem 1988;263:16709–13.
15. Rao AG. Conformation and antimicrobial activity of linear derivatives of tachyplesin lacking disulfide bonds. Arch Biochem Biophys 1999;361:127–34.
16. Alberti S, Marques G, Hernandez-Alles S, et al. Interaction between complement subcomponent C1q and the *Klebsiella pneumoniae* porin OmpK36. Infect Immun 1996;64:4719–25.
17. Barilla-LaBarca ML, Liszewski MK, Lambris JD, Hourcade D, Atkinson JP. Role of membrane cofactor protein (CD46) in regulation of C4b and C3b deposited on cells. J Immunol 2002;168:6298–304.
18. Underhill CB, Chi-Rosso G, Toole BP. Effects of detergent solubilization on the hyaluronate-binding protein from membranes of simian virus 40-transformed 3T3 cells. J Biol Chem 1983;258:8086–91.
19. Agren UM, Tammi R, Tammi M. A dot-blot assay of metabolically radiolabeled hyaluronan. Anal Biochem 1994;217:311–5.
20. Xu XM, Chen Y, Chen J, et al. A peptide with three hyaluronan binding motifs inhibits tumor growth and induces apoptosis. Cancer Res 2003;63:5685–90.
21. Uliasz TF, Hewett SJ. A microtiter trypan blue absorbance assay for the quantitative determination of excitotoxic neuronal injury in cell culture. J Neurosci Methods 2000;100:157–63.
22. Kishore U, Reid KB. C1q: structure, function, and receptors. Immunopharmacology 2000;49:159–70.
23. Kohro-Kawata J, Wener MH, Mannik M. The effect of high salt concentration on detection of serum immune complexes and autoantibodies to C1q in patients with systemic lupus erythematosus. J Rheumatol 2002;29:84–9.
24. Liu N, Gao F, Han Z, Xu X, Underhill CB, Zhang L. Hyaluronan synthase 3 overexpression promotes the growth of TSU prostate cancer cells. Cancer Res 2001;61:5207–14.
25. Pan T, Wong BS, Liu T, Li R, Petersen RB, Sy MS. Cell-surface prion protein interacts with glycosaminoglycans. Biochem J 2002;368:81–90.
26. Hautmann SH, Lokeshwar VB, Schroeder GL, et al. Elevated tissue expression of hyaluronic acid and hyaluronidase validates the HA-HAase urine test for bladder cancer. J Urol 2001;165:2068–74.
27. Bullard KM, Kim HR, Wheeler MA, et al. Hyaluronan synthase-3 is upregulated in metastatic colon carcinoma cells and manipulation of expression alters matrix retention and cellular growth. Int J Cancer 2003;107:739–46.
28. Posey JT, Soloway MS, Ekici S, et al. Evaluation of the prognostic potential of hyaluronic acid and hyaluronidase (HYAL1) for prostate cancer. Cancer Res 2003;63:2638–44.
29. Rooney P, Kumar S, Ponting J, Wang M. The role of hyaluronan in tumour neovascularization (review). Int J Cancer 1995;60:632–6.
30. Kishore U, Gupta SK, Perdikoulis MV, Kojouharova MS, Urban BC, Reid KB. Modular organization of the carboxyl-terminal, globular head region of human C1q A, B, and C chains. J Immunol 2003;171:812–20.
31. Nauta AJ, Daha MR, Tijsma O, van de WB, Tedesco F, Roos A. The membrane attack complex of complement induces caspase activation and apoptosis. Eur J Immunol 2002;32:783–92.
32. Cragg MS, Howatt WJ, Bloodworth L, Anderson VA, Morgan BP, Glennie MJ. Complement mediated cell death is associated with DNA fragmentation. Cell Death Differ 2000;7:48–58.
33. Bohnsack JF, Tenner AJ, Laurie GW, Kleinman HK, Martin GR, Brown EJ. The C1q subunit of the first component of complement binds to laminin: a mechanism for the deposition and retention of immune complexes in basement membrane. Proc Natl Acad Sci U S A 1985;82:3824–8.
34. Arlaud GJ, Gaboriaud C, Thielens NM, Budayova-Spano M, Rossi V, Fontecilla-Camps JC. Structural biology of the C1 complex of complement unveils the mechanisms of its activation and proteolytic activity. Mol Immunol 2002;39:383–94.
35. Bos JD, Pasch MC, Asghar SS. Defensins and complement systems from the perspective of skin immunity and autoimmunity. Clin Dermatol 2001;19:563–72.
36. Eggleton P, Tenner AJ, Reid KB. C1q receptors. Clin Exp Immunol 2000;120:406–12.
37. Blok VT, Daha MR, Tijsma OM, Weissglas MG, van den Brock LJ, Gorter A. A possible role of CD46 for the protection *in vivo* of human renal tumor cells from complement-mediated damage. Lab Invest 2000;80:335–44.
38. Dillman RO. Antibodies as cytotoxic therapy. J Clin Oncol 1994;12:1497–515.

Proceedings of the American Association for Cancer Research • Volume 42 • March 2001

★ **#382 Hyaluronan Binding Motifs Inhibit Tumor Growth.** Ningfei Liu, Xue-Ming Xu, Charles B. Underhill, Yixin Chen, Jinguo Chen Chen, Feng Gao, Zeqiu Han, and Lurong Zhang. *Lombardi Cancer Center, Washington, DC.*

Cartilage, enriched with hyaluronan (HA) binding proteins, has been proved to have anti-tumor effect in some clinical trails. To explore if HA binding motif is responsible for anti-tumor effect, a 39 peptide (called P4) containing three HA binding motifs was linked with NGR homing motif on its N-terminal and tested for anti-tumor function. The synthetic P4 could bind to 3H-HA with high capacity. When TSU prostate cancer cells, MDA-435 breast cancer cells and/or endothelial cells were treated with 50-100 ug/ml of P4, their growth was strongly inhibited in either anchorage-dependent or anchorage-independent conditions. This inhibitory effect was abolished by pre-incubation of P4 with HA, indicating the activated HA binding sites are crucial for the effect. In addition, when 100 ug of P4 was i.v. injected into CAM of chicken embryo bearing with tumors formed by B16 melanoma or MDA-435 cells, the tumor sizes were greatly reduced compared to the control. To see the potential of P4 for gene therapy, the amino acid sequence of P4 was back-translated into nucleotide sequence. The cDNA coding for P4 was inserted into the pSecTag2 vector with a signal peptide and transfected into TSU and MDA-435 cells. The growth of tumors formed by cells expressing P4 was inhibited compared to the control cells in both CAM and nude mice models. The angiogenesis in P4 tumors was reduced as determined by endothelial cells staining. Furthermore, the apoptotic indexes (Annexin-π staining and nuclear fragmentation) were increased in both tumor cells and endothelial cells upon the treatment of P4, indicating that the inducing of apoptosis is one of action mechanisms by which P4 exerts anti-tumor effect. The involvement of lysosome and mitochondria in the P4 induced cell death has been investigated.

★ **#383 Targeted Peptide of Human Brain Hyaluronan Binding Protein Inhibits Tumor Growth.** Xueming Xu, Yixin Chen, Ningfei Liu, Jinguo Chen, Feng Gao, Zeqiu Han, Charles B. Underhill, and Lurong Zhang. *Dept. of Biology, Xiamen University, Xiamen, China, and Lombardi Cancer Ctr., Washington, DC.*

In previous studies, we have found that human brain hyaluronan binding protein (b-HABP) inhibits tumor growth. To explore the functional domain of this anti-tumor protein, 33 amino acids containing three hyaluronan binding motifs from N-terminal of b-HABP were linked with NGR homing motif to better target tumor cells. The synthetic peptide exerted an inhibitory effect on the proliferation of both TSU prostate cancer cells and HUVEC endothelial cells at a dose of 100 ug/ml. It also inhibited the colony formation of TSU and MDA-435 cells. When the targeted b-HABP peptide was tropically administrated to TSU and MD-A435 cells on top of the chorioallantoic membranes (CAM) of 10 days chicken embryos, the tumor growth was greatly inhibited. In addition, when 100 ug of b-HABP peptide was i.v. injected once into CAM bearing with established B16 melanomas, the growth of tumor xenografts was greatly inhibited. Then, the peptide sequence was back-translated into nucleotide sequence. The cDNA coding for the peptide was obtained using overlap-PCR and inserted into the pSecTag2 vector with a signal peptide for the secretion. The pSecTag2 vector alone (as control) or pSecTag2-peptide vectors (as tests) were transfected into MDA-435 cells. The in vivo results indicated that cells expressing targeted b-HABP peptide formed smaller tumors as compared to vector alone in both the CAM and nude mice model systems. Additional studies indicated that the targeted b-HABP peptide could damage the both the plasma membrane and mitochondrial membrane that triggered the apoptosis cascade.

★ **#369 Anti-Tumor Effect of RGD-Tachyplesin.** Yixin Chen, Xue-Ming Xu, Jinguo Chen, Ningfei Liu, Charles B. Underhill, Karen Creswell, Shuigen Hong, and Lurong Zhang. *Dept.of Biology, Xiamen University, Xiamen, China, and Lombardi Cancer Center, Washington, DC.*

Tachyplesin, an anti-microbial peptide present in leukocytes of horseshoe crab (Tachypleus tridentatus), was conjugated to the integrin homing domain RGD and tested for anti-tumor activity. Initial experiments indicated that RGD-tachyplesin could inhibit the proliferation of both cultured tumor and endothelial cells and could block the colony formation of TSU prostate cancer cells. The RGD-tachyplesin appeared to compromise the integrity of the plasma membrane as well as those associated with the mitochondria and nuclei, as evidenced by the changes in the staining with the fluorescent probes JC-1, annexin V, dextran-FITC and YO-PRO-1. In addition, Western blotting showed that the Fas ligand, FADD, Caspase 7, Caspase 6 and activated subunits of Caspase 8 (18 kDa) and Caspase 3 (20 kDa) were up-regulated following treatment with RGD-tachyplesin, suggesting that it induces apoptosis through elements of the Fas dependent pathway. And finally, in vivo studies indicated that the RGD-tachyplesin could inhibit the growth of tumor cells on the chorioallantoic membranes of chicken embryos and in syngenic mice. The results of this study suggests that the RGD-tachyplesin can inhibit tumor growth by impairing the function of vital membranes and by inducing apoptosis in both tumor cells and endothelial cells.

#4375 Human Brain Hyaluronan Binding Protein Inhibits Tumor Growth VIA Induction of Apoptosis. Feng Gao, Xue-Ming Xu, Charles B. Underhill, Shimin Zhang, Ningfei Liu, Zeqiu Han, Jiaying Zhang, and Lurong Zhang. *Lombardi Cancer Ctr., Washington, DC.*

Naturally existing anti-tumor substance are less toxic and implicated a promising feature in cancer therapy. In this study, a new protein, termed human brain hyaluronan (HA) binding protein (b-HABP) was found to have an anti-tumor effect. The cDNA coding for N-terminal of human b-HABP was cloned and found to consist of 1,548 bp coding for 516 amino acids with signal peptide. When malignant MDA-435 breast cancer cells were transfected with b-HABP-pcDNA3, their ability to grow in anchorage-dependent conditions and to form colonies was greatly reduced compared to the mock transfectants. In addition, the conditioned media from b-HABP-pcDNA3 transfectants inhibited the growth of endothelial cells. Furthermore, studies revealed that the FasL, Caspase 3, p53, p27 were induced while bcl2 and cyclin E were reduced in b-HABP-pcDNA3 transfectants. Finally, the growth of tumors formed by b-HABP-pcDNA3 transfectants was greatly inhibited compared to the mock transfectants in CAM system and in nude mice model. This study suggests that HABP may represent a new category of naturally existing anti-tumor substance via induction of apoptosis.

#3465 Inhibition of Tumor Growth by Hyaluronan Binding Motifs (P4) is Mediated by Apoptosis Pathway Related with Lysosome and Mitochondria. Ningfei Liu, Xue-Ming Xu, Charles Underhill, Susette Mueller, Karen Creswell, Yixin Chen, Jinguo Chen, and Lurong Zhang. *Lombardi Cancer Ctr., Washington, DC.*

We have demonstrated that the tumor growth can be greatly suppressed by hyaluronan binding motifs (P4) either exogenous administration of synthetic P4 peptide or endogenous expressing of P4. To explore the underlying mechanism for the anti-tumor effect, FITC-P4 was used for its intracellular tracing and the alterations in apoptotic molecules were studied. The results of confocal microscopy indicated that the P4 bound to cell surface, which could be partially blocked by anti-CD44, heparin and chondroitin sulfate, indicating that the binding may indirectly mediated by CD44 and interaction anionic substances on the membrane. Following the binding on cell surface, the FITC-P4 was up-taken by lysosomes and partially entered mitochondria, as evidenced by co-localization staining. At the molecular level, Fas ligand, FADD, caspase 8 (activated 18 kDa subunit) and caspase 3 were up-regulated upon the treatment of P4 in both MDA-435 tumor cells and ABAE endothelial cells, indicating that the apoptosis is triggered by P4. As a result, other vital membranes were greatly damaged as demonstrated by 1) positive Annexin V staining, an increased inflow of FITC-Dextran (MW 40,000) and exflow of LDH for the damage of plasma membrane; 2) an increased inflow of YO-Pro-1 for the damage of nuclear membrane; and 3) the shifted JC-1 staining for the depolarization of mitochondrial potential. Furthermore, the P4-induced cell death could be partially reversed by inhibitors (NH_4Cl) specific for lysosomal functions and inhibitor (Z-VAD-FMK) for caspases, suggesting that the pro-apoptotic molecules associated with lysosome and mitochondria might be released by P4 and then activate the caspases in cytoplasm.

#4358 Effect of Tachyplesin on MDR Overexpressing Tumor Cells. Jinguo Chen, Yixin Chen, Shuigen Hong, Fabio Leonessa, Robert Clarke, Xue-Ming Xu, Ningfei Liu, Charles B. Underhill, Karen Creswell, and Lurong Zhang. *Lombardi Cancer Center, Georgetown University, Washington, DC, and The Key Lab of China Education Ministry on Cell Biology and Tumor Engineering, Xiamen University, Xiamen, China.*

Tachyplesin is an anti-microbial peptide, consisting of 17 amino acids with a molecular weight of 2,269 Dalton and pI of 9.93. It has two disulfide linkages, which exposes all six positively charged basic amino acids on its surface. This cationic peptide can interact with anionic phospholipids present in the prokaryotic cytoplasmic membrane and eukaryotic mitochondrial membrane. We have found that tachyplesin could inhibit the growth of tumor cells. To see the effect of tachyplesin on the tumor cells that are resistant to first line chemotherapeutic drugs, we used a pair of breast cancer cell lines, LCC6-MDR (a MDA435 cells transduced with MDR1-retroviral vector) and LCC6-vector as control. Due to the over-expression of MDR1, LCC6-MDR cells resisted to Taxol with an EC50 of 1000 nM, while LCC6-vector had an EC50 of 10 nM. However, when treated with tachyplesin, both cell lines showed a similar sensitivity (EC50 of 40 nM) in response to the inhibitory effect of tachyplesin. The confocal analysis indicated that the FITC- tachyplesin bound to cell surface, entered the cells and localized in mitochondria. The flow cytometer analysis indicated that the mitochondria potential was depolarized and that both plasma membrane and nuclei membrane were damaged, as evidenced by staining with JC-1, FITC-Dextran and YO-Pro-1. This study suggests that the cationic peptide, such as tachyplesin, may be a promising alternative agent to treat the chemotherapy resistant tumor cells.

Abstracts presented in AACR meeting in year 2002

Proceedings of the American Association for Cancer Research • Volume 43 • March 2002

#4404 Targeted hyaluronan binding peptide inhibits the growth of ST88-14 Schwann cells. Yixin Chen, Shuigen Hong, Xiaolin Chen, Shanmin Yang, Ningfei Liu, Xu-Fang Pei, Luping Wang, Xue-Ming Xu, Jinguo Chen, Charles B. Underhill, and Lurong Zhang. *The Cell and Tumor Key Lab of China Education Ministry at Xiamen University, Xiamen, China, and Georgetown University Medical Center, Washington, DC.*

We have reported that the hyaluronan (HA) binding proteins/peptides possess anti-tumor effect, in part, due to the induction of apoptosis and p53. The loss of neurofibromin, a tumor suppressor corded by NF1 (Neurofibromatosis Type 1) gene, results in the accumulation of hyperactive Ras-GTP due to a reduced conversion of active Ras-GTP to inactive Ras-GDP, which turns on uncontrolled mitogenic signals in the nucleus. Therefore, neurofibromatosis can be regarded as a disease resulting from the disruption of the balance between cell proliferation and apoptosis. To determine if the abnormality of neurofibromatosis can be interrupted by HA binding peptide, a naturally existing HA binding peptide, tachyplesin with RGD domain (for a better targeting) and its scramble peptide were synthesized. When ST88-14 Schwann cells were treated with this targeted peptide for 24 hours, the cells underwent apoptosis and began to die. The 3H-TdR incorporation rate of targeted HA binding peptide treated cells was greatly reduced compared to that of the control peptide treated cells. This inhibitory effect was in a dose-dependent manner. Similarly, the ability to form colony in soft agar was also remarkably reduced. Western blot analysis showed that the cell cycle key molecules, such as cyclin B1 and cdc2, were reduced. In addition, the targeted HA binding peptide could reduce the phosphorylation of mitogen-activated protein kinase. The data suggest that the targeted HA binding peptide could inhibit the growth of ST88-14 Schwann cells via suppression of some key molecules in cell proliferation process.

Proceedings of the American Association for Cancer Research • Volume 43 • March 2002

#5364 Peptides derived endostatin and angiostatin inhibits tumor growth. Xueming Xu, Jinguo Chen, Luping Wang, Xue-Fang Pei, Shanmin Yang, Charles B. Underhill, and Lurong Zhang. *Georgetown University, Washington, DC.*

Endostatin and angiostatin are well-known anti-tumor/angiogenesis agents. We have found that there are several hyaluronan (HA) binding motifs existing in these two proteins. In previous studies, we have found that HA binding proteins / peptides inhibited the growth of tumor cells. In this study, two peptides with HA binding motifs derived from endostatin and angiostatin were tested to confirm that the HA binding motifs are the critical effector in the bioactivity of their parental molecules. Two peptides that containing 2-3 HA binding motifs and NGR homing domain or the control scramble peptide were chemically synthesized. When the peptides were added to endothelial cells (HUVEC and ABAE) or tumor cells (TSU prostate or MDA435 breast cancer), they inhibited the cell growth in a dose-dependent manner. When 100 μg of peptides was tropically administrated to TSU tumors grown on chorioallantoic membrane of chicken embryo, the sizes of tumors in the peptide-treated groups were smaller than the control, while the development of chick embryos were not affected. The results of Western blot and flow cytometry analysis indicated that the peptides could trigger the depolarization of mitochondrial, induce the expression of p16 and p21 and increase the cleaved caspase 8. It seems that the HA binding motifs in endostatin and angiostatin are the key factor for the anti-tumor/angiogenesis effects of their parental proteins.

#3618 **Expression pattern of extracellular matrix protein 1 (ECM1) in human tumors.** Luping Wang, Jianjin Wang, Jiyao Yu, Haoyong Ning, Xu-Fang Pei, Xue-Ming Xu, Jinguo Chen, Shanmin Yang, Charles B. Underhill, Lei Liu, Jian Ni, and Lurong Zhang. *Beijing General Hospital, Beijing, China, Changhai Hospital, Shanghai, China, Naval General Hospital, Beijing, China, Georgetown University Medical Center, Washington, DC, The Cell and Tumor Key Lab of China Education Ministry at Xiamen University, Xiamen, China, Chaoyingbiotech Inc, Xian, China, and HGS, Rockville, MD.*

In a previous study, we found that the human extracellular matrix protein 1 (ECM1) possessed angiogenic activity and was expressed with a high incidence in human breast cancers. To determine the expression pattern of ECM1 in human tumors, we stained 191 samples with affinity purified antibodies to ECM1. These samples included normal and tumor tissue from the breast, prostate, stomach, esophagus, intestines, liver, pancreas, rectum, kidney, brain and uterus. Positive staining was observed in the following cases: invasive breast ductal carcinoma (31/37, 83%); esophagus squamous carcinoma (6/6, 100%); gastric cancer (23/26, 88%); rectal cancer (25/32, 78%); pancreas ductal carcinoma (2/2, 100%); hepatocellular carcinoma (1/6, 16.7%); and prostate adenocarcinoma (3/3, 100%). In contrast, there was no obvious staining in normal lobular breast tissue, intestinal mucosa adjacent to tumor tissue, gastrointestinal leiomyosarcoma, liposarcoma, renal clear cell carcinoma, uterine leiomyoma and mediastinum neurofibroma. The ECM1 positive rate can be summarized as follows: carcinomas 76.6%; sarcomas 16.6%; benign lesions of epithelial origin 16%; benign lesions of non-epithelial origin 5%; and normal tissue adjacent to tumors 7%. Importantly, metastatic tumors had a higher rate of positive staining than those without metastasis (primary breast cancer with metastasis 76%; metastatic foci in lymph node 85%; and breast cancer without metastasis 33.3%). These results indicate that ECM1 tends to be preferentially expressed by carcinomas and suggests that it may be a useful marker for these tumors

Proceedings of the American Association for Cancer Research • Volume 43 • March 2002

#3502 **A peptide (DGI201) antagonist of Fas acts as a strong stimulus for cell proliferation.** Ku-Chuan Hsiao, Shanmin Yang, Xue-Ming Xu, Jinguo Chen, Luping Wang, Jing Yang, Neil Goldstein, Charles B. Underhill, and Lurong Zhang. *DGI Biotechologies Inc., Edison, NJ, and Georgetown University Medical Center, Washington, DC.*

We have utilized a random and highly diverse phage-displayed peptide library (RAPIDLIB20) to generate a 20-mer peptide (called DGI201) with specificity for human FAS. The phage clone was able to compete with human Fas ligand (FasL) for FAS. Using an in-house amino acid alignment program, no appreciable sequence homology was observed between the peptide sequence and the natural ligand FasL. To test whether this peptide acts as an agonist or antagonist for Fas, the peptide and control scramble peptide were chemically synthesized and tested in several different cell lines, including endothelial cells (human umbilical vein endothelial cells), immobilized Cos 7 and 3T3 cells as well as several tumor cell lines (MDA435, TSU, L929, U937, B16 and Jurkat). Compared to the control, the DGI201 showed an antagonistic effect, inducing the treated cells to proliferate by 3 to 6 folds in a dose dependent fashion. The stimulatory effect of DGI201 could be abolished by addition of FasL, especially when the ligand was in a dimer form via antibody. In an assay with Jurkat cells, the apoptosis effect induced by FasL at a concentration of ED50 could be inhibited by DGI201. These results further confirmed that the peptide is a Fas specific antagonist. We are currently investigating the utility of this peptide.

#794 A peptide derived from the hemopexin-like domain of matrix metalloproteinase 9 exerts an anti-tumor effect. Luping Wang, Xu-Fang Pei, Jinguo Chen, Xue-Ming Xu, Shanmin Yang, Ningfei Liu, Charles B. Underhill, and Lurong Zhang. *Beijing General Hospital, Beijing, China, Georgetown Univ. Med. Ctr, Washington, DC, and The Cell and Tumor key Lab of China Education Ministry in Xiamen University, Xiamen, China.*

Previously, we have reported that hyaluronan (HA) binding proteins, such as Metastatin from cartilage inhibits tumor growth and metastasis. To determine if a peptide that possesses HA binding activity has similar anti-tumor properties, we chemically synthesized a peptide (PEX-P) with two HA binding motifs derived from the hemopexin-like domain of human matrix metalloproteinase 9 linked to a NGR homing domain (32 amino acids, MW of 3,621 Dalton). The peptide specifically bound to 3H-HA. It inhibited the proliferation of both endothelial cells (ABAE and HUVEC) and MDA-435 cells in a dose-dependent manner. When 100 mg of the peptide was applied tropically to tumor cells growing on the chorioallantoic membranes of chicken embryos daily, the xenografts were smaller than those treated with vehicle alone or control peptide. However, the peptide had no obvious effect on the development of the chicken embryos based upon their weights. Western blot analysis of these tumor cells indicated that treatment with PEX-P caused a reduction in the levels of cell cycle promoters (such as cyclin A, cyclin B1/cdc2, cyclin D1) and the oncogene c-myc. In addition, the inactive form of phosphorylated Rb was decreased, suggesting that more Rb remained in the active form to suppress tumor cell growth. Furthermore, treatment of tumor cells with PEX-P increased the active form of PARP, suggesting the induction of apoptosis. This was further supported by flow cytometry showing that treatment with PEX-P increased the number of Annexin V positive, propidium iodide negative cells to 30% as compared to <5% in controls. In addition, staining with JC-1 suggested that PEX-P could induce mitochondrial depolarization, which might be one of the initial steps in the apoptotic cascade. The therapeutic value of PEX-P will be further investigated using adenovirus carrying cDNA coding for PEX-P

#4233 Triptolide, a potent antitumor agent. Shanmin Yang, Jinguo Chen, Xue-Ming Xu, Luping Wang, Shimin Zhang, Xu-Fang Pei, Jing Yang, Charles B. Underhill, and Lurong Zhang. *the Cell and Tumor Key Lab of China Education Ministry at Xiamen University, Xiamen, China, Georgetown University Medical Center, Washington, DC, and PowerTech Inc., Bethesda, MD.*

Triptolide (TPL) is a compound (MW 360) purified from the herb Tripterygium wilfordii Hook F that has been used in China as a natural medicine for hundreds of years. In China, clinical trials have indicated that TPL could achieve complete or partial remission in patients with leukemia. In the present study, we examined the effects of TPL on cell lines derived from human cancers of the breast, prostate, stomach and liver. In addition, mouse B16 melanoma cells were used as an experimental model of metastasis. In the case of cultured tumor cells, TPL at 4 ng/ml inhibited cell growth to a similar extent as taxol at 100 ng/ml both under anchorage-dependent and -independent conditions. When mice with tumor xenografts formed by several different cell lines were injected i.v. with TPL at a dose of 0.25 mg/kg/ twice a week, the sizes of the tumor xenografts were reduced to 10-50% of the controls. This was comparable or superior to that achieved with the commonly used chemotherapeutic drugs adrimycin, cisplatin and mitomycin. Importantly, TPL could inhibit both spontaneous and experimental metastasis. Additional studies revealed that treatment of tumor cells with 10 ng/ml of TPL for 24 hours resulted in decreased levels of c-myc, cyclin A/cdk2 and cyclin B/cdc2 while increasing the level of cleaved PARP, an indicator of apoptosis. Furthermore, TPL also decreased the telomerase activity as measured by both the TRAP assay and PicoGreen staining. These results strongly suggest that TPL can potentially be developed as a new anti-tumor/metastasis agent.

Proceedings of the American Association for Cancer Research • Volume 43 • March 2002

#3962 Overexpression of tumor necrosis factor-stimulated gene-6 protein (TSG-6) suppresses tumor growth *in vivo*. Jinguo Chen, Xue-Ming Xu, Shanmin Yang, Luping Wang, Charles B. Underhill, and Lurong Zhang. *Georgetown University Medical Center, Washington, DC, The Cell and Tumor Key Lab of China Education Ministry at Xiamen University; Xiamen, China, and Beijing General Hospital, Beijing, China.*

Tumor necrosis factor-stimulated gene-6 protein (TSG-6) is an anti-inflammatory factor that is produced in response to TNF and contains a link module that allows it to bind hyaluronan. In this study, we examined the effects of overexpression of TSG-6 on tumor progression. The cDNA coding for human TSG-6 gene (782bp) was cloned, inserted into an expression vector (pSecTag2/Hygro B) and transfected into TSU human prostate cancer cells. The positive clones were identified by RT-PCR and the biological activity of the TSG-6 protein was confirmed by its ability to bind hyaluronan. The TSG-6 positive clones were then pooled and compared with control cells (transfected with vector) with regard to cell behaviors. In culture, the TSG-6 transfected TSU cells grew at the same rate as control cells as measured by cell number and by incorporation of radioactive thymidine. However, when the cells were inoculated on the chorioallantoic membrane of chicken embryos, the TSG-6 transfected TSU cells grew at a slower rate than the control cells (mean xenograft weight in TSG-6 16.3 mg vs. control 39.6 mg). Similarly, when cells were injected s.c. into nude mice, the xenografts formed by the TSG-6-transfected cells were smaller than that of the control cells (mean xenograft weight 0.72 g vs. 2.16 g). Western Blot analysis of lysates from these xenografts indicated that the TSG-6 transfected cells had increased levels of Fas, cleaved caspase 8 and cleaved PARP, but no change in the levels of cyclin D1, B1, Rb, ERK. These preliminary results suggest that TSG-6 could function as a tumor suppressor *in vivo*, in part, through the induction of apoptosis.

#149 Decoy TR6 protects tumor cells from apoptosis. Luping Wang, Sunghee Kim, Jinguo Chen, Xue-Ming Xu, Shanmin Yang, Charles B. Underhill, and Lurong Zhang. *Beijing General Hospital, Beijing, China, Human Genome Sciences, Inc., Rockville, MD, Lombardi Cancer Center, Washington, DC, Xiamen University, Xiamen, China, and Fujian Medical University, Fuzhou, China.*

Recently, TR6, a decoy receptor of the TNFR super-family, has been shown to bind to three ligands: FasL, LIGHT and TL1. Since TR6 lacks a transmembrane domain, it can bind to these ligands and competitively block their interaction with Fas and HVEM and as a consequence inhibit apoptosis. In a series of experiments, we examined the role of TR6 in tumor progression, and obtained the following results: 1) in transwell chambers, the TR6 expressed by SW480 cells in the top well could inhibit apoptosis in MDA-435 tumor cells growing in the bottom well; 2) recombinant TR6 could block apoptosis induced by exogenous FasL and this effect could be reversed by the addition of neutralizing antibodies to TR6; and 3) cell death induced by endogenous FasL could be blocked by the addition of TR6. We then examined the expression of TR6 in a panel of human tissues by immunohistochemical staining with a monoclonal antibody and found that while normal tissue demonstrated little or no staining, a significant fraction of breast cancer tissue was positive. This fraction depended in part on the stage of the tumor. In the case of tumors that had not metastasized to the lymph nodes, the staining rate was 44% (4 out of 9) and for tumors that had metastasized the rate was 70% (14 out of 20). For lymph node metastases themselves, the rate was 80% (16 out of 20). Furthermore, ELISA assays showed that the level of TR6 in the serum of cancer patients was higher than that from normal individuals (2.3 + 0.2 ng/ml vs. 0.46 + 0.07 ng/ml). These results suggest that TR6 plays a critical role in preventing tumor cells from undergoing apoptosis and thereby promotes their progression. Thus, it may be possible to reduce tumor malignancy by inhibiting the function of TR6.

#5589 A hyaluronan binding peptide can trigger apoptosis by antagonizing members of the bcl-2 family. Xueming Xu, Ningfei Liu, Jinguo Chen, Luping Wang, Shanmin Yang, Charles B. Underhill, and Lurong Zhang. *Georgetown University Medical Center, Washington, DC, Shanghai 9th Hospital, Shanghai, China, Lombardi Cancer Center, Washington, DC, Beijing General Hospital, Beijing, China, and Xiamen University, Xiamen, China.*

In previous studies, we have demonstrated that the growth of tumor cells can be suppressed by a peptide termed P4 that can bind to hyaluronan. This effect appeared to be due to the induction of apoptosis, since treatment of cultured cells with P4 resulted in the fragmentation of the DNA, characteristic apoptotic cells. Confocal microscopy of cells treated with FITC tagged P4, revealed that it quickly became associated with mitochondria. This was further supported by the fact that treatment of cells with P4 induced a spectral change in the dye JC-1 indicating the loss of membrane potential in the mitochondria. Western blotting of cultured MDA-435 tumor cells following treatment with P4 revealed increased levels of activated caspase 9, caspase 3 and PARP, suggesting that P4 upregulated a Fas-independent pathway leading to apoptosis. Using immunoprecipitation, we found that the P4 peptide could bind to Bcl-2 and Bcl-xL which are predominately located in the membranes of mitochondria. And finally, in an in vitro assay with cytoplasmic extracts of tumor cells, we found that P4 caused the release of cytochrome c from the mitochondria. Taken together, these results suggest that P4 targets mitochondria by binding to Bcl-2 family members and this induces the release of cytochrome c leading to apoptosis.